LETTER FROM THE EDITOR

Our lead article this month is a timely exploration of the mathematics underlying the spread of disease on a college campus. Though this article was written and accepted for publication prior to the outbreak of the COVID-19 pandemic, it clearly has relevance to understanding the awful year we have all been muddling through. Authors John Mayberry, Maria Nattestad, and Austin Tuttle provide a lively and accessible introduction to some mathematical issues in epidemiology, and I urge everyone to have a look at their work.

Our co-lead article comes from Thomas Clark and Anil Venkatesh. Inspired by the mobile app *Flappy Bird*, in which a player tries to navigate a small bird through an obstacle course by applying upward thrusts against gravity, they consider several difficult problems in orbital mechanics. Their exploration takes them through a variety of topics in mathematical physics, including the calculus of variations, interpolation problems, and the construction of spline minimizers.

If you prefer combinatorics to physics, then we have several items for your consideration. Michael Spivey offers a novel take on the venerable topic of sums of integer powers. He shows how Stirling numbers (of the second kind) and Eulerian numbers can be used to prove some classic identities. For their part, Sam Chow, Ayla Gafni, and Paul Gafni consider a seemingly simple question: Can we connect all of the dots in a square grid to form a polygon with n^2 sides, with the restriction that no two consecutive segments can be collinear? Their clever and complete solution to this puzzle will definitely make you smile.

Jimmy Dillies provides a sort of transitional form between the continuous and the discrete, as he shows how to use graph theory to explain the concept of an "orientable" manifold. This can be a tricky concept for newcomers to manifold theory, so anything that provides an engaging way in is welcome.

The shorter pieces will likewise make you smile. Giovanni Vincenzi and Bonaventura Paolillo provide a pleasingly elementary proof for a classic result in elementary trigonometry: that if the sine of a rational angle is a rational number, then that number is either 0, ± 1, or $\pm 1/2$. This can be a surprisingly difficult result to prove, making their contribution all the more welcome. Nam Gu Heo also provides an elementary proof for a difficult result: the Ionescu–Weitzenböck inequality from Euclidan geometry. And Roger Nelsen closes out the articles with some observations on a famous observation: that $\sqrt{2} + \sqrt{3}$ provides a surprisingly good approximation to pi.

We also have the problems and solutions from the 49th Annual USA Mathematical Olympiad, a couple of proofs without words, original problems and solutions, and reviews. There's a little something for everyone!

Jason Rosenhouse, Editor

Math. Mag. **94** (2021) 82. doi:10.1080/0025570X.2021.1872221

ARTICLES

The Structure of an Outbreak on a College Campus

JOHN MAYBERRY
University of the Pacific
Stockton, CA 95211
jmayberry@pacific.edu

MARIA NATTESTAD
Google, Inc.
Palo Alto, CA 94306
maria.nattestad@gmail.com

AUSTIN TUTTLE
Open Systems International
Minneapolis, MN 55455
tuttl059@umn.edu

Disclaimer. *This article was written prior to the COVID-19 pandemic, and it is in no way meant to replace or supersede the advice of expert epidemiologists. We are grateful to those in the scientific community whose work is helping to combat this outbreak. We only hope that the simple models presented here will serve as motivation to dive more deeply into their work.*

Mathematical modeling is a nebulous process because it is based on an underlying principle best stated by the statistician George Box: "All models are wrong; some models are useful" [9]. This innate ambiguity makes the transition between traditional "textbook" mathematics and real world applications particularly challenging for students and requires a complete change in perspective. Nevertheless, in summer 2012, we ventured into this mysterious realm and applied for a grant through our home institution, the University of the Pacific, to investigate the following three questions:

1. How fast will a typical outbreak of seasonal influenza spread throughout the student population at Pacific?
2. If a limited number of vaccinations are available, how should these vaccinations be distributed in order to minimize the number of infected students?
3. How do the answers to questions (1) and (2) depend on parameters related to the severity of the epidemic and the structure of the student contact network?

This process led us on an interesting journey through the history of mathematical epidemiology, the recent rise of the "science of networks," and the mathematical theory of random graphs. Our purpose here is to provide a brief introduction to this exciting area of mathematical research through the backdrop of our own summer investigations.

In 1766, Daniel Bernoulli published the first known mathematical model for the spread of small pox [7]. His work provides an example of "good" mathematical modeling leading to meaningful results. The benefits of smallpox inoculation were disputed in the medical community at this time, and Bernoulli's goal was to argue in favor of

Math. Mag. **94** (2021) 83–98. doi:10.1080/0025570X.2021.1867450
MSC: 05C80, 92D30

universal inoculation against this often fatal disease. His (differential equation based) model provided evidence in support of this strategy by showing that universal inoculation would increase the expected life expectancy in Britain by over three years [**8**]. Despite Bernoulli's seminal work, it was not until the 20th century that the now well known Susceptible-Infected-Removed (SIR) model was introduced as a more general model for the spread of infectious diseases (like smallpox) which partition society into three classes of individuals: those who are susceptible to infection (S), those who are currently infected (I), and those who have been "removed" (R). Removed can mean one of two things: (i) the individual was infected, but recovered, consequently developing immunity to further infection, or (ii) the individual was infected and died. Since our main interest here is in modeling seasonal influenza, we will typically think of the first (less morbid) interpretation.

The literature on deterministic epidemiological models is extensive; most introductory textbooks on differential equations or dynamical systems contain exercises about SIR type models, and there are entire books dedicated to explaining variations at a level suitable for undergraduates (see [**10**], for example). Here we mention such models only to point out two underlying assumptions that are often unrealistic:

1. The "homogeneously mixing" or "everyone knows everyone" assumption, which states that an infected person is able to spread their infection to any susceptible individual in the network.
2. The "law of large numbers" assumption, which states that the population size is sufficiently large to accurately describe microscopically random dynamics with macroscopic averages.

In situations where these assumptions are not met, models which account for random fluctuations and variable differences in individual behavior are more appropriate. One such class of models is based on the mathematical theory of random graphs. The basic idea is to represent our underlying network of interest (students at Pacific) as a graph where each node is a student and edges between nodes represent potential disease-spreading contacts. For example, if Jane and Jill are roommates, our graph would contain an edge which connects Jane and Jill. The randomness comes in two places:

1. We assign to each student a random number of potential contacts representing roommates, classmates, teammates, and other individuals whom the student encounters on a daily basis. While the assignment can be done in many ways, one of the most common methods (called the *configuration model*) is to assign contacts based on a probability distribution (called the *degree distribution*) which accurately reflects the empirical distribution of contacts in the population.
2. If a student becomes infected with influenza, then during each day of their infectious period, we allow them to infect contacts with some probability λ called the *transmissibility* or *transmission rate* of the disease.

A simple illustration is provided in Figure 1, but further details and the history of such models will be developed in the next section. We start by describing the Erdős–Renyi model, one of the simplest and earliest examples of a random graph. After showing that this model does not fit the degree distribution of student connections from a sample survey, we then develop the more flexible configuration model, which achieves a more accurate fit. We then present the results of Monte Carlo simulations of epidemics with different transmissibilities. We suggest a "three phase" model for the study of outbreaks in a closed environment and present some related conjectures for future research. Finally, we compare random vs. optimal vaccination strategies and conclude with some limitations and questions for future work.

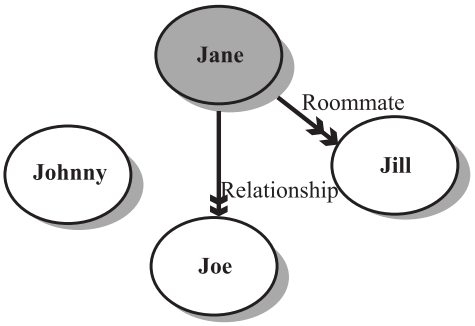

Figure 1 An example of a student network consisting of four students. Here, Jane has just been infected and has probability λ of infecting Jill or Joe during each day of her infectious period. Johnny is a loner and has no risk of infection.

Random graph models

The first random graph SIR type model was proposed by Reed and Frost in the 1920s although the analysis of this model was not published until the 1950s [1]. Later in the same decade, Austin, Fagen, Penny, and Riordan [3], Gilbert [15], and Erdős and Renyi [14] considered similar models for the construction of random graphs on N vertices. Of all these possible models which one could use as a launching point for our discussion, we choose to use Gilbert's model because it most naturally extends to random graph models with arbitrary degree distributions. Following the convention of random graph literature however, we shall refer to graphs generated using Gilbert's model as Erdős–Renyi random graphs.

The Erdős–Renyi model Consider a set of vertices or nodes labeled with the integers $1, 2, \ldots, N$ where in our specific application of interest, a node represents a student enrolled in classes at Pacific. We draw an edge e_{ij} between students i and j if students i and j "interact" on a daily basis. Informally speaking, an interaction is an encounter which could potentially lead to the transfer of an influenza virus if either individual is infected; see below for a more detailed description. The collection of all student nodes and their corresponding edges is called a graph and in our work, we shall refer to such graphs as student connectivity networks. Note that there are $\binom{N}{2} = \frac{N(N-1)}{2}$ possible edges which can be formed in a population of N students and a graph which includes all these edges is called *complete*. In a complete graph, "everyone knows everyone." But in reality, students interact with a relatively small number of students on any given day. Hence, only a small fraction of possible edges are contained in an actual graph of student interactions. The "random" part of our random graph models comes from the method by which edges are formed. In an Erdős–Renyi random graph, we form each possible edge in the graph with probability p, independently of all other edges. Here, p is a parameter which measures the approximate fraction of possible connections which are formed. For example, let's say that Jane is a student at Pacific. Jane could potentially have $N - 1$ connections. Each connection is formed with probability p independently of the rest and therefore the number of connections Jane ends up with is distributed according to a binomial random variable with parameters $N - 1$ and p. More specifically, if D_J is the number of Jane's connections, then

$$\Pr(D_J = k) = \binom{N-1}{k} p^k (1-p)^{N-1-k}$$

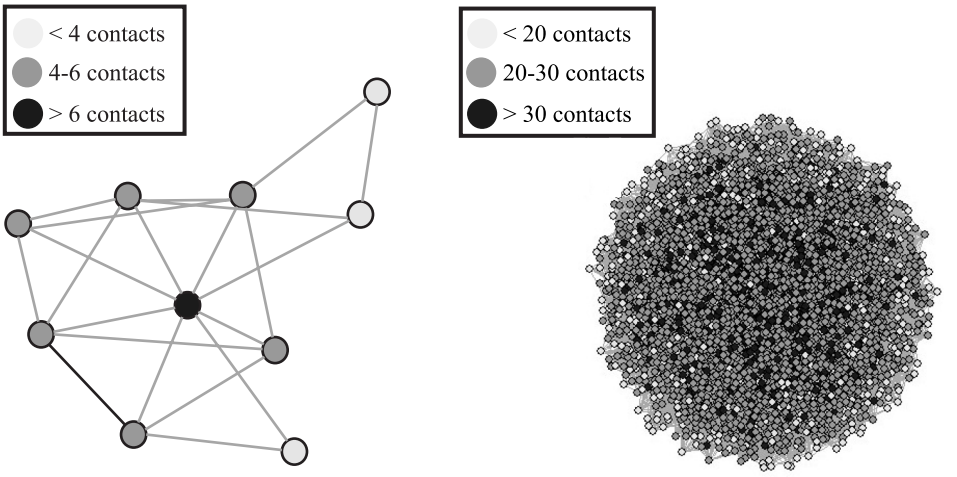

Figure 2 Examples of student connectivity network generated using the Erdos–Renyi model. Left: A small network of $N = 10$ students and connection probability $p = 1/2$. Right: An Erdos–Renyi approximation of the Pacific network with $N = 4000$ students and connection probability $p = 0.00625$. Parameters were chosen to match survey data.

for $k = 0, 1, \ldots, N - 1$ where $\Pr(A)$ is and will be our shorthand notation for the probability of event A throughout this paper. Note that Jane's expected number of connections is $(N - 1)p \approx Np$ since N is relatively large ($\approx$4000 at Pacific). Hence, p is approximately equal to the relative fraction of students with whom Jane interacts on a daily basis.

Figure 2 shows two examples of Erdős–Renyi random graphs. In the first example, the student body is small (10 students) and each edge is connected with probability $1/2$. The majority of students have an intermediate number of connections (4–6) with one "super-connector" who knows almost everyone. The second example uses Pacific relevant parameters based on data obtained from a student survey (see the Comparison with student data section below for details).

There are two problems with using Erdős–Renyi random graphs to model a student connectivity network. The first involves a phenomenon known as *clustering* (or rather, lack thereof). Clustering occurs when two of a student's connections are more likely to interact with one another than two randomly chosen students in the network. Since Jane's friends will also tend to be friends with one another (similarly, if Jane interacts with two students in class, those two students will also interact with one another), we would expect an accurate representation of a student connectivity network to exhibit a fair amount of clustering. In an Erdős–Renyi random graph, connections between students form independently with probability p regardless of who the two students know so there is no clustering in such models.

Comparison with student data The second problem with Erdős–Renyi random graphs is their lack of flexibility when it comes to matching qualitative shapes of real networks: any choice of degree distribution should reflect the empirical degree distribution of the population under consideration. To obtain a better picture of what this empirical distribution should look like at our institution, we sent out a survey to Pacific students which contained the following two questions:

- How many Pacific students do you currently live with? (If living in a dorm or Greek house only include roommates).

Mean	StDev	Min	First quartile	Median	Third quartile	Max
25	23	1	10	18	32	144

TABLE 1: Summary statistics for the average number of daily contacts (rounded to the nearest integer). The average number of daily contacts for each student was obtained by averaging the reported number of contacts for each day of the week and adding the number of roommates.

- Estimate how many Pacific students (excluding roommates) you typically interact with on each of the following days (Mon–Sun). By interact, we mean sit near enough to hit with a meter stick, have a face to face conversation beyond a simple "Hi, how are you?," or have any sort of physical contact (like a handshake), but not a simple bump in the hallway. Make sure to consider the following activities in answering this question: class schedule, work schedule, shared meals, hanging out, studying, playing sports, working out, and any other extracurricular activities you are involved with on a regular basis.

A full copy of the survey questions is included in the appendix in the online version of the article. The survey was posted on Pacific's Facebook pages and sent out to the authors' classes so while a wide range of students had access to the survey, participation was voluntary. We received a total of 127 responses although ten were excluded from further analysis because of missing or ridiculous answers (e.g., one student claimed to have 400 roommates). Summary statistics for the average number of daily contacts of the remaining 117 students are shown in Table 1.

A histogram of the average number of daily contacts per student is shown in Figure 3. Notice that the distribution is right-skewed with a positive mode of around 5–10 contacts per day. Most students tend to have relatively few connections with a small number of highly connected students on the upper end of the distribution. Although our survey data is privy to a number of selection biases (for example, only eight freshmen filled out the survey as opposed to 54 juniors), we believe that the qualitative shape of our sample distribution is an accurate representation of the actual population degree distribution. In contrast, a binomial degree distribution would suggest a symmetric degree distribution with a mode of about 25 contacts per student. Furthermore, the maximum and minimum numbers of contacts for the Erdős–Renyi graph shown in the right side of Figure 2 were 45 and 10, respectively, whereas 21 students in our survey had more than 45 contacts and 30 students had less than 10. Therefore, the class

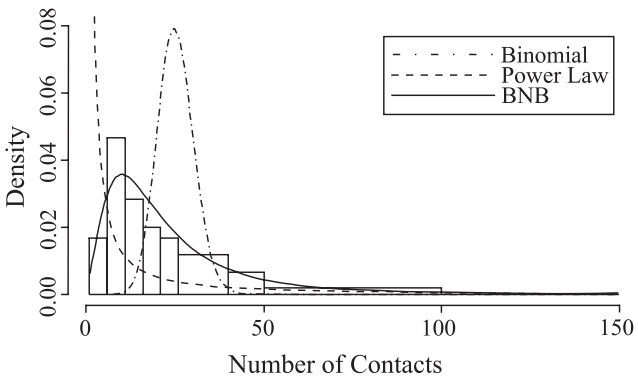

Figure 3 Histogram of average daily contacts based on survey data along with maximum likelihood fits of binomial, power law, and BNB distributions.

Erdős–Renyi random graph model does not provide us with an accurate description of real life student connectivity networks and an alternative approach is required.

The configuration model At the end of the 20th century, the publication of two papers by Watts and Strogatz [21] and Barabasi and Albert [5] spawned a new area of research they jointly dubbed "the science of networks." The goal of this field was to develop models for real world networks which allowed for more flexible degree distributions as well as the incorporation of clustering effects. In fact, related models were independently developed and studied within the probability community during the mid 1990s ([2], [19]). We shall focus here on describing one simple method for generating random graphs with arbitrary degree distributions that most closely follows the development of [20] and is often referred to in the literature as the *configuration model*. For more detailed coverage of modern issues in random graphs and the science of networks, see [26] for an informal read or the textbooks [13], [22] for more rigorous developments.

In the configuration model, we begin by choosing a degree distribution D with

$$\Pr(D = k) = r_k$$

for some sequence of numbers $\{r_k\}_{k=0}^{\infty}$ with $\sum r_k = 1$. The Erdős–Renyi model is a special case in which the distribution of D is binomial. We generate N random draws from D, $d_1, \ldots, d_N$, and assign d_i "half-edges" or stubs to student i. We then connect these half-edges using a form of weighted-attachment: at each step, we select two half-edges at random from the set of remaining stubs to connect. There are two problems which could occur during this process: two half-edges may attempt to connect students who are already connected (forming *parallel edges* in the resulting graph) and two half-edges may attempt to connect students with themselves (forming a *self-loop* in the graph). A graph which has no parallel edges or self-loops is called *simple*. Theorem 3.1.2 of [13] shows that as long as r_k has a finite second moment, there is a positive probability of forming a simple graph through the above process so we restrict our attention to such situations in what follows.

Barabasi and Albert [5] popularized the use of a power law degree distribution which sets

$$r_k = \frac{1}{\zeta(s)k^s}$$

where $\zeta(s)$ denotes the Riemann-Zeta function and is included as a normalizing constant. Power law distributions are a natural model for large-scale networks such as the world wide web because the long tails leave room for the creation of super-connectors, and the power-law form is capable of capturing a "scale-free" structure often observed in such networks [6]. However, we can see from Figure 3 that a power law distribution provides a relatively poor fit for our student contact network. Our empirical degree distribution exhibits a mode of 5–10 interactions per week whereas the power law distribution is a strictly decreasing function of degree and hence, grossly overestimate the number of students with 1–5 contacts.

To address the existence of a non-zero mode, we appeal instead to an interesting and less discussed probability distribution first used in [16]. This distribution goes by the name of the "Waring distribution" in some circles, but here we use the more probabilistically-relevant name of the beta negative binomial (BNB) distribution. The BNB arises as a mixture of the more well known beta and negative binomial distributions. To give a simple probabilistic derivation of its mass function, suppose we have in our possession a biased coin in which the probability of obtaining heads on a given

flip is p. We perform a random experiment in which we toss the coin until we see some predetermined number of heads, n and record X, the number of tails obtained in the process. Then X has a *negative binomial distribution* and its probability mass function is given by

$$\Pr(X = k) = \binom{n+k-1}{n-1} p^n (1-p)^k$$

for $k = 0, 1, \ldots$. To derive this formula, note that for the event $X = k$ to occur, $n-1$ of the first $n+k-1$ trials must be heads, the nth head must occur on the $(n+k)$th trial, and there must be a total of n heads and k tails.

The BNB distribution puts an interesting twist on this classic probability model by assuming that p, the success probability, is itself a random variable. Clearly, any reasonable choice of a random variable to model this variability in success probabilities should be continuous and supported on the interval $[0, 1]$. One natural choice would be to assume that p is uniformly distributed across the interval [0,1]. However, this forces upon us a "flatness" assumption: p is as likely to be between 0 and 0.1 as it is to be between 0.5 and 0.6. A more flexible choice is to assume that p follows a Beta distribution with parameters α, β. In this case, p has density function

$$f(x) = cx^{\alpha-1}(1-x)^{\beta-1}, \quad 0 \le x \le 1$$

where c is a normalization constant that depends on α, β. In fact, it is usually shown in an introductory course on undergraduate probability that c can be computed in terms of the Gamma function, but for our purposes it is easier just to write $c = B(\alpha, \beta)^{-1}$ where

$$B(\alpha, \beta) = \int_0^1 x^{\alpha-1}(1-x)^{\beta-1}\, dx$$

is the well-known Beta function.

To derive the mass function of X, we condition on the possible values of p to obtain

$$\begin{aligned}
\Pr(X = k) &= \int_0^1 \Pr(X = k \mid |p = x) f(x)\, dx \\
&= \binom{n+k-1}{n-1} B(\alpha, \beta)^{-1} \int_0^1 x^n (1-x)^k x^{\alpha-1}(1-x)^{\beta-1}\, dx \\
&= \binom{n+k-1}{n-1} \frac{B(n+\alpha, k+\beta)}{B(\alpha, \beta)} \\
&= \begin{cases} \frac{B(n+\alpha,k+\beta)}{kB(n,k)B(\alpha,\beta)} & k \ge 1 \\ \\ \frac{B(n+\alpha,\beta)}{B(\alpha,\beta)} & k = 0. \end{cases}
\end{aligned} \tag{1}$$

Note that while the probabilistic interpretation of the BNB requires n to be an integer, this last line makes sense for any positive n. We therefore define a BNB random variable as any random variable whose mass function is given by equation (1). We fit a BNB distribution to our given empirical student connectivity data using maximum likelihood estimation ; the resulting distribution is shown overlaid in Figure 3 and provides a much better fit than either the binomial or power law distributions. Figure 4 illustrates the differences between a binomial and BNB degree distribution. Clearly, the BNB allows for a greater amount of variability in connections.

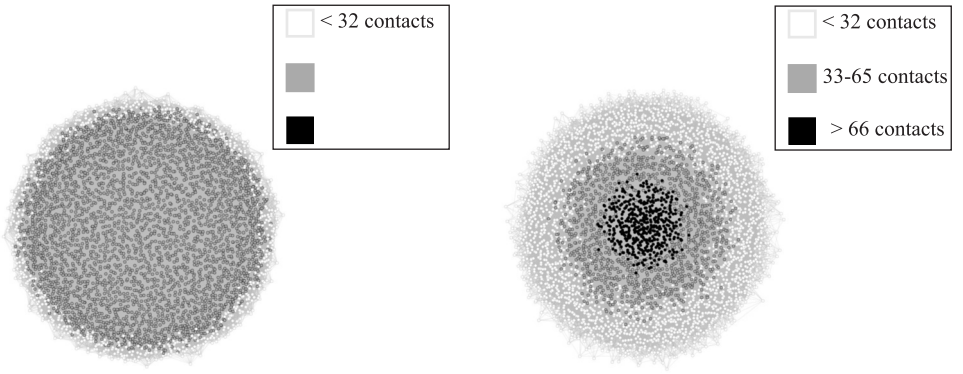

Figure 4 A comparison of the structure of student connectivity graphs generated using a Binomial degree distribution (left) and a BNB degree distribution (right).

Is there an a priori reason to suspect that the BNB is a reasonable degree distribution for a student interaction network? We have only conjectures at this time, but one amusing explanation is as follows. Every student can tolerate a certain number of miserable, relational experiences. We will call this number n. Every time a student forms a new relationship, the relationship is either ended because of one such experience (a "heads" outcome) or ends in a sustained interaction (a "tails" outcome). To take into account individual student difference in affability, we allow the probability p of misery to vary from student to student. Under these assumptions, the number of daily contacts X of a given student would follow the BNB model.

Simulating an epidemic

Once we have set-up our student interaction network, the next step is to simulate the disease spread. To formally define this process, we introduce the following notation: $|A|$ will denote the cardinality of a set A and 2^A will denote the power set of A. We then define a *potential outbreak* on a random graph of N vertices labeled $1, 2, \ldots, N$ with degree distribution $\{r_k\}_{k=0}^{\infty}$, *transmissibility* $\lambda > 0$, and *infection duration* $\gamma \in \mathbb{N}$ as any stochastic process $(S_n, I_n, F_n)_{n=0}^{\infty}$ with state space

$$2^{\{1,\ldots,N\}} \times 2^{\{1,\ldots,N\}} \times \{0, 1, \ldots \gamma\}^N$$

that evolves according to the following rules:

1. We initially have $S_0 = \{1, \ldots, N\}$, $I_0 = \emptyset$, and $F_0(j) = 0$ for all $j = 1, \ldots, N$.
2. At step $n = 1$, we choose a random $j \in \{1, \ldots, N\}$, setting $I_1 = \{j\}$, $F_1(j) = \gamma$, and $S_1 = S_0 - \{j\}$.
3. At the beginning of step $n \geq 2$, we search through all nodes $j \in S_{n-1}$ and move them to I_n with probability $1 - (1 - \lambda)^{i_j}$ where i_j is the number of j's neighbors in I_{n-1}.
4. At the end of step $n \geq 2$, we set

$$F_n(j) = F_{n-1}(j) - 1$$

for all $j \in I_{n-1}$ and $F_n(j) = \gamma$ for all $j \in I_n - I_{n-1}$. Any vertex $j \in I_n$ with $F_n(j) = 0$ is removed from the graph before the next step.

To decode the above conditions in the context of our previous informal descriptions of an SIR random graph model, S_n and I_n are the lists of susceptible and infected individuals, respectively, on Day n of the potential outbreak. F_n is a vector of length N whose jth entry tells us the remaining length of infection for person j. Conditions (A)–(D) can informally be restated in the following way:

1. Initially, all individuals are susceptible.
2. On day 1, a single individual (who we often call Patient Zero) is infected and will remain infected for the first γ days of the outbreak.
3. On each subsequent day of the process, infected individuals infect each of their susceptible contacts independently with probability λ. Once infected, an individual remains latent until the next day of the outbreak.
4. The number of remaining days in an infected individual's infectious period decreases by one with each passing day. After their infectious period is up, an individual can no longer infect other susceptibles and is immune to further infection, effectively removing them from the population.

Note that since we are assuming a finite population of size N, a potential outbreak will end in a maximum of $\gamma \times N$ days and hence, the above process is well-defined.

We call the above process a *potential* outbreak because there is no guarantee that Patient Zero will spread their infection to a significant fraction of the population. In fact, we presume that a typical influenza outbreak would proceed after one of an initial number of "seeded" infections in the student body manages to spread to a significant fraction of the population. We call any realization of an outbreak which spreads to at least 1% of the population an *outbreak*. The choice of 1% is rather arbitrary, but as we shall see, most potential outbreaks either die out with Patient Zero or initiate an outbreak so the exact cutoff is not important.

We shall study the dynamics of potential outbreaks via stochastic simulations, generating 1000 random realization

$$(s_{m,n}, i_{m,n}, f_{m,n})_{m=1}^{1000}$$

of a potential outbreak for each given parameter pair (λ, γ) of interest. For each simulation, the fitted BNB from The configuration model section was used to generate a random student connectivity network and then the potential outbreak played out according to the rules in (A)–(D) above. Based on our research objectives, we compute four important disease statistics for each simulation:

1. $o_m = 1$ if an outbreak occurred and 0 otherwise.
2. $\ell_m =$ the length of the potential outbreak $= \min\{n \geq \gamma : |i_{m,n+1}| = 0\}$.
3. $t_m =$ the total fraction of students infected by the potential outbreak $= \lim_{n\to\infty}(1 - |s_{m,n}|/N)$.
4. $p_m =$ the peak day of the potential outbreak $= \arg\max\{|i_{m,n} : n \geq 1|\}$ where in the case of multiple peaks, we take the first.

We shall also be interested in looking at the values of the latter three statistics restricted to outbreaks and use the notation $\tilde{\ell}_m$, $\tilde{t}_m$, and $\tilde{p}_m$ when we refer to the corresponding statistics restricted to samples with $o_m = 1$. In reality, each set of statistics $\{o_m\}$, $\{\ell_m\}$, etc. represents a set of independent and identically distributed observations from a random variable associated with potential outbreaks and hence, we can use the central limit theorem to form confidence intervals for the theoretical expected values of each variable of interest.

Since generating a random graph of 4000 students and running a potential outbreak are time consuming ventures, we will restrict our attention to parameter values relevant

to the influenza virus. Choosing a value for γ is simple since previous research has placed the average length of flu transmissibility at around 5 days [11]. However, λ is more difficult to estimate for two reasons. First of all, each year brings new strains of influenza with different rates of infectiousness. However, between-strain differences aside, even within a particular strain, the transmissibility will be highly heterogeneous and will vary depending on the strength of the individual interactions between students. For example, a student may be more likely to contract a disease from a roommate, close friend, or significant other than from a casual encounter in the hallway or during class. Longini et al. [18] distinguish between household interactions, which describe the former type of interaction, and community interactions. They were able to estimate household transmission rates in several different influenzas strains and found that estimates range from around 0.03 for the less virulent Influenza B strain to around 0.09 for the highly contagious A(H1N1) strain. The community transmissibility is more difficult to estimate, as one can imagine, although the same paper did obtain estimates on the chances of contracting a particular strain from someone in the community over the course of an influenza season. Without knowledge of the individual interaction structure which led to this estimate, however, little can be said about the per interaction transmissibility. In any case, student networks are different from the broader city networks considered in [18], and it may be more realistic to assume a higher rate of household type interactions due to the more closed off environment in which students interact.

We start our investigations by choosing a compromise between the two situations and use the best case household transmission probability of 0.03 for λ. The resulting disease statistics are shown in Table 2 and the rightmost graph in Figure 5 illustrates several sample realizations of outbreaks.

Notice that with $\lambda = 0.03$, almost 90% of potential outbreaks initiate an actual outbreak and when they do, they infect almost 90% of the student body with very little variability in the fraction of infected students (in fact, 884 of the 885 outbreaks infected between 85% and 89% of the students). We also note that the average length is about twice the average peak day of an outbreak with little difference in variability between the two statistics. We discuss these observations in greater detail below.

How do these numbers compare with empirical influenza rates on campus? Since students rarely visit the doctor for official influenza tests, we cannot get an exact incidence rate for a typical season, but in our survey, only 58 of 120 students (approximately 50%) reported having both a fever and at least one of the other common flu symptoms (runny nose, sore throat, body aches) during the previous flu season. Therefore, using $\lambda = 0.03$ seems to represent an extreme epidemic. To investigate other scenarios, we performed stochastic simulations of potential outbreaks with $\lambda = 0.01$ and $\lambda = 0.02$ as well. The results are summarized in Table 2 and Figure 5.

Clearly, the probability of an outbreak and the mean fraction of infected individuals are both monotonically increasing functions of λ as we should expect. When $\lambda = 0.01$, about half of all potential outbreaks initiate outbreaks which, in turn, infect about half the population. Looking at other disease statistics suggest two other interesting conjectures for future work:

1. As we observed in the case $\lambda = 0.03$, the average peak day is always around half the length of the outbreak for all values of λ and only slightly less variable than the length.
2. The mean of the length and peak day both increase as λ decreases.

All three of these observations can be explained by comparison with the "three phases of fixation" for a selectively advantageous allele in the theory of population genetics. These three phases are described in Chapter 6 of [12] as follows:

Statistic	Mean	StDev	95% CI for mean
Outbreak (o)			
$\lambda = 0.03$	0.885	0.319	(0.865, 0.905)
$\lambda = 0.02$	0.776	0.417	(0.750, 0.802)
$\lambda = 0.01$	0.531	0.499	(0.500, 0.562)
$\lambda = 0.03,\ R3$	0.801	0.399	(0.776, 0.826)
$\lambda = 0.03,\ H3$	0.518	0.500	(0.487, 0.549)
Length of outbreak ($\hat{l}$)			
$\lambda = 0.03$	27.75	2.73	(27.57, 27.93)
$\lambda = 0.02$	33.01	3.58	(32.76, 33.26)
$\lambda = 0.01$	46.80	5.85	(46.31, 47.30)
$\lambda = 0.03,\ R3$	31.70	3.44	(31.45, 31.93)
$\lambda = 0.03,\ H3$	59.23	8.30	(58.51, 59.94)
Fraction infected ($\hat{t}$)			
$\lambda = 0.03$	0.873	0.006	(0.873, 0.873)
$\lambda = 0.02$	0.780	0.008	(0.779, 0.780)
$\lambda = 0.01$	0.537	0.012	(0.536, 0.538)
$\lambda = 0.03,\ R3$	0.516	0.008	(0.515, 0.516)
$\lambda = 0.03,\ H3$	0.333	0.016	(0.329, 0.331)
Peak day ($\hat{p}$)			
$\lambda = 0.03$	13.09	2.01	(12.96, 13.22)
$\lambda = 0.02$	15.40	2.53	(15.23, 15.58)
$\lambda = 0.01$	22.15	4.17	(21.79, 22.50)
$\lambda = 0.03,\ R3$	14.96	2.59	(14.78, 15.14)
$\lambda = 0.03,\ H3$	29.54	5.66	(29.05, 30.03)

TABLE 2: Sample mean and standard deviations of our four primary sample statistics along with the corresponding 95% confidence intervals for their mean values for the three values of $\lambda = 0.01, 0.02, 0.03$ as well as the two vaccination strategies of vaccinating a random 1/3 of the population ($R3$) and targeted vaccination of the top 1/3 most highly connected individuals ($H3$), both for the extreme case of $\lambda = 0.03$.

Phase 1: While the advantageous allele is rare, its growth in the population is well-approximated by a supercritical branching process with a nontrivial survival probability. In a potential outbreak, the infected individuals play the role of the advantageous alleles and the "survival" probability is the probability that an actual outbreak is initiated. We call this the *critical phase* of a potential outbreak.

Phase 2: While the advantageous allele is at intermediate frequencies, its growth is "almost deterministic" and can be well-approximated by an appropriate logistic equation. This is like the early stages of an outbreak when the bulk of the population is susceptible and the disease has plenty of "food for fodder." We call this the *apocalyptic phase* because it occurs quickly and most of the final removed class is infected during this phase.

Phase 3: Once the disadvantageous allele is rare, its decline is well-approximated by a sub-critical branching process as the advantageous alleles attempt to sweep up the remnant of their weaker counterparts. This period is like the final phase of an outbreak. We call this the *post-epidemic* phase because the virus is no longer spreading quickly through the population.

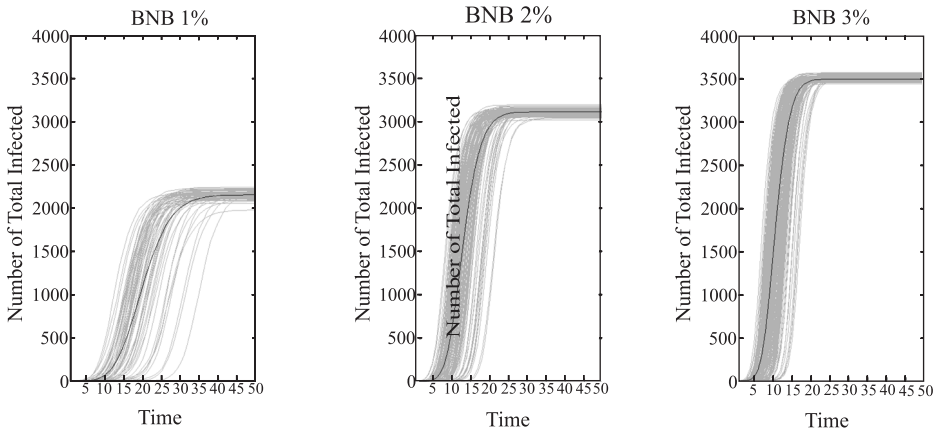

Figure 5 A comparison of the outbreak dynamics for three different disease transmissibilities (*left*: $\lambda = 0.01$; *center*: $\lambda = 0.02$, *right*: $\lambda = 0.03$). The black lines show the average values of the total number of infected individuals for all outbreaks as a function of n while the gray lines show the total numbers of infected individuals after n days in individual outbreaks.

The plots in Figure 5 further demonstrate these dynamics. For all three values of λ, the logistic nature of the apocalyptic phase is evident and while the length of this phase varies with λ, simulations with the same transmissibility proceed through this phase in a similar fashion. We can see that most of the variability in outbreak dynamics comes from the critical phase which is more variable when λ is small. For example, when $\lambda = 0.01$ it takes anywhere from three to 25 days for an infection to initiate an outbreak while for $\lambda = 0.03$, all outbreaks have begun by around Day 10. These observations provide further insights into our two earlier conjectures:

1. (*Peak day vs. total length*): If we consider the discrete time logistic equation

$$x_{n+1} = \beta x_n(1 - x_n) - x_n/\gamma,$$

then we believe that during the apocalyptic phase on an outbreak, the fraction of individuals who have been infected by day n will be close to x_n for an appropriate value of β which depends on λ and the degree distribution r_k. It is easy to verify that the difference $x_{n+1} - x_n$ is maximized when x_n reaches half of its limiting value $x_\infty = 1 - (\gamma + 1)/(\gamma\beta)$. This explains why the peak day is half the total length of the outbreak.

2. (*Dependence of length on* λ): For small λ, there will be a slower mean growth rate during the critical phase (the supercritical branching process which governs the dynamics here will have a mean growth rate which is a decreasing function of λ) followed by slower logistic growth rate during the apocalyptic phase (β will be a decreasing function of λ).

Providing specific formulas for the logistic parameter β and the offspring distribution for the super-critical branching process in terms of λ would be an interesting project for future work.

Vaccinations

In the final stage of our investigations, we look at the impact of vaccinations on the dynamics of a potential outbreak. We define a vaccination strategy for a potential out-

break as the removal of some subset of vertices from a randomly generated connectivity network. As such, a vaccination strategy could also refer to quarantines or shelter in place protocols. We compare the impact of two classes of specific strategies.

Random vaccinations. The vertices are chosen uniformly at random from all possible subsets of $V = \lfloor v \times N \rfloor$ vertices for some parameter $v \in (0, 1)$.

Targeted vaccinations. The vertices are chosen at random from all possible subsets of $V = \lfloor v \times N \rfloor$ vertices for some parameter $v \in (0, 1)$, but vertices are weighted by their number of connections. In other words, we sample V vertices without replacement and at each step, choose vertex i with weight proportional to $d_i =$ the degree of vertex i.

The comparison of these two vaccination strategies is not so much about which strategy is better (clearly, targeting more highly connected individuals will do more to slow down and reduce the severity of an outbreak), but how much better targeted strategies are compared to random vaccinations. If the benefit of targeted vaccinations is small compared to the cost of finding and targeting highly connected students, then the costs would outweigh the benefits and universities can shift resources away from such strategies.

We use two different values for v: $1/4$, which is based on numbers given by Pacific's Cowell Wellness center on the number of available vaccinations, and $1/3$ which is taken from our survey data as the estimated fraction of individuals who said they received a vaccination last year. Figures 6 and 7 illustrate the resulting outbreaks and Table 2 summarizes the disease statistics. Note that the targeted strategies drastically decrease the severity of the outbreak. For example, with $v = 1/3$, the targeted strategy decreased the total fraction of infected individuals from almost 90% to around 30% while the random strategy still left more than half the population infected.

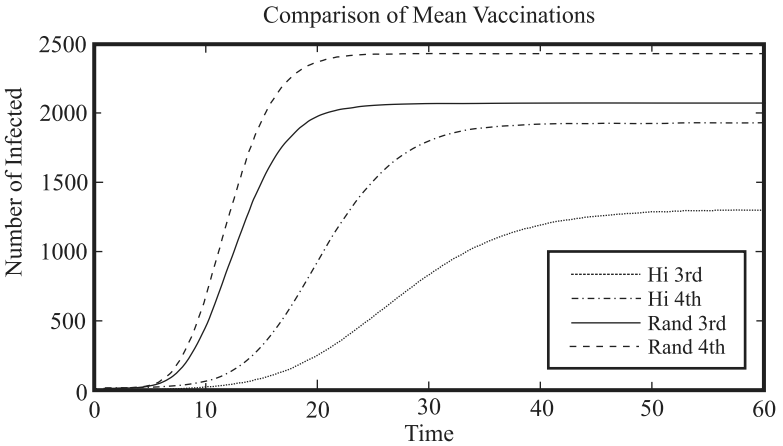

Figure 6 A comparison of the mean number of infected individuals as a function of n for each vaccination strategy.

Conclusions and limitations

Dynamic random graphs present greater flexibility in modeling small population outbreaks than their differential equation based cousins. They can be tailored to fit real world connectivity networks and allow for variability in interaction rates amongst

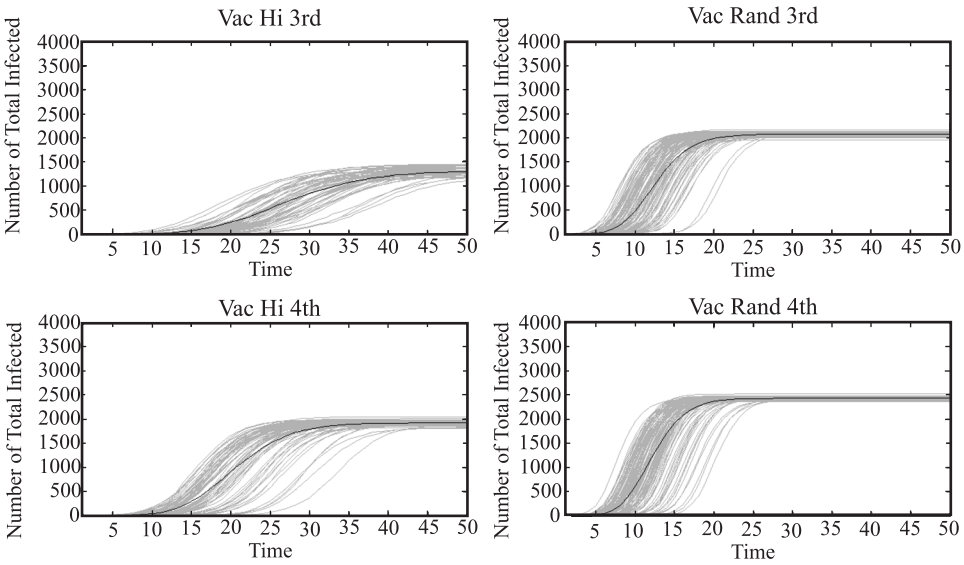

Figure 7 A comparison of number of infected individuals vs. time (days) for the four vaccination strategies discussed in the text (*top left*: hi third; *top right*: random third, *bottom left*: hi fourth; *bottom right*: random fourth

students. Here we have used Monte Carlo simulations to compare epidemics with different transmission rates as well as to explore the impact of various vaccination strategies. While the results of these investigations may be interesting, there are numerous unrealistic assumptions and limitations to our models which limit the scope of their applications.

First, we would like to point out that our models make the unrealistic assumption of a completely closed college environment. To incorporate external contacts, we could assume that each student in the network has a daily probability

$$1 - (1 - \lambda \times f_E)^{\mu_E} \approx \lambda \times f_E \times \mu_E$$

of contracting the disease from an outside source, where μ_E is the average number of external contacts for students at the university and f_E is the fraction of infected individuals outside the university. This would imply that an average of $N \times \lambda \times f_E \times \mu_E$ infections are added to the network each day and each one initiates a new potential outbreak. One interesting question for future investigations is whether most epidemics result from a single external infection that initiated a large scale outbreak, a large number of external infections which initiated potential outbreaks, or a few external infections which initiated small outbreaks.

A second limitation is our static assumption about the student connectivity network. Although a different network was randomly generated at the start of each simulation, it remained fixed throughout the remainder of the potential outbreak. Previous studies have shown that information induced behavioral responses such as increased hand washing, mask wearing, and social distancing can drastically alter the scope of an outbreak ([**23**], [**24**], [**25**]). Such changes could be incorporated in future work by allowing the student connectivity network to change from day to day or lowering the transmissibility as a simulation progresses. A second unrealistic assumption of our models is the use of a constant infection duration. Several recent studies related to the novel COVID-19 virus have demonstrated that the incubation time, defined as the amount of time between when an individual is first exposed to a virus and when they start

showing symptoms, can vary dramatically between individuals according to a Weibull, Gamma, or Lognormal distribution ([**4**], [**17**]). Incorporating such random incubation times into our models would further increase the variability of disease statistics and provide additional insights into disease dynamics on a college campus.

REFERENCES

[1] Abbey, H. (1952). An examination of the Reed-Frost theory of epidemics. *Hum. Biol.* 24(3): 201. PMID: 12990130

[2] Andersson, H. (1998). Limit theorems for a random graph epidemic model. *Ann. Appl. Probab.* 8(4): 1331–1349. doi.org/10.1214/aoap/1028903384

[3] Austin, T. L., Fagen, R. E., Penney, W. F., Riordan, J. (1959). The number of components in random linear graphs. *Ann. Math. Stat.* 30(3): 747–754. doi.org/10.1214/aoms/1177706204

[4] Backer, J. A., Klinkenberg, D., Wallinga, J. (2020). Incubation period of 2019 novel coronavirus (2019-nCoV) infections among travellers from Wuhan, China, 20–28 January 2020. *Eurosurveillance.* 25(5): 2000062. doi.org/10.2807/1560-7917.ES.2020.25.5.2000062

[5] Barabási, A. L., Albert, R. (1999). Emergence of scaling in random networks. *Science.* 286(5439): 509–512. doi.org/10.1126/science.286.5439.509

[6] Barabási, A. L., Albert, R., Jeong, H. (2000). Scale-free characteristics of random networks: The topology of the world-wide web. *Phys. A*. 281(1–4): 69–77. doi.org/10.1016/S0378-4371(00)00018-2

[7] Bernoulli, D. (1760). Essai d'une nouvelle analyse de la mortalité causée par la petite vérole, et des avantages de l'inoculation pour la prévenir. *Hist. Acad. R. Sci. (Paris) avec Mem*. 1–45.

[8] Bernoulli, D., Blower, S. (2004). An attempt at a new analysis of the mortality caused by smallpox and of the advantages of inoculation to prevent it. *Rev. Med. Virol.* 14(5): 275. doi.org/10.1002/rmv.443

[9] Box, G. E. (1976). Science and statistics. *J. Amer. Statist. Assoc*. 71(356): 791–799. doi.org/10.1080/01621459.1976.10480949

[10] Brauer, F., Castillo-Chavez, C., Castillo-Chavez, C. (2012). *Mathematical Models in Population Biology and Epidemiology*, Vol. 2. New York: Springer.

[11] Carrat, F., Vergu, E., Ferguson, N. M., Lemaitre, M., Cauchemez, S., Leach, S., Valleron, A. J. (2008). Time lines of infection and disease in human influenza: A review of volunteer challenge studies. *Amer. J. Epidemiol.* 167(7): 775–785. doi.org/10.1093/aje/kwm375

[12] Durrett, R. (2008). *Probability Models for DNA Sequence Evolution*. New York: Springer Science and Business Media.

[13] Durrett, R. (2007). *Random Graph Dynamics*. Cambridge: Cambridge University Press.

[14] Erdős, P., Rényi, A. (1960). On the evolution of random graphs. *Publ. Math. Inst. Hung. Acad. Sci.* 5(1): 17–60.

[15] Gilbert, E. N. (1959). Random graphs. *Ann. Math. Stat.* 30(4): 1141–1144. doi.org/10.1214/atoms/1177706098

[16] Irwin, J. O. (1975). The generalized Waring distribution. Part I. *J. R. Stat. Soc. Ser. A Gen.* 138(1): 18–31. doi.org/10.2307/2345247

[17] Lauer, S. A., Grantz, K. H., Bi, Q., Jones, F. K., Zheng, Q., Meredith, H. R., Azman, A. S., Reich, N. G., Lessler, J. (2020). The incubation period of coronavirus disease 2019 (COVID-19) from publicly reported confirmed cases: Estimation and application. *Ann. Intern. Med.* doi.org/10.7326/M20-0504

[18] Longini Jr, I. M., Koopman, J. S., Monto, A. S., Fox, J. P. (1982). Estimating household and community transmission parameters for influenza. *Amer. J. Epidemiol.* 115(5): 736–751. doi.org/10.1093/oxfordjournals.aje.a113356

[19] Molloy, M., Reed, B. (1995). A critical point for random graphs with a given degree sequence. *Random Structures Algorithms.* 6(2–3): 161–180. doi.org/10.1002/rsa.3240060204

[20] Newman, M. E. (2002). Spread of epidemic disease on networks. *Phys. Rev. E.* 66(1): 016128. doi.org/10.1103/PhysRevE.66.016128

[21] Watts, D. J., Strogatz, S. H. (1998). Collective dynamics of "small-world" networks. *Nature*. 393(6684): 440. doi.org/10.1038/30918

[22] Newman, M. (2018). *Networks.* Oxford: Oxford University Press.

[23] Shang, Y. (2013). Discrete-time epidemic dynamics with awareness in random networks. *Int. J. Biomath.* 6(2): 1350007. doi.org/10.1142/S1793524513500071

[24] Shang, Y. (2013). Modeling epidemic spread with awareness and heterogeneous transmission rates in networks. *J. Biol. Phys.* 39(3): 489–500. doi.org/10.1007/s10867-013-9318-8

[25] Shang, Y. (2015). Degree distribution dynamics for disease spreading with individual awareness. *J. Syst. Sci. Complexity*. 28(1): 96–104. doi.org/10.1007/s11424-014-2186-x

[26] Watts, D. J. (2004). *Six Degrees: The Science of a Connected Age*. New York: W. W. Norton and Company.

Summary. We provide a brief introduction to a class of flexible random graph SIR models that allow for a random number of connections per student and are relatively easy to simulate. We present an application of these individual-based models to study a seasonal outbreak of influenza at our home institution. Using data obtained from a survey of students, we find that the right skewed beta negative binomial distribution provides a good fit to the degree distribution of student contacts with a mean of about 25 contacts per student. With no vaccinations or change in student behavior, our model predicts that a highly contagious influenza virus would spread to about 90% of the student body while even a less virulent strain would infect about one-half of the population. Our investigations conclude with an exploration of targeted vs random vaccination strategies. Individual based random graphs models not only provide exciting opportunities for undergraduate research, but provide insights into the structure of epidemics on college campuses.

JOHN MAYBERRY is an associate professor of mathematics at the University of the Pacific. He currently lives in Stockton, CA with his wife and their three kids. He received his B.A. in Mathematics from California State University, Fullerton in 2003 and his Ph.D. from the University of Southern California in 2008. Prior to joining the math department at Pacific, he spent two years at Cornell University as a postdoc under an NSF Research and Training Grant. His research interests include mathematical biology, applied probability, statistics, and sports analytics. Highlights of his time at Pacific include collaborating with the school's water polo team to analyze game data, teaching a first year seminar class called "Punk, Metal, and the Meaning of Life," and advising the Pacific math club. He spends his spare time biking or hiking with his family, reading science fiction, cooking, and listening to music.

MARIA NATTESTAD (ORCID: 0000-0002-4796-2894) graduated from the University of the Pacific in 2013 with a B.S. in Biology. She went on to complete her Ph.D. in Bioinformatics at Cold Spring Harbor Laboratory in 2017 and founded her own data visualization software company OMGenomics. She currently works for Google as a software engineer on the Genomics Team in Google Health.

AUSTIN TUTTLE (ORCID: 0000-0001-6629-8506) graduated from the University of the Pacific in 2014 with a double major in Applied Mathematics and Physics. He went on to complete his Ph.D. at the University of Minnesota in 2019 where he specialized in numerical analysis, partial differential equations and mathematical biology. His dissertation focused on mathematical models for spreading depression and seizures. He currently works as a software developer for Open Systems International. He lives in Minneapolis where he enjoys biking the lakes and eating good food with his fiance.

Flappy Bird in Space: An Impulse Minimization Problem

THOMAS J. CLARK
Dordt University
Sioux Center, IA 51250
Tom.Clark@dordt.edu

ANIL VENKATESH
Adelphi University
Garden City, NY 11530
avenkatesh@adelphi.edu

In 2013, the mobile game *Flappy Bird* was released and quickly became a sensation. In this game, the player navigates a cartoon bird through an obstacle course by repeatedly applying upward boosts against gravity. What does *Flappy Bird* have to do with orbital mechanics? While spaceflight is complicated by the Tsiolkovsky rocket equation and moving gravitational sources, its core question is the same as *Flappy Bird*'s: can we find a pattern of acceleration that results in a given desired trajectory?

We use a variant of *Flappy Bird* with continuous acceleration as a model to study orbital mechanics. Specifically, we aim to demonstrate how the objective of fuel conservation affects optimal flight paths. With elementary calculus and numerical methods, we use our model to reproduce the concentration of impulse observed in orbital maneuvers such as the powered slingshot. Along the way, we present several new constructions of spline minimizers for interpolation problems in norms other than $\mathcal{L}^2$.

Introduction

It's hard to change direction in space! Unlike its depiction in popular science fiction, spaceflight is much more about gravity than rockets. One of the main reasons for this is laid out by the Tsiolkovsky rocket equation, which states that the amount of fuel required for a maneuver is exponential in the desired change in velocity. Put another way, changing velocity is expensive and adding extra fuel to your ship will barely increase its maneuvering capacity.

The rocket equation implies that orbital maneuvers are only efficient when a relatively small change in velocity is required, since this value governs the amount of fuel needed for the maneuver. More technically, the quantity to minimize is delta-v, the time-integral of thrust per mass in (1).

$$\Delta v = \int_{t_0}^{t_1} \frac{|T(t)|}{m(t)}\, dt \tag{1}$$

Integrating force with respect to time results in impulse, a measurement of the change in momentum. Consequently, delta-v measures the impulse per mass of an orbital maneuver, roughly describing the change in velocity. Depending on the geometry of the initial and desired orbits, the Hohmann transfer, bi-elliptic transfer, and powered slingshot are all strategies for changing trajectory with minimal delta-v. They are characterized by brief, intense fuel burns at optimal moments, with long periods of coasting in between [**2**].

Math. Mag. **94** (2021) 99–112. doi:10.1080/0025570X.2021.1886807
MSC: 00A69, 49-04, 65D07

The 2013 mobile game *Flappy Bird* also revolves around the concept of delta-v. In *Flappy Bird*, the player navigates a cartoon bird through an obstacle course by applying a series of upward impulses to the bird. Between impulses, the bird experiences freefall. While *Flappy Bird* is much simpler than orbit transfer for spacecraft, the two scenarios have a common objective: can we find a pattern of acceleration that results in a given desired trajectory?

We study the mathematics underlying such maneuvers as the powered slingshot, in which a spacecraft applies a brief fuel burn while on close approach to a celestial object in order to alter its trajectory. If it were possible for the spacecraft to condense the entire fuel burn into a single instant, this would achieve the lowest delta-v and the highest fuel economy, but doing so would require infinite instantaneous acceleration. Why do brief, intense fuel burns result in greater fuel economy than slow, gradual changes to trajectory? The mathematics behind this question are complicated in multiple ways: parametric curves in $\mathbb{R}^3$, differential equations, and moving gravitational sources. If we pare away all complexity except the concept of delta-v, is there still an interesting problem to understand?

Motivated by this question, we wrote down a simple model for orbital mechanics with inspiration from *Flappy Bird*. We assume constant mass and constant horizontal velocity, but allow continuous upward and downward acceleration (and we dispense with gravity since downward acceleration is enabled). In our model, which we term "continuous *Flappy Bird*," the goal is to find a path through the obstacle course with minimum delta-v, as opposed to solving the original game for its own sake as demonstrated in [4]. We got excited about this model when we noticed that an impulse-minimizing path would involve a famous integral, the $\mathcal{L}^1$ norm of the second derivative. Equation (2) displays this integral, where $f(t)$ is the vertical position at time t. Since we use constant horizontal velocity in our model, we can identify t with x going forward.

$$\Delta v = \int_{t_0}^{t_1} |f''(t)|\, dt \tag{2}$$

The integral in (2) has an even more famous sibling: the $\mathcal{L}^2$ norm. In general, finding a function that minimizes a certain norm is a problem in the calculus of variations. Consider a function $y = f(x)$ that passes through a given set of points $\{(x_i, y_i)\}_{i=0}^n$. This function is called an *interpolant*. In the $\mathcal{L}^2$ case, we look for an interpolant that minimizes the integral $\int_{x_0}^{x_n} |f''(x)|^2\, dx$. The solution to this problem is a function that is built piecewise from cubic polynomial segments [5]. Such piecewise solutions to interpolation problems are called splines, and they are an important tool in numerical analysis and approximation theory due mainly to their utility in applications. In addition to their use in interpolation, they have applications in computer assisted design, fonts, and solutions to control problems [6].

Interpolants that minimize acceleration in other norms are not as well known [1]. This is in part because the proof in $\mathcal{L}^2$ employs a clever algebraic technique that does not generalize to other norms. Without this trick, it's not even clear that an optimal solution exists, much less how to obtain an explicit formula for a hypothetical solution. Our quest to solve continuous *Flappy Bird* took us on a journey through the $\mathcal{L}^1$ and $\mathcal{L}^\infty$ norms, and finally arrived at a sort of compromise between them. In each case, we were able to conjecture an explicit formula for a most efficient path and then prove, using elementary calculus techniques, that our conjecture was right. This usually does not happen in the calculus of variations [3]!

In the next section, we use elementary methods to solve the impulse-minimizing interpolation problem. Our results led us to examine a different variant of the problem

in the section "Minimizer of Maximum Acceleration": navigating an obstacle course with minimum fixed-magnitude acceleration throughout. This equates to minimizing the acceleration in $\mathcal{L}^\infty$, that is, minimizing $\max_{[x_0,x_n]} |f''(x)|$. In the section "Capped $\mathcal{L}^1$ Minimizer," we bring the results of the previous two sections together to study impulse-minimization subject to a cap on instantaneous acceleration.

Minimizer of total impulse

We got a surprise when we solved the $\mathcal{L}^1$ norm interpolation problem: the solution was *Flappy Bird*! It turns out that the best strategy for minimizing delta-v is to concentrate the acceleration into "boosts" and coast in between. This is just like an idealized powered slingshot, with instantaneous impulses concentrated at certain points and coasting in between them.

A continuous function f that interpolates the points $\{(x_i, y_i)\}_{i=0}^n$ and also minimizes $\int_{x_0}^{x_n} |f''(x)|\,dx$ has the physical interpretation of minimizing the total acceleration needed to navigate the set of points. Given the constant horizontal velocity of this formulation of the problem, this integral also represents the total impulse (change in momentum) necessary to interpolate the points. We show in this section that there is no $\mathcal{C}^2$ or even $\mathcal{C}^1$ solution to this problem. The critical insight here is to concentrate all the acceleration into as short an amount of time as possible. Pushing that to the limit creates a piecewise linear interpolation of the points. In this case f'' exists not as a function, but as a set of instantaneous infinite accelerations at the points (x_i, y_i). We refer to these accelerations as *Dirac impulses* in reference to the concept of Dirac delta function, a generalized function that models the density of a point mass (that is, zero density everywhere except for the location of the mass, at which the density is infinite). In the case of f'', we describe each instantaneous acceleration by a Dirac impulse with magnitude equal to the amount by which the velocity needs to change to reach the next point. While this continuous interpolant is not in $\mathcal{C}^2$, it is the limit of a $\mathcal{C}^2$ solution this is constructed from linear and cubic polynomials, stitched together to maintain continuity and differentiability.

For example on the set of points $\{(0, 0), (1, 1), (2, 0)\}$, for each $0 < h < 1$, the function

$$f(x) = \frac{3}{3-h}\begin{cases} x & 0 \le x \le 1-h \\ \frac{-1}{3h^2}(x-(1-h))^3 + x & 1-h \le x \le 1 \\ \frac{1}{3h^2}(x-1)^3 - \frac{1}{h}(x-1)^2 + 1 - \frac{h}{3} & 1 \le x \le 1+h \\ -x+2 & 1+h \le x \le 2 \end{cases}$$

is a $\mathcal{C}^2$ function that interpolates the given points. See Figure 1. Moreover, by symmetry

$$\int_0^2 |f''(x)|\,dx = 2\int_0^1 |f''(x)|\,dx = 2|f'(1) - f'(0)| = 2f'(0) = 2 \cdot \frac{3}{3-h}.$$

As $h \to 0$, the integral approaches 2, which is the magnitude of the difference in the velocities 1 and -1. A similar construction can be done in general. There is no $\mathcal{C}^2$ minimizer to the minimum total acceleration problem, but a clear candidate for the "appropriate" minimizer is evident and it can be approximated by $\mathcal{C}^2$ functions as closely as desired. More generally, if f is the piecewise linear interpolation of $\{(x_i, y_i)\}_{i=0}^n$, then f'' as a set of $n-2$ Dirac impulses at the interior points. Defining the slopes

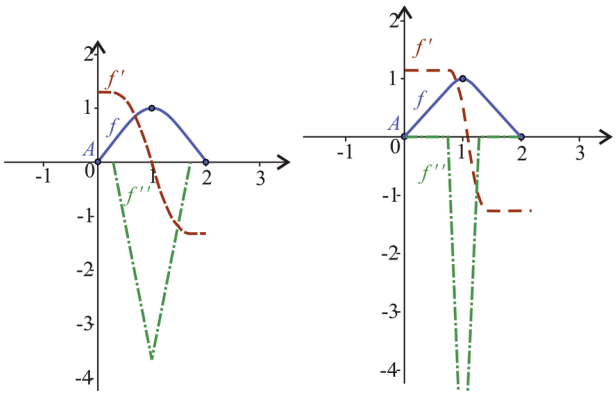

Figure 1 This figure displays $\mathcal{C}^2$ interpolants of $\{(0, 0), (1, 1), (2, 0)\}$.

as $m_i = \dfrac{y_i - y_{i-1}}{x_i - x_{i-1}}$ for $1 \le i \le n$, the required magnitudes of the impulses are equal to $|m_{i+1} - m_i|$. We can think of the total $\mathcal{L}^1$ norm of f'' as $\sum_{i=1}^{n-1} |m_{i+1} - m_i|$, and this would be achieved in the limit from an appropriately constructed $\mathcal{C}^2$ function built from cubics as above.

If the set of points are all collinear then a linear interpolation is smooth and also requires no acceleration. In the interesting case where the points are not collinear we have the following:

Proposition 1 (Piecewise linear is "optimal")**.** *For a set of noncollinear points* $\{(x_i, y_i)\}_{i=0}^n$ *and any interpolant* $f \in \mathcal{C}^2$*, if* $m_i = \dfrac{y_i - y_{i-1}}{x_i - x_{i-1}}$ *then*

$$\int_{x_0}^{x_n} |f''(x)|\, dx > \sum_{i=1}^{n-1} |m_{i+1} - m_i| \tag{3}$$

Proof. Let a set of points $\{(x_i, y_i)\}_{i=0}^n$ be given with slopes $m_i = \dfrac{y_i - y_{i-1}}{x_i - x_{i-1}}$ for $1 \le i \le n$. Let $f \in \mathcal{C}^2$ interpolate $\{(x_i, y_i)\}_{i=0}^n$. By the mean value theorem, there exists $c_i \in (x_{i-1}, x_i)$ such that $f'(c_i) = m_i$. We then have:

$$\begin{aligned}
\int_{x_0}^{x_n} |f''(x)|\, dx &\ge \int_{c_1}^{c_n} |f''(x)|\, dx \\
&= \sum_{i=1}^{n-1} \int_{c_i}^{c_{i+1}} |f''(x)|\, dx \\
&\ge \sum_{i=1}^{n-1} \left| \int_{c_i}^{c_{i+1}} f''(x)\, dx \right| \\
&= \sum_{i=1}^{n-1} |f'(c_{i+1}) - f'(c_i)| = \sum_{i=1}^{n-1} |m_{i+1} - m_i|.
\end{aligned}$$

This inequality shows that the $\mathcal{L}^1$ norm of any $\mathcal{C}^2$ interpolant is at least as great as $\sum_{i=1}^{n-1} |m_{i+1} - m_i|$, the sum of the Dirac impulse magnitudes of the piecewise linear interpolant. This implies that a $\mathcal{C}^2$ interpolant cannot improve on the piecewise linear

interpolant. In the case that the points are collinear, the problem is trivial and equality holds. To show the inequality in (3) can be made strict, assume without loss of generality that $\{(x_i, y_i)\}_{i=0}^{2}$ are noncollinear. Since $x_0 < c_1 < x_1$ either

$$\int_{x_0}^{c_1} |f''(x)|dx > 0$$

and the inequality in (3) becomes strict, or f is linear on $[x_0, c_1]$. If f is linear up to c_1, let $c_{1^*} = \sup\{c \mid f''(x) = 0 \text{ on } [x_0, c]\}$. Then if $c_{1^*} < x_1$, the mean value theorem can be reapplied to $\{(c_{1^*}, f(c_{1^*}), (x_1, y_1)\}$ to find $c_{1'}$ with $f'(c_{1'}) = m_1$ and $c_{1^*} < c_{1'} < x_1$ (since the linearity on the first portion means the average rate of change remains the same). The lack of linearity implies that

$$\int_{c_{1^*}}^{c_{1'}} |f''(x)|dx > 0,$$

establishing the strictness of the inequality. If, on the other hand, $c_{1^*} = x_1$, we repeat the procedure on $[x_1, x_2]$. The same conclusion is reached, except that f cannot be linear on both segments because it is a $\mathcal{C}^2$ function and the points are not collinear. ■

As we sketched above, it is possible to get as close as desired with a $\mathcal{C}^2$ function, but the optimal solution is not physically achievable. Nonetheless, the concept of instantaneous impulse is commonly used in video games such as *Flappy Bird*.

Minimizer of maximum acceleration

The impulse-minimizing interpolant of the previous section requires Dirac impulses to change velocity instantaneously. This behavior cannot be realized physically, although video games like Flappy Bird make extensive use of it. To extend the analysis to physical interpolation problems, we now turn our attention to impulse-minimizing paths that are subject to a physical cap on acceleration magnitude.

Before we can analyze this new problem, we first note that some nonzero acceleration is necessary to interpolate any collection of noncollinear points. For a given point set, we must first determine the minimum magnitude acceleration necessary for any successful interpolation, and only then return to the question of impulse minimization. Without this consideration, we would be unable to say whether the problem was well posed for a given acceleration cap.

The question of minimizing $\max_{x\in[x_0,x_n]} |f''(x)|$ amounts to minimizing the $\mathcal{L}^\infty$ norm of f''. In this section, we reprise the previous work with respect to this new norm. The result is a strategy that uses the least magnitude acceleration required for interpolation. This analysis will be a stepping stone in the following section, as the acceleration value obtained in this way is used to determine whether a given impulse-minimization problem has a solution. However, the $\mathcal{L}^\infty$ solution to the interpolation problem has its own applications to spaceflight as well, as long as a little suspension of disbelief is indulged. The popular sci-fi television series *The Expanse* explores the fictional conceit of a non-reactive rocket engine: instead of expelling fuel to generate thrust, the engines in the story are capable of generating a fixed level of thrust indefinitely. While our primary goal for studying the $\mathcal{L}^\infty$ norm is to marry thrust limitations with the foregoing analysis of delta-v, we remark that this section coincidentally solves the interpolation problem for spaceflight in *The Expanse*.

For the $\mathcal{L}^1$ problem, the key idea was to concentrate all the acceleration at each point and coast in between them. In this section, since we wish to minimize pointwise

acceleration, the key will be to spread out the required acceleration as uniformly over the interval as possible. In view of this, an obvious candidate to try is to construct a solution from piecewise quadratic functions since they have constant acceleration on each subinterval. However, such a spline is generally not $\mathcal{C}^2$. In this section, we extend the definition of the $\mathcal{L}^\infty$ norm of f'' to functions with absolutely continuous first derivative. This extension allows us to state meaningfully that a certain piecewise quadratic interpolant minimizes the $\mathcal{L}^\infty$ norm of second derivative over all $\mathcal{C}^2$ functions. We begin by establishing some basic results in the $\mathcal{L}^\infty$ norm.

Proposition 2 (Quadratic interpolant is locally optimal)**.** *Let $f(x)$ represent the unique quadratic interpolant of the ordered set of points (x_0, y_0), (x_1, y_1), (x_2, y_2). If $g \in \mathcal{C}^2$ interpolates the points and satisfies $|g''(x)| \leq |f''(x)|$ for all $x \in [x_0, x_2]$, then $g(x) = f(x)$.*

Proof. Let $f(x)$ represent the unique quadratic interpolant of the ordered set of points (x_0, y_0), (x_1, y_1), (x_2, y_2), and let $g(x)$ be a $\mathcal{C}^2$ interpolant satisfying $|g''(x)| \leq |f''(x)|$. Let $c = f''(x)$, a constant since f is quadratic. Without loss of generality, suppose $c > 0$. The hypothesis that $|g''(x)| \leq c$ induces the following conditions on g':

$$g'(x) \geq g'(x_2) + c(x - x_2) \tag{4}$$

$$g'(x) \leq g'(x_0) + c(x - x_0) \tag{5}$$

Since $g''(x) \leq f''(x)$, we have that $g'(x) \geq f'(x)$ on $[x_0, x_1]$ and $g'(x) \leq f'(x)$ on $[x_1, x_2]$. If $g'(x_1) > f'(x_1)$, g obtains more displacement on $[x_0, x_1]$ than f. By symmetry, $g'(x_1) < f'(x_1)$ is impossible as g would obtain less displacement on $[x_1, x_2]$ than f. Neither case can occur since both f and g are interpolants. We conclude that $g'(x_1) = f'(x_1)$. In order for the functions to obtain the same displacement, further conclude that $g'(x) = f'(x)$ on the entire domain. Consequently, the functions are equal. ■

Construction of $\mathcal{L}^\infty$ spline minimizer for two points and two slopes Let $(x_0, y_0; m_0)$ and $(x_1, y_1; m_1)$ represent a pair of points in $\mathbb{R}^2$ together with slopes m_0 and m_1, respectively. For certain values of these parameters, a quadratic interpolant between the points coincidentally satisfies both slope conditions. However, this does not occur in general. Except when a single quadratic interpolant is obtained, there exists a $\mathcal{C}^1$ piecewise quadratic interpolant of two segments. We construct such an interpolant and demonstrate that every $\mathcal{C}^2$ interpolant has $\mathcal{L}^\infty$ norm of the second derivative at least as great as that of either of the parabolic segments of the piecewise solution. Consequently, we prove by construction the existence of a $\mathcal{C}^1$ solution to the $\mathcal{L}^\infty$ spline minimizer problem.

Construction of piecewise interpolant For any interpolant $f(x)$ of the given data, it must hold that $f'(x)$ interpolates between (x_0, m_0) and (x_1, m_1). We will consider solutions for $f'(x)$ of the form

$$f'(x) = \begin{cases} k(x - x_0) + m_0 & x_0 \leq x < x^* \\ -k(x - x_1) + m_1 & x^* \leq x \leq x_1 \end{cases} \tag{6}$$

where x^* denotes the unique value in $[x_0, x_1]$ that makes this function continuous. Note that $f'(x)$ can also be expressed as a shifted and scaled absolute value function with slopes k and $-k$. Note also that $|k| \geq \left|\frac{m_1 - m_0}{x_1 - x_0}\right|$ must hold in order for $f'(x)$ to be continuous. We first solve for x^* in terms of k.

$$k(x^* - x_0) + m_0 = -k(x^* - x_1) + m_1$$

$$2kx^* = (m_1 - m_0) + k(x_1 + x_0)$$

$$x^* = \frac{m_1 - m_0}{2k} + \frac{x_1 + x_0}{2}$$

Not all values of k give rise to a function $f(x)$ that interpolates between (x_0, y_0) and (x_1, y_1). For this property to hold, we impose the following condition on $f'(x)$.

$$y_1 - y_0 = \int_{x_0}^{x_1} f'(x)\, dx \tag{7}$$

Equation (7) imposes a condition on k as follows.

$$y_1 - y_0 = \frac{(m_1 - m_0)^2}{4k} + \frac{k(x_1 - x_0)^2}{4} + m_0\left(\frac{m_1 - m_0}{2k} + \frac{x_1 - x_0}{2}\right) - m_1\left(\frac{m_1 - m_0}{2k} - \frac{x_1 - x_0}{2}\right) \tag{8}$$

Equation (9) is quadratic in k with at least one solution satisfying the condition $x_0 \leq x^* \leq x_1$. This can be proven by observing that $\int_{x_0}^{x_1} f'(x)\, dx$ is continuous in k and that the value of this integral ranges both below and above $y_1 - y_0$ as k varies. Multiplying by $4k$ and rearranging the terms leads to:

$$0 = (x_1 - x_0)^2 k^2 + k\,(2(x_1 - x_0)(m_1 + m_0) - 4(y_1 - y_0)) - (m_1 - m_0)^2 \tag{9}$$

Solving for k we find

$$k = \frac{-(x_1 - x_0)(m_1 + m_0) + 2(y_1 - y_0) \pm \sqrt{R}}{(x_1 - x_0)^2} \tag{10}$$

where we introduce the nonce notation

$$R = 2((x_1 - x_0)m_0 - (y_1 - y_0))^2 + 2((x_1 - x_0)m_1 - (y_1 - y_0))^2$$

for visual clarity. Note that k is well-defined since $x_1 > x_0$ by assumption.

For clarity, if we define $a := x_1 - x_0$, $b = y_1 - y_0$, $x = m_0$ and $y = m_1$ then (10) can be written as

$$k = \frac{-(ax - b) - (ay - b) \pm \sqrt{2(ax - b)^2 + 2(ay - b)^2}}{a^2} \tag{11}$$

In the case where

$$m_0 = m_1 = \frac{y_1 - y_0}{x_1 - x_0}$$

we get $k = 0$ which corresponds to the special case where a line through (x_0, y_0) and (x_1, y_1) satisfies the conditions.

In the case where $(x_1 - x_0)m_0 - (y_1 - y_0)$ and $(x_1 - x_0)m_1 - (y_1 - y_0)$ are equal in absolute value, but of opposite sign, the values of k are also equal in absolute value, but of opposite sign. In this case, a parabola satisfies the conditions and this parabola is given by (6) where for one value of k, $x^* = x_0$ and for the other we have $x^* = x_1$.

In any other case, there are always exactly two values for k, one of which is non-negative and one of which is non-positive (since $|X + Y| \leq \sqrt{2X^2 + 2Y^2}$ for any values of X and Y). For only one of these values of k will the value of x^* lie between x_0 and x_1.

Theorem 1. *Given* $(x_0, y_0; m_0)$ *and* $(x_1, y_1; m_1)$*, let* k *be the smallest-magnitude solution of* (10) *and let* f *be the unique interpolant constructed according to* (6)*. There is no* $\mathcal{C}^2$ *interpolant* g *that satisfies* $\max|g''(x)| < |k|$.

Proof of Theorem 1. Suppose $k > 0$, $g(x)$ is a $\mathcal{C}^2$ interpolant of $(x_0, y_0; m_0)$, and $(x_1, y_1; m_1)$ with $\max|g''(x)| \leq k$.

By construction,

$$f'(x) = k(x - x_0) + m_0$$

on the interval $[x_0, x^*]$. Since $f''(x) = k$ and $|g''(x)| \leq k$, it holds that $g'(x) \leq f'(x)$ on the interval $[x_0, x^*]$. For all x in $[x^*, x_1]$, it holds that

$$g'(x_1) - g'(x) \geq -k(x_1 - x) = f'(x_1) - f'(x).$$

Since $f'(x_1) = g'(x_1)$, we obtain $f'(x) - g'(x) \geq 0$. This proves that $g'(x) \leq f'(x)$ on the interval $[x_0, x_1]$.

Taking integrals, we find that $g(x_1) = f(x_1)$ only if $g'(x) = f'(x)$ on the entire domain of integration. Taking $k < 0$ leads to the same result. This implies that $g = f$ and thus $\max|g''(x)| = k$. ∎

Corollary 1. *Changing the hypothesis of Theorem 1 to* $k < 0$ *results in* $g'(x) > f'(x)$ *on the interval* $[x_0, x_1]$*. Consequently, the condition* $|g''(x)| < k$ *implies that* $|g'(x)| \leq |f'(x)|$ *on the interval* $[x_0, x_1]$.

Corollary 2. *If the function* f *in Theorem 1 is not* $\mathcal{C}^2$*, then*

$$\max|f''(x)| < \max|g''(x)|$$

for any $\mathcal{C}^2$ *interpolant* g.

Construction of convex program for $\mathcal{L}^\infty$ spline minimizer The previous work establishes the existence of a particular piecewise quadratic spline interpolant. Now we demonstrate uniqueness. We also show that the magnitude of the acceleration is a convex function of the slopes m_0 and m_1. These provisions are sufficient for constructing a convex program on the slopes $m_0, \ldots, m_n$ that minimizes the magnitude of the acceleration of the spline.

The acceleration equation is quadratic in the slopes m_0 and m_1, giving rise to a pair of solutions k^+ and k^-. We first show that $k^+ \geq 0$ and $k^- \leq 0$ for all values of m_0 and m_1. For any nonzero k, let

$$x^* = \frac{m_1 - m_0}{2k} + \frac{x_1 + x_0}{2},$$

as in the previous section. Taking integrals, we compute the total displacement of the spline on $[x_0, x_1]$ as follows:

$$\int_{x_0}^{x^*} (k(x - x_0) + m_0)\, dx + \int_{x^*}^{x_1} (-k(x - x_1) + m_1)\, dx$$
$$= \frac{k}{2}(x^* - x_0)^2 + \frac{k}{2}(x^* - x_1)^2 + m_0(x^* - x_0) - m_1(x^* - x_1).$$

Noting that x^* depends on k and then differentiating with respect to k, we obtain

$$\frac{1}{4k^2}(k^2(x_1 - x_0)^2 + (m_1 - m_0)^2)$$

which is strictly greater than zero since $x_1 > x_0$. Consequently, the displacement of the spline is monotonically increasing in k whenever $k \neq 0$. Given two nonzero values of k that achieve the same displacement, it follows that these solutions must have opposite signs. Since $k^+ \geq k^-$, it follows that $k^+ \geq 0$ and $k^- \leq 0$ in all cases.

Moreover, an acceleration value is not admissible if it gives rise to an x^* that does not lie in the interval $[x_0, x_1]$. We deduce that the admissible k values are bounded away from zero according to the condition

$$|k| \geq \frac{|y_1 - y_0|}{x_1 - x_0},$$

with equality obtained only in case a single quadratic arc that successfully interpolates with given slopes m_0 and m_1. Lastly, inspection of the definition of x^* confirms that exactly one of k^+ and k^- is admissible, and in particular that the unique admissible value of k is given by whichever of k^+ and k^- has greater magnitude. Note that $|k|$ is a convex function of m_0 and m_1 since (11) is essentially of the form $\sqrt{X^2 + Y^2}$ which can be seen to be convex by the second derivative convexity test. Since k^+ in (11) is convex in $x = m_0$ and $y = m_1$, and thus also is $-k^-$, the convexity of $|k|$, the quantity of interest, is established.

For a given interpolant of a set of points, the $\mathcal{L}^\infty$ norm of acceleration on each segment is a convex function of the initial and final tangent line slopes. By extension, the $\mathcal{L}^\infty$ norm of acceleration of the entire interpolant is the maximum of the accelerations of each segment and is a function of the tangent line slopes at each point in the set. Since the maximum of a finite set of convex functions is itself a convex function, the $\mathcal{L}^\infty$ norm of acceleration of any interpolant is a convex function of the interpolant's tangent line slopes at the points in the set. Given any set of points

$$(x_0, y_0), (x_1, y_1), \ldots, (x_n, y_n)$$

with monotonically increasing x-coordinates, we solve the convex program on the slope values $m_0, m_1, \ldots, m_n$ with objective function given by the maximum of the k-values for each segment of the interpolant. The solution is a $\mathcal{C}^1$ function with piecewise linear (hence absolutely continuous) first derivative, and has minimal $\mathcal{L}^\infty$ norm of acceleration among all functions in its class. Figure 2 shows an example of such a function and its derivative. Note that the derivative of the interpolant is continuous and piecewise linear.

Capped $\mathcal{L}^1$ minimizer

As discussed previously, the impulse-minimizing solution in the $\mathcal{L}^1$ sense is unsatisfying because it concentrates all acceleration into Dirac impulses. This led us to formulate a new problem: Given a set of points and a fixed maximum acceleration value, find an interpolant that minimizes total impulse subject to this maximum acceleration. In the context of continuous *Flappy Bird*, we want to navigate a set of points using minimum total impulse, but with a maximum level of thrust at our disposal. Again, we aim to minimize the $\mathcal{L}^1$ norm, $\int_{x_0}^{x_n} |f''(x)|dx$, but now under the additional condition that $|f''(x)|$ is capped by some finite bound. What is the optimal path in this case? When is it even possible to navigate a set of points?

We saw in the previous section that a given set of points determines an $\mathcal{L}^\infty$ norm, and we constructed an interpolant that achieves this norm. In the $\mathcal{L}^1$-cap problem, as long as the imposed cap is above the $\mathcal{L}^\infty$ norm, at least one interpolation must exist.

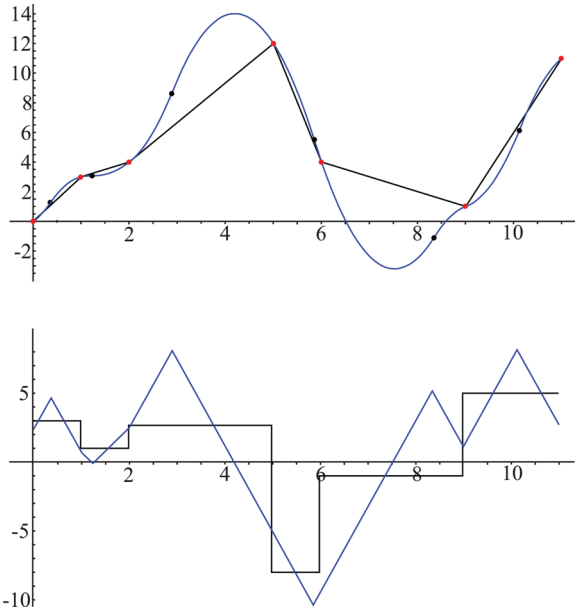

Figure 2 This figure displays the graphs of the piecewise linear interpolant and an interpolant that minimizes the $\mathcal{L}^\infty$ norm of acceleration. The graphs of the derivatives are also shown.

The goal is to minimize the $\mathcal{L}^1$ norm within the set of admissible interpolants. To achieve this we build a family of functions on each interval, show that an admissible interpolant can be constructed from this family, prove that no $\mathcal{C}^2$ function can improve on the $\mathcal{L}^1$ norm, and finally build a numerical solver to find such a solution.

Construction of capped $\mathcal{L}^1$ minimizer To begin our construction of the capped $\mathcal{L}^1$ minimizer, we start with a simple construction. Take $(x_0, y_0; m_0)$ and $(x_1, y_1; m_1)$ as before and a fixed maximum allowed acceleration $k > 0$. Later it will be necessary that k be at least as large as the minimal $\mathcal{L}^\infty$ norm required by the given set of points. We then create a basic function $f(x)$ consisting of two parabolic arcs connected with a line segment that interpolates $\{(x_i, y_i; m_i)\}_{i=0}^1$. There are four possibilities since each arc could either be concave up or down.

We first note that for f to be described as above, it is necessary that

$$f''(x) = \begin{cases} (-1)^\alpha k & x_0 \le x \le x_* \\ 0 & x_* < x < x^* \\ (-1)^\beta k & x^* \le x \le x_1 \end{cases},$$

for $\alpha, \beta \in \{-1, 1\}$ and some $x_1 \le x_* \le x^* \le x_1$ yet to be determined. It follows that

$$f'(x) = \begin{cases} (-1)^\alpha k(x - x_0) + m_0 & x_0 \le x \le x_* \\ \tilde{C} & x_* < x < x^* \\ (-1)^\beta k(x - x_1) + m_1 & x^* \le x \le x_1 \end{cases}, \tag{12}$$

for the value of $\tilde{C}$ that makes f' continuous. The key is to determine the signs of the coefficients of k and the values of x_* and x^* such that f' ranges from m_0 to m_1 and

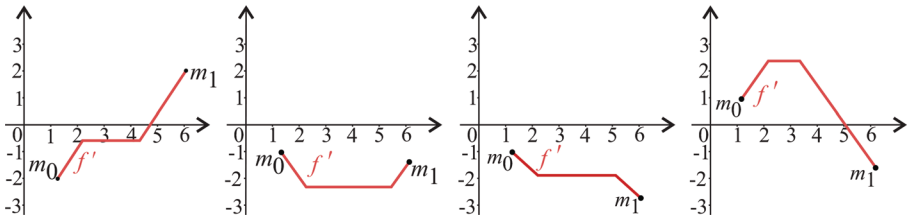

Figure 3 This figure displays the four possible shapes for f', the derivative of a hypothetical interpolant.

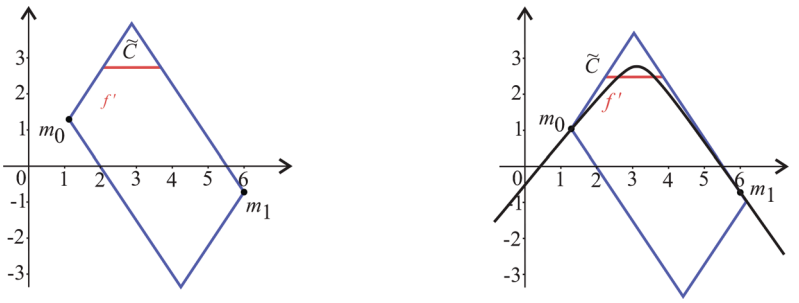

Figure 4 This figure displays "trapezoid" diagrams for f', the derivative of a hypothetical interpolant.

also

$$f := y_0 + \int_{x_0}^{x} f'(t)dt$$

ranges from y_0 to y_1. To achieve this, note that f' must take one of the shapes in Figure 3.

The shapes in Figure 3 are entirely specified by the value of $\tilde{C}$, the height of the central plateau. We now demonstrate that exactly one value of $\tilde{C}$ gives rise to a successful interpolation f. While there is a whole family of functions f' in (12) that interpolate (x_0, m_0) and (x_1, m_1), there is only one value of $\tilde{C}$ that achieves any particular displacement in f, computed by $\int_{x_0}^{x_1} f'(x)dx$. This is because the displacement integral is monotone increasing in $\tilde{C}$. Therefore, exactly one value of $\tilde{C}$ gives rise to a function f that interpolates $(x_0, y_0; m_0)$ and $(x_1, y_1; m_1)$ (provided k is large enough for a solution to exist). We can conclude that given a fixed admissible cap k, there is exactly one interpolant of $(x_0, y_0; m_0)$ and $(x_1, y_1; m_1)$ with the construction above.

Optimality of capped $\mathcal{L}^1$ minimizer The previous section gives just one possible construction of an interpolant in $\mathcal{L}^1$-cap, but there are many other possible constructions to consider. The following theorem establishes the optimality of the interpolant constructed in the previous section.

Theorem 2. *Given $(x_0, y_0; m_0)$ and $(x_1, y_1; m_1)$ and an admissible $k > 0$, let f be the unique interpolant defined in (12). There is no $\mathcal{C}^2$ interpolant g with $|g''(x)| \leq k$ that satisfies*

$$\int_{x_0}^{x_1} |g''(x)|dx < \int_{x_0}^{x_1} |f''(x)|dx.$$

Proof. Without loss of generality assume $x_0 = 0$, $m_0 = 0$, since a linear shift can accomplish this with no effect on the second derivative. Further assume that $m_1 \geq m_0$ since the other case will hold by a symmetrical argument. Let f and g be given as in the theorem statement. There are three possibilities for f depending on the value of $\tilde{C}$ as shown in Figure 4.

In the case where $f' \geq 0$, (the "up over up" option), then

$$\int_{x_0}^{x_1} |g''(x)|dx \geq \int_{x_0}^{x_1} g''(x)dx = m_1 - m_0$$
$$= \int_{x_0}^{x_1} f''(x)dx = \int_{x_0}^{x_1} |f''(x)|dx,$$

as desired.

In the case where f' is initially positive, then negative, the displacement in f must be such that an excess in acceleration is needed to achieve the interpolation. Because g must also achieve the same net displacement, the area under the graph of g' must equal that of f' as shown in Figure 4. However, the value of $\int_{x_0}^{x_1} |f''(x)|dx$ is equal to the sum

$$(\tilde{C} - m_0) + (\tilde{C} - m_1)$$

in this case, and if g' exceeds the value of $\tilde{C}$ at any point, $\int_{x_0}^{x_1} |g''(x)|dx$ will necessarily exceed that quantity. Because f was constructed to minimize $\tilde{C}$ to capture as much area as possible, g cannot meet the displacement condition without exceeding $\tilde{C}$ while remaining inside the parallelogram as shown in Figure 4. This establishes that the proposed construction of f is at least as good as any $\mathcal{C}^2$ interpolation in this case and the other cases follow similarly. ■

Corollary 3. *If the function f in Theorem 2 is not $\mathcal{C}^2$, then*

$$\int_{x_0}^{x_1} |f''(x)|dx < \int_{x_0}^{x_1} |g''(x)|dx$$

for all $\mathcal{C}^2$ interpolants g.

Existence of a minimizer Given any interpolant g of $\{(x_i, y_i)\}_{i=0}^n$, we can evaluate $g'(x_i)$ for each i, and apply our construction to that set of points and slopes. Since our construction is locally optimal on each subinterval, it must be globally optimal as well by the linearity of the integral. Hence the given construction is at least as good as any other interpolant.

We note here that the objective function is not convex, in contrast to the $\mathcal{L}^\infty$ case. As a result, the numerical solver in the capped $\mathcal{L}^1$ case is not guaranteed to converge, and indeed encounters difficulty when the imposed acceleration cap is close to the minimum admissible cap. However, Theorem 2 ensures that any solution candidate constructed by the solver is in fact optimal.

Examples from numerical implementation Given an acceleration cap and a set of points $(x_0, y_0), (x_1, y_1), \ldots, (x_n, y_n)$ with monotonically increasing x-coordinates, for any set of slope values $m_0, m_1, \ldots, m_n$ there either exists a unique interpolant of the form (12), or no interpolant of any kind exists that respects the acceleration cap. Our numerical solver converges to values for $m_0, m_1, \ldots, m_n$ whose resulting interpolant

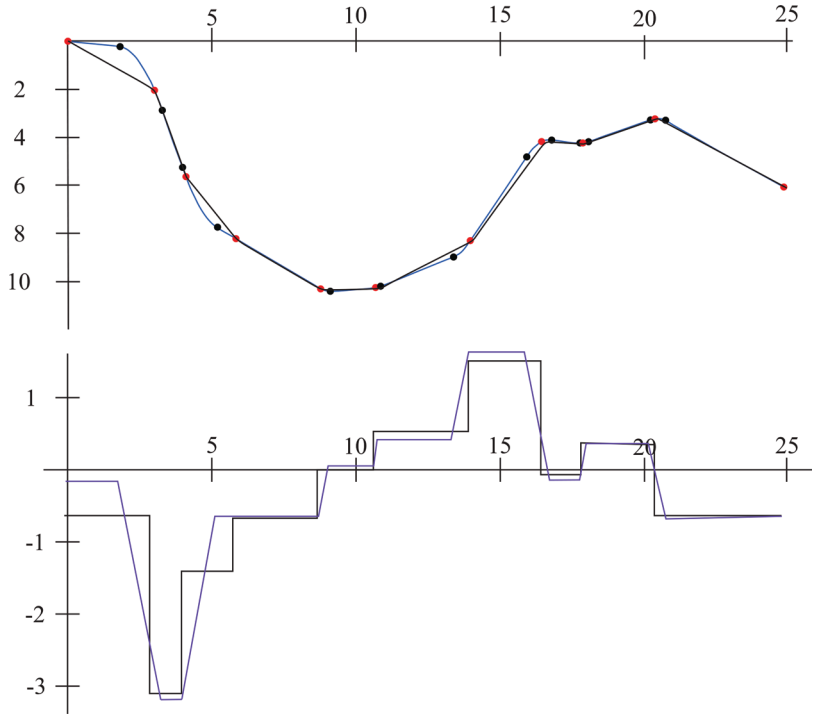

Figure 5 This figure displays graphs of the piecewise linear interpolant and an interpolant that minimizes the $\mathcal{L}^1$ norm of acceleration with an acceleration cap imposed. The graphs of the derivatives are also shown, with the distinctive trapezoidal shape clearly visible.

achieves minimum $\mathcal{L}^1$ norm of acceleration compared to all $\mathcal{C}^2$ functions that respect the given acceleration cap. Figure 5 shows an example of such a function and its derivative. In this example, we used an acceleration cap of that was 30% above the minimum feasible acceleration from the $\mathcal{L}^\infty$ solver of section "Minimizer of maximum acceleration." We chose an acceleration cap somewhat above the minimum feasible value in order to illustrate the distinctive trapezoidal shape of the interpolant's derivative graph.

Conclusion

We studied a hypothetical continuous variant of the game *Flappy Bird*. Our interest in this variant stemmed from the application to orbit transfer in spaceflight. By replacing discrete impulses with continuously varying acceleration and seeking impulse-minimizing paths, we envisioned a *Flappy Bird* variant that contained a core principle of orbital mechanics: the minimization of delta-v. We found that minimizing total impulse in continuous *Flappy Bird* reduced the problem to the original game, since concentration of impulse is optimal in the $\mathcal{L}^1$ norm. The concentration of impulse is also consistent with an idealized orbital transfer maneuver, lending credence to the continuous *Flappy Bird* model as a productive simplification of orbital mechanics.

Our results in the $\mathcal{L}^1$ norm led us to formulate a new objective: minimizing total impulse subject to a cap on acceleration. It was first necessary to establish what minimum cap on acceleration was required in order to interpolate a given set of points, or equivalently, what interpolant obtained minimum acceleration in the $\mathcal{L}^\infty$ norm. After constructing a piecewise-quadratic solution in this norm, we used this information to

construct an explicit solution to the capped $\mathcal{L}^1$ problem as well, in both cases using numerical methods to identify the correct constants.

Our goal throughout this project was to use elementary calculus to shed light on the optimality of maneuvers like the powered slingshot. To gain purchase, we proposed a dramatically simplified model of orbital mechanics that we termed "continuous *Flappy Bird*" for its similarities to the video game. Our model collapsed all the complexity of orbital mechanics to a single concept of study: the minimization of delta-v. Using elementary techniques, we were to prove optimality of several new interpolant constructions, and thereby reproduce the concentration of impulse exhibited in real-life orbital maneuvers.

REFERENCES

[1] Atkinson, K., Han, W. (2004). *Elementary Numerical Analysis*, 3rd ed. Indianapolis, IN: Wiley.
[2] Doody, D. (2011). *Basics of Space Flight.* Pasadena: Blüroof Press.
[3] Gelfand, I. M., Fomin, S. V. (2000). *Calculus of Variations.* Mineola, NY: Dover.
[4] Piper, M. (2017). How to beat Flappy Bird: A mixed-integer model predictive control approach. Master's thesis. http://aux.coe.utsa.edu/~pab/reports/Matthew_Piper_MSThesis.pdf
[5] Prenter, P. M. (1975). *Splines and Variational Methods.* Indianapolis, IN: Wiley.
[6] Schumaker, L. L. (2007). *Spline Functions: Basic Theory*, 3rd ed. Cambridge: Cambridge University Press.

Summary. We propose a simple model for orbital mechanics with inspiration from the video game *Flappy Bird*. We study impulse-minimizing paths in our model, producing new constructions of spline minimizers of acceleration in the $\mathcal{L}^1$ and $\mathcal{L}^\infty$ norms. Our work illustrates the concentration of impulse observed in real-world orbital maneuvers. We use elementary techniques that are accessible to college mathematics students, including integrals and derivatives of polynomials, applications of the mean value theorem, and numerical optimization.

THOMAS J. CLARK (ORCID 0000-0002-5160-4782) earned his Ph.D. in mathematics from the University of Nebraska – Lincoln. He is an associate professor of mathematics at Dordt University. While trained in the area of numerical PDEs, he is additionally active in both the scholarship of teaching and learning and math circles communities.

ANIL VENKATESH (MR Author ID 1347306, ORCID 0000-0001-9893-7704) earned his Ph.D. in mathematics from Duke University. He is an assistant professor in the Department of Mathematics and Computer Science at Adelphi University. His primary work is in mathematical applications to music theory, acoustics, and music information retrieval. He also works in the scholarship of teaching and learning with a focus on formative assessment in college mathematics.

Edge Coloring and the Möbius Strip

JIMMY DILLIES
University of Georgia
Athens, GA 30602
jimmy.dillies@uga.edu

From the work of M.C. Escher to the universal recycling logo, no mathematical object is more ubiquitous than the Möbius strip. Introduced independently by Listing and Möbius in 1858, the Möbius strip illustrates in a very tangible way the concept of (non)orientability and even characterizes non-orientable surfaces (which contain a copy of it). While the Möbius strip is a concrete object for which it is easy to develop a feeling, when venturing away from it and introducing orientability, students often face a mental barrier. Part of the difficulty lies in the use of the language of atlases and manifolds which have been freshly introduced—we will quickly recollect these notions in the first Section. As we will see below, orientability can actually be determined using elementary graph theoretic tools. Moreover, this new characterization of orientability also facilitates the construction of related objects such as the oriented double cover of manifolds.

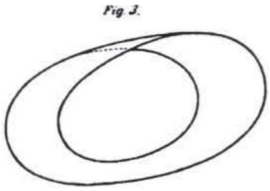

Figure 1 Möbius strip as represented in Johann Listing's book [4].

A small refresher on manifolds

Up to the nineteenth century, geometric objects were perceived globally. For example, surfaces lived in $\mathbb{R}^3$, and mathematicians studied them using calculus. However, a new door was opened when Gauss [2] and Riemann [6] showed in their work that it is possible to do geometry in spaces that only look like $\mathbb{R}^n$ once restricted to small chunks. In a sense, Gauss and Riemann gave a mathematical framework to our perception of the universe. As sensible beings, we can only perceive our direct surroundings. This new geometry was not very different from the work of cartographers of bygone times, they had access to scattered knowledge of different regions and the game was to understand how to patch these pieces together. Take the example of an atlas: each page corresponds to a small patch of Earth and using latitude and longitude one can identify the edges of pages describing neighboring pieces of land.

A manifold is the formalization of this idea: A *manifold* M is a separated topological space which is locally homeomorphic to $\mathbb{R}^n$, that is, each point x is contained in some open neighborhood U for which there exists a homeomorphism

$$\phi : U \to \phi(U) \subset \mathbb{R}^n.$$

Math. Mag. **94** (2021) 113–117. doi:10.1080/0025570X.2021.1867452
MSC: 55-01; 57-01; 57N65

The pair (U, ϕ) is called a *chart*, and an *atlas* is a collection of charts $\{(U_i, \phi_i)\}$ covering the manifold, that is, $M = \cup_i U_i$. The patching between charts is encoded by the transition maps:

$$\psi_j^i = \phi_j \circ \phi_i^{-1} : \phi_i(U_i \cap U_j) \to \phi_j(U_i \cap U_j).$$

The nature of the transition maps (topological, differentiable, analytics, ...) is paramount to the nature of the manifold. For example, a manifold is differentiable if and only if all of its transition maps are differentiable. The reader can refer to the book by Borceux [1] for an elegant and comprehensive introduction to geometric spaces and manifolds.

Orientability

While the notion of orientability is quite intuitive, students often struggle with the definition found in a first course on the geometry of manifolds, i.e.

Definition (Orientability—Version 1)**.** A manifold is orientable if it admits an atlas all of whose charts have compatible orientation.

Two charts U_i and U_j have compatible orientation if and only if the determinant of the Jacobian of their transition maps ψ_j^i or ψ_i^j is positive:

$$\det D\psi_j^i > 0.$$

This is the local notion of preservation of orientation for linear maps. If one is lucky and starts with an atlas of compatible charts, all ambiguity is removed: the manifold is orientable. How about when the charts are not compatible? Is the manifold non-orientable, or was it simply an unsuitable choice of atlas?

Listing graph

Given an atlas, we will construct its associated *Listing graph* which we name in honor of German mathematician *Johann Benedict Listing*, a contemporary of August Möbius, who discovered the eponymous strip independently and who studied circuits on graphs in the context of "positional geometry" [4].

A graph G is given by two sets, a set of vertices V and a set of edges E, where edges are required to be bound by vertices of the graph. The vertices of the Listing graph will represent the charts of the atlas, and two vertices will be connected by an edge if and only if the intersection of the corresponding charts is not empty. Moreover, the graph will carry some extra information—and some charm—in the form of a coloring of the edges. When the transition function between two charts preserves the orientation, the associated edge will be marked in blue (or $+1$), and when the transition function inverts the orientation, it will colored in red (or -1).* Figure 2 shows two examples of surfaces, a cylinder and a Möbius strip, each described by three charts, together with the associated Listing graph.

To be able to rephrase the notion of orientability in terms of Listing graphs, recall the notion of a circuit. A *circuit* $c = [e_1, e_2, \ldots, e_N]$ is a sequence of consecutive edges forming a closed loop. We will denote the set of circuits on a graph G by $\mathrm{Circ}(G)$. In Figure 3, a sample circuit is represented by dashed edges.

*Note that the online version of this article features color graphics.

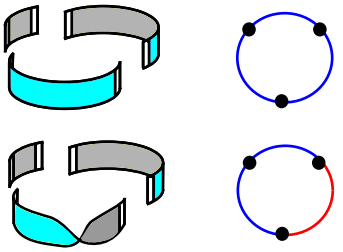

Figure 2 Listing graph of a cylinder and a Möbius strip.

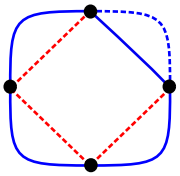

Figure 3 Circuit on a graph.

Proposition 1 (Orientability—Version 2)**.** *A manifold is orientable if and only if all circuits on the Listing graph of one of its atlases have an even number of red edges.*

Proof. One direction is obvious once one starts with compatible charts. In the other direction, fix a base vertex on the Listing graph. Since all circuits contain an even number of red edges, there is a well-defined list of vertices separated from the base vertex by an odd number of red edges. Change the orientation of the charts represented by these vertices by, for example, making a suitable change of coordinates and, *mutatis mutandis*, adapting the transition functions. All charts are now compatible. ■

Looking back at the examples in Figure 2, the criterion of Proposition 1 is quickly verified as each graph contains an essentially unique circuit. In the case of the cylinder, no edges are red, so the surface is orientable. For the Möbius strip, there is a single red edge and it cannot be avoided: the surface is not orientable.

Example. The real projective space, $\mathbb{RP}^3$, can be identified with the space of lines in $\mathbb{R}^4$ passing through the origin. We can use 4 charts to cover it,. Specifically, we use the open sets $U_k = \{(x_1, x_2, x_3, x_4), x_k \neq 0\}$, where all $(\lambda x_1, \lambda x_2, \lambda x_3, \lambda x_4)_{\lambda \neq 0}$ are identified—for $k = 1, 2, 3, 4$ and the coordinate maps

$$\phi_k : U_k \to \mathbb{R}^3 : (x_1, x_2, x_3, x_4) \mapsto \left(\frac{x_1}{x_k}, \ldots, \frac{\widehat{x_k}}{x_k}, \ldots, \frac{x_4}{x_k} \right)$$

where the hat means that the entry is omitted.

All charts overlap and any two have a compatible orientation if and only if the sum of their indices is even. For example, U_1 and U_2 do not have a compatible orientation because the transition map

$$\psi_2^1 : \mathbb{R}^3_{X \neq 0} \to \mathbb{R}^3 : (X, Y, Z) \mapsto \left(\frac{1}{X}, \frac{Y}{X}, \frac{Z}{X} \right)$$

has a Jacobian determinant equal to $-X^{-4}$.

The Listing graph in this situation is therefore a complete graph on 4 vertices all of whose edges but two are red (see Figure 4). One sees immediately that the projective space in three dimensions is orientable as all circuits contain 2 or 4 red edges.

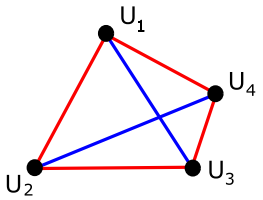

Figure 4 Listing graph of a projective space.

Orientation double cover

Besides being a tool to measure orientability, Listing graphs can be used constructively. Take the example of the oriented double cover: to each manifold X, we can associate an oriented manifold Y which admits a two to one map to the initial space, $\pi : Y \xrightarrow{2:1} X$. A direct application of the Listing graph is its use is the construction of the oriented double cover. Using the prescription given in Figure 5 one obtains immediately an atlas for the double cover.

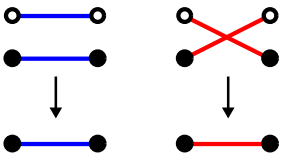

Figure 5 Local cover of Listing graph.

The key element of the Listing graph of the orientation cover is that edges above red edges switch "levels." This guarantees that the double cover is orientable: any circuit finishes on the same level, that is, has to go through an even number of red edges. Once the covering graph is constructed, the covering manifold is then obtained by using copies of the original charts and gluing them according to the new Listing graph. This construction is illustrated for the running examples in Figure 6. These examples illustrate the more general fact that the orientation double cover is connected if and only if the original manifold is not orientable.

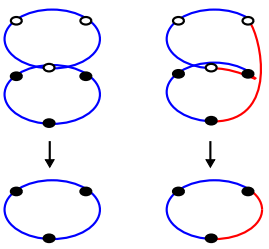

Figure 6 Listing graph of oriented cover.

Final remarks

This note is only the tip of the iceberg, and many features of a manifold can be read off its Listing graph. For example: the universal cover, the computation of Cartesian products, the calculation of the Euler characteristic of surfaces (through ribbon graphs). More generally, there is a blooming literature on topological graph theory, and the books by Mohar and Thomassen [5], and Lando and Zvonkin [3] offer a perfect gateway for the interested reader. We limited ourself to describing the Listing graph, which can be seen as the poor man's *nerve* of an atlas, but yet holds many virtues, not the least of which is offering an effective entry to the combinatorics of an atlas pertinent to orientation.

Stiefel–Whitney

In this appendix, we will succinctly describe a bridge to algebraic topology by formalizing the above characterization of orientability. First, the coloring of the edges can be encoded by means of a *coloring map*: Let the function $\omega : E \to \mathbb{Z}/2\mathbb{Z}$ take the value 1 if the edge was previously colored in red and the value 0 if the edge was blue. We can associate an element of $\mathbb{Z}/2\mathbb{Z}$ to each circuit on the Listing graph by extending ω additively:

$$w_1 : \mathrm{Circ}(G) \to \mathbb{Z}/2\mathbb{Z} : [e_1, e_2, \ldots, e_N] \mapsto \sum_{i=1}^{N} \omega(e_i)$$

The characterization of orientability in the previous section can now readily be rephrased in terms of the function w_1:

Proposition 2 (Orientability—Version 3)**.** *A manifold is orientable if and only if the function w_1 is trivial, i.e., $w_1 \equiv 0$.*

The map w_1 is a special case of the *orientation character*, which is itself an instantiation of the first *Stiefel–Whitney class* of the manifold.

Acknowledgments The author thanks Joe Hoisington and the anonymous referees for their suggestions and constructive advice.

REFERENCES

[1] Borceux, F. (2014). *A Differential Approach to Geometry: Geometric Trilogy III*. New York: Springer.
[2] Gauss, C. F. (1828). *Disquisitiones Generales Circa Superficies Curvas*. Göttingen: Typis Dieterichianis.
[3] Lando, S. K., Zvonkin, A. K. (2004). *Graphs on Surfaces and Their Applications*. Berlin: Springer Verlag.
[4] Listing, J. B. (1862). *Der Census Räumlicher Complexe oder Verallgemeinerung des Euler'schen Satzes von den Polyedern*. Göttingen: In der Dieterischschen Buchhandlung.
[5] Mohar, B., Thomassen, C. (2001). *Graphs on Surfaces*. Baltimore: Johns Hopkins University Press.
[6] Riemann, B. (1868). Ueber die Hypothesen, welche der Geometrie zu Grunde liegen. In: *Abhandlungen der Königlichen Gesellschaft der Wissenschaften zu Göttingen*.

Summary. We present an elementary, graph-theoretic characterization of orientability for manifolds equipped with an atlas. This method focuses on the essential information needed to determine orientability and gives an elegant application of graph theory to geometry. The approach that we take also provides students with a straightforward tool to study orientation.

JIMMY DILLIES (MR Author ID: 794407, ORCID: 0000-0003-4757-0820) received his Licence en sciences mathématiques from the Université catholique de Louvain and his Ph.D. from the University of Pennsylvania. In his spare time, he enjoys reading.

Connecting the Dots: Maximal Polygons on a Square Grid

SAM CHOW
University of Warwick
Coventry, United Kingdom
Sam.Chow@warwick.ac.uk

AYLA GAFNI
University of Mississippi
University, MS 38677
argafni@olemiss.edu

PAUL GAFNI
Seattle Country Day School
Seattle, WA 98109
paul.gafni@gmail.com

Given an $n \times n$ grid of dots, where $n > 1$, when is it possible to connect all of the dots to give a polygon with n^2 sides? One is not allowed to have two consecutive segments be collinear, since that would merge two sides of the polygon. Figure 1 gives an example of a valid solution when $n = 4$.

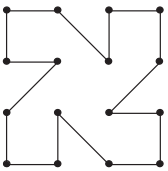

Figure 1 A 16-sided polygon on a 4×4 grid of dots.

We want to know: Which values of n permit such a polygon to be drawn?*

How might one attack such a problem? As a first step, we gave it to some schoolchildren to try. The children came back with solutions for $n = 6, 7$, and 9. Figure 2 shows a somewhat devious construction in the case $n = 7$. Even after a long time, the students couldn't find solutions to the cases $n = 3, 5$, so we figured they were probably impossible. Now the problem is to prove that there are no solutions.

Solutions do not exist on the 3 × 3 and 5 × 5 grids

We'll show that it is impossible to draw an n^2-sided polygon on an $n \times n$ grid if $n = 3$ or 5. By playing with the grid for a few minutes, one can readily see that the 3×3 grid has no solution. The 5×5 grid is more subtle. We begin with a short proof of the $n = 3$ case, which contains ideas that will be used for $n = 5$.

Theorem 1. *There is no way to draw a* 9*-sided polygon on a* 3×3 *grid of points.*

Proof. Classify the points on the grid as corners (○), sides (×), and center (★), as shown in Figure 3.

*The task is straightforward if one is allowed to have two consecutive segments be collinear. In this case, it is easy to construct many solutions, even if one only uses horizontal, vertical, and 45° segments of minimal length; see the article [1] enumerating Hamiltonian cycles in king's graphs. The non-collinearity condition is highly restrictive, and is non-standard in graph theory. Our problem can be formulated in terms of non-uniform hypergraphs, but such a formulation is neither natural nor helpful.

Math. Mag. **94** (2021) 118–124. doi:10.1080/0025570X.2021.1869493
MSC: 05B30, 05B99

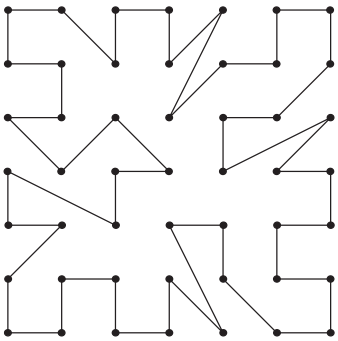

Figure 2 A 49-sided polygon on a 7×7 grid of dots.

Figure 3 Points in a 3×3 grid classified as corners ($\circ$), sides ($\times$), and center ($\star$).

Consider the edges through the $\times$ point on the left side. These edges can only connect to the top-left corner, bottom-left corner, or the center. Connecting to another side or a non-adjacent corner would cut off part of the grid and prevent the polygon from going through all the points, as shown in the right-most grid in Figure 4. Further, we cannot have edges from this point to both the top and bottom corner, since that would decrease the number of sides in our polygon. Since there must be two edges through every point, we must have that this point connects to the center ($\star$).

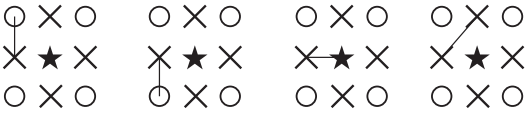

Figure 4 The first three diagrams show potentially valid edges through the left side point. The right-most grid shows how a side-to-side ($\times \to \times$) edge would prevent the polygon from reaching all 9 points.

By the same reasoning, each of the four side ($\times$) points must connect to the center ($\star$). This is a contradiction since we must have exactly two edges through each point. ■

A similar combinatorial argument can be used to show the $n = 5$ case also has no solution.

Theorem 2. *There is no way to draw a* 25*-sided polygon on a* 5×5 *grid of points.*

Proof. Again, we classify the points in three categories. This time we will consider "outer" ($\circ$), "inner" ($\times$), and "center" ($\star$) points, as shown in Figure 5. Count the edges according to which types of point they connect:

$a =$ number of edges connecting two outer points ($\circ \to \circ$)

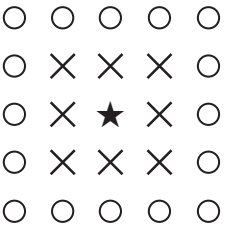

Figure 5 Points in a 5×5 grid classified as outer ($\circ$), inner ($\times$), and center ($\star$).

$b =$ number of edges connecting an inner point to an outer point ($\times \to \circ$)

$c =$ number of edges connecting two inner points ($\times \to \times$)

$d =$ number of edges connecting the center to an outer point ($\star \to \circ$)

$e =$ number of edges connecting the center to an inner point ($\star \to \times$)

Suppose we have a solution that forms a 25-sided polygon. Each edge in the polygon is counted by one of the above categories, so we have that

$$a + b + c + d + e = 25. \tag{1}$$

Consider first the possible edges counted by a. These can only be vertical or horizontal edges connecting adjacent points on the same side of the grid. Otherwise the edge would cut off part of the grid. Further, we cannot have two "adjacent" $\circ \to \circ$ edges on the same side, since that would decrease the number of sides in the polygon. Thus we can have at most two $\circ \to \circ$ edges on each side, i.e., $a \leq 8$.

We next count the total number of times an edge touches an inner point ($\times$). On the one hand, this is equal to $b + 2c + e$ (since each $\times \to \times$ edge touches two inner points). On the other hand, there are 8 inner points and each point touches two edges, for a total of 16. Therefore,

$$b + 2c + e = 16. \tag{2}$$

Subtracting (2) from (1), we see that

$$a - c + d = 9.$$

Since $a \leq 8$ and $c \geq 0$, this implies that $d \geq 1$. Hence we must have at least one edge from the center ($\star$) to an outer ($\circ$) point. If $\star$ connects to two outer ($\circ$) points, then the grid is split and we cannot reach all the points. Therefore we must have one $\star \to \circ$ edge and one $\star \to \times$ edge, i.e., $d = e = 1$.

We now have the restrictions

$$\begin{cases} a + b + c &= 23, \\ b + 2c &= 15, \\ a &\leq 8. \end{cases} \tag{3}$$

The only solution to (3) in non-negative integers is $a = 8,\ b = 15,\ c = 0$. Thus the edge counts are:

$$\#\{\circ \to \circ\} = 8,\ \ \#\{\times \to \circ\} = 15,\ \ \#\{\times \to \times\} = 0,$$
$$\#\{\star \to \circ\} = 1,\ \ \#\{\star \to \times\} = 1.$$

In particular, we have no $\times \to \times$ edges, and exactly two $\circ \to \circ$ on each side.

We now consider the possible ways these edge counts can be laid out on the grid. Label the points on the grid by their row (A, B, C, D, E) and column (1, 2, 3, 4, 5) , as shown in Figure 6. Without loss of generality, we may assume that the $\star \to \circ$ edge

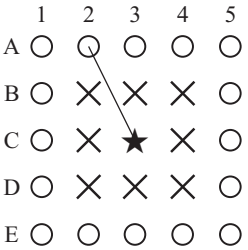

Figure 6 By rotational symmetry, we can assume that (A3,C2) is an edge without loss of generality.

connects C3 to A2. Recall that row A must have two horizontal edges, which are not "adjacent." Thus, exactly one of the edges (A1, A2) and (A2, A3) must occur.

Case 1: (A1, A2) is an edge. Consider the path in the polygon starting at A1 and moving with negative orientation (A1, A2, C3, . . .). The next $\circ$-point in the sequence must be A3, since otherwise the grid is split. We have no $\times \to \times$ edges, so the sequence must be

$$(\text{A1},\ \text{A2},\ \text{C3},\ \times,\ \text{A3},\ \ldots).$$

If the $\times$ is B3, then we have (C3, B3, A3), and we have too few sides in the polygon. If the $\times$ is not B3, then B3 is cut out of the polygon (see Figure 7). So this case is impossible.

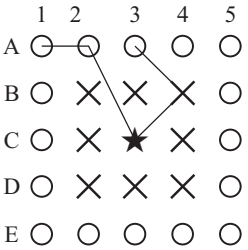

Figure 7 If (A1,A2) is an edge, then there is no way to reach B3 and maintain 25 sides.

Case 2: (A2, A3) is an edge. Consider the path in the polygon starting at A3 and moving with positive orientation

$$(\text{A3},\ \text{A2},\ \text{C3},\ \ldots).$$

By a similar argument, the next $\circ$-point in the sequence must be A1. As above, the path to A1 is (A3, A2, C3, $\times$, A1, . . .). If the $\times$ is B2, we have too few sides. If the $\times$ is not B2, then B2 is cut out of the polygon (see Figure 8). So this case is also impossible.

Therefore, there is no way to draw a 25-sided polygon on a 5×5 grid of points. ■

The main obstruction to creating an n^2-sided polygon when $n = 3, 5$ is that there simply isn't enough space for all the edges without having consecutive collinear edges. For larger grids, there is a lot of space, so we should expect there to be solutions. And, in fact, there are.

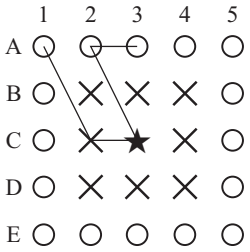

Figure 8 If (A2,A3) is an edge, then there is no way to reach B2 and maintain 25 sides.

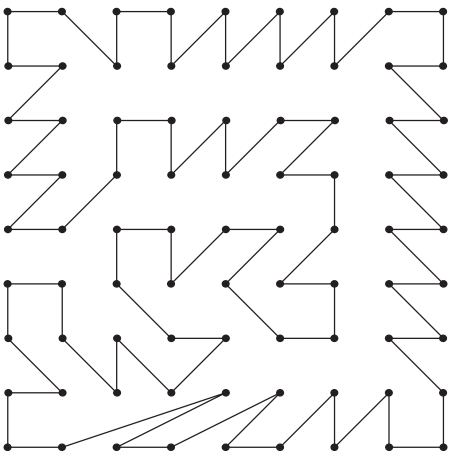

Figure 9 An 81-sided polygon on a 9×9 grid of dots.

Solutions exist on any other square grid

The case $n = 2$ is trivial, and we've seen that a solution exists for $n = 4$ but not for $n = 3$ or 5. Now let's complete our answer by seeing how to construct a valid polygon when the grid has side-length $n \geq 6$.

Theorem 3. *Let $n \geq 6$. Then one can draw an n^2-sided polygon on an $n \times n$ grid of points.*

Our proof will induct from n to $n + 4$. Since we have constructions for $n = 2, 4, 7$, the other base case we will need is $n = 9$. Figure 9 gives one such solution.

The induction. To complete the proof, we describe the induction. It's helpful to follow Figure 10 to keep track of how it works. Let $n \geq 2$, and suppose a maximal polygon exists for the $n \times n$ grid with horizontal and vertical segments out of the southwest corner, such that the horizontal segment does not connect to a 45° segment. We construct a maximal polygon for $n + 4$ as follows.

1. Construct a maximal polygon in the central $n \times n$ subgrid, having horizontal and vertical segments in the southwest corner, such that the horizontal segment does not connect to a 45° segment.
2. Remove the aforementioned horizontal segment, and from each of the two affected vertices draw a southwest and then a south segment. (This path takes us to the southern edge of the grid, just east of the southwest corner.)

3. Zigzag around the outside, with every corner having a horizontal and a vertical segment; just west of the northeast corner insert two consecutive right angles on the northern border.

By induction, we can now construct a solution for any n except for $n = 3$ and $n = 5$.

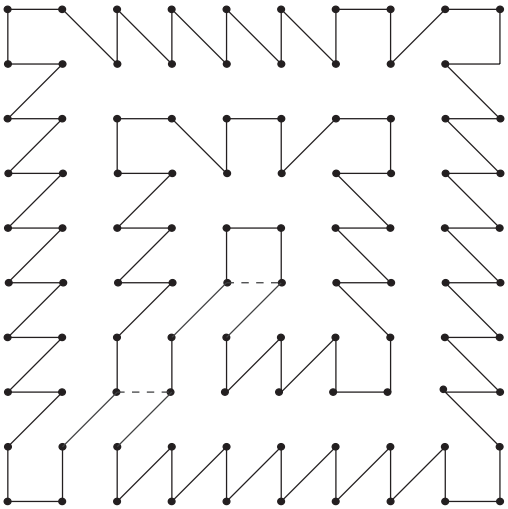

Figure 10 The inductive step to turn a solution for n into a solution for $n + 4$. The dotted blue line is removed from the n solution, and the outer path is added, beginning and ending with the diagonal blue edges.

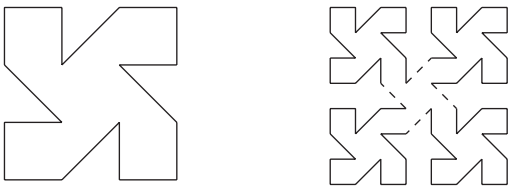

Figure 11 By copying the solution and connecting in the middle, we can create a $2n$ solution from an n solution.

Further discussion

There is another induction one could use, which would go from n to $2n$. Given a maximal polygon for n, we can generate a solution for $2n$ using four copies of the smaller polygon and connecting in the middle. This is cumbersome to use in the proof of Theorem 3 because it would require infinitely many base cases. However, it does lead to some interesting patterns. In particular, for n a power of 2, this construction gives rise to an unfamiliar fractal (see Figure 11), which is reminiscent both of a Sierpinski Curve and a Hilbert Curve. If you've encountered this fractal before, we'd love to hear about it.

We have settled the problem of existence of n^2-sided polygons on the $n \times n$ grid, but the story does not end here. One might consider rectangular grids that are not square. Alternatively, one might consider the problem in which only axis-parallel and 45° segments are allowed. Finally, if there isn't an n^2-gon, what is the largest number

of sides that one can achieve—is it possible to make an octagon on a 3×3 grid? We leave these for the interested reader to share and enjoy.

Acknowledgments This material is based upon work supported by the National Science Foundation under Grant No. DMS-1440140 while Sam Chow and Ayla Gafni were in residence at the Mathematical Sciences Research Institute in Berkeley, California, during the Spring 2017 semester. Sam Chow was also supported by EPSRC Fellowship Grant EP/S00226X/1, EPSRC Fellowship Grant EP/S00226X/2, and EPSRC Programme Grant EP/J018260/1. The authors would like to thank the anonymous referees for helpful comments which improved the exposition.

REFERENCE

[1] Pettersson, V. H. (2014). Enumerating Hamiltonian cycles. *Electron. J. Combin.* 21: Paper 4.7, 15 pp. doi.org/10.37236/4510

Summary. Given an $n \times n$ grid of dots, we wish to connect all of the dots and end up with a non-degenerate n^2-gon. Sometimes this is possible, and other times it is not.

SAM CHOW (MR Author ID: 1077989, ORCID: 0000-0001-7651-4831) is an assistant professor at the University of Warwick. He is an analytic number theorist with particular interests in Diophantine equations and Diophantine approximation. He grew up in Melbourne, and enjoyed competition mathematics in his youth, earning a bronze medal at the International Mathematical Olympiad. Sam is a keen chess player, and holds the FIDE Master title.

AYLA GAFNI (MR Author ID: 1081891, ORCID: 0000-0003-4226-2175) is an assistant professor at the University of Mississippi. She received her Ph.D. from Pennsylvania State University in 2016. Her research explores connections between analytic number theory and harmonic analysis, with an emphasis on integer partitions and Diophantine approximation. In addition to mathematics, Ayla is passionate about theater and music, and she currently serves on the board of Theatre Oxford, the local community theater organization.

PAUL GAFNI spends his professional energy bringing genuine mathematics to the K-12 world. He's constantly on the hunt for ways to strip the technical and the jargon away in order to invite students at all ages to marvel in the delight of mathematical inquiry and exploration. His teaching experience includes work with Math for Love, the Robinson Center for Young Scholars at the University of Washington, and Seattle Country Day School, and he has presented at conferences for the National Council of Teachers of Mathematics and the National Association for Gifted Children. When he's not thinking about teaching or curriculum, he's likely making mathematical art using laser cutters or musical instruments.

A Combinatorial View of Sums of Powers

MICHAEL Z. SPIVEY
University of Puget Sound
Tacoma, WA 98416-1043
mspivey@pugetsound.edu

The sum of powers of the first n positive integers,

$$1^m + 2^m + 3^m + \cdots + n^m,$$

has been a topic of mathematical study for centuries. For example, the formulas for this sum when m equals 1, 2, and 3 are widely known:

$$1 + 2 + 3 + \cdots + n = \frac{n(n+1)}{2},$$
$$1^2 + 2^2 + 3^2 + \cdots + n^2 = \frac{n(n+1)(2n+1)}{6},$$
$$1^3 + 2^3 + 3^3 + \cdots + n^3 = \frac{n^2(n+1)^2}{4}.$$

In this note, we describe a simple combinatorial way to view the power sum. Then we use this perspective to give combinatorial proofs of two known formulas for the power sum: one involving Stirling numbers of the second kind and one involving Eulerian numbers. Finally, we make a minor modification to the latter proof to produce a combinatorial proof of Worpitzky's identity.

A convention and some notation: Throughout this note we assume that m, n, and x are nonnegative integers, and we use the symbol $[n]$ to denote the set $\{1, 2, \ldots, n\}$.

The power sum, combinatorially

Here is our combinatorial interpretation of the power sum.

Theorem 1. *The power sum $\sum_{k=1}^{n} k^m$ is the number of functions $f : [m+1] \mapsto [n+1]$ such that, for all $i \in [m]$, $f(i) < f(m+1)$.*

Before we prove Theorem 1, let's take a look at a couple of its special cases in order to understand a little better what it says.

- With $m = 1$, Theorem 1 says that the sum $\sum_{k=1}^{n} k$ is the number of functions f from $\{1, 2\}$ to $\{1, 2, \ldots, n+1\}$ with $f(1) < f(2)$.
- With $m = 2$, Theorem 1 says that the sum $\sum_{k=1}^{n} k^2$ is the number of functions f from $\{1, 2, 3\}$ to $\{1, 2, \ldots, n+1\}$ with $f(1) < f(3)$ and $f(2) < f(3)$.

In other words, the power sum can be thought of as the number of functions $f : [m+1] \mapsto [n+1]$ for which $f(m+1)$ is larger than any of the other function values.

Proof. For such a function f, let $k \in [n]$, and suppose $f(m+1) = k+1$. Since we must have $f(1) < f(m+1)$, there are k choices for $f(1)$; that is, we must have

Math. Mag. **94** (2021) 125–131. doi:10.1080/0025570X.2021.1869481
MSC: 05A19, 11B73, 05A10

$f(1) \in \{1, 2, \ldots, k\}$. Similarly, there are k choices for $f(2)$, k choices for $f(3)$, and so forth, up to $f(m)$, so that we have k^m total choices for the values of $f(1)$, $f(2)$, $\ldots$, $f(m)$. Summing over all possible values of k yields $\sum_{k=1}^{n} k^m$ as the total number of functions $f : [m+1] \mapsto [n+1]$ satisfying $f(i) < f(m+1)$ for all $i \in [m]$. ■

The power sum via Stirling numbers

Theorem 1 leads to a quick combinatorial proof of a formula for the power sum featuring the Stirling numbers of the second kind. Let's talk a little about these numbers before we discuss the formula.

The Stirling numbers of the second kind $\left\{ {n \atop k} \right\}$ can be generated by the following recursion:

$$\left\{ {n \atop k} \right\} = k \left\{ {n-1 \atop k} \right\} + \left\{ {n-1 \atop k-1} \right\},$$

valid for $n > k \geq 1$. For the boundary cases, we have $\left\{ {n \atop n} \right\} = 1$, and, for $n > 0$, $\left\{ {n \atop 0} \right\} = 0$. The first several rows of the triangle of Stirling numbers of the second kind are given in Figure 1.

n	$\left\{ {n \atop 0} \right\}$	$\left\{ {n \atop 1} \right\}$	$\left\{ {n \atop 2} \right\}$	$\left\{ {n \atop 3} \right\}$	$\left\{ {n \atop 4} \right\}$	$\left\{ {n \atop 5} \right\}$	$\left\{ {n \atop 6} \right\}$	$\left\{ {n \atop 7} \right\}$
0	1							
1	0	1						
2	0	1	1					
3	0	1	3	1				
4	0	1	7	6	1			
5	0	1	15	25	10	1		
6	0	1	31	90	65	15	1	
7	0	1	63	301	350	140	21	1

Figure 1 Rows 0 through 7 of the triangle of Stirling numbers of the second kind.

The Stirling numbers of the second kind have a combinatorial interpretation as well: They count the number of ways to partition n objects into k nonempty subsets. For example, suppose we want to partition the set $\{1, 2, 3, 4\}$ into two nonempty subsets. Here are the possibilities:

$$\{1\} \cup \{2, 3, 4\}, \quad \{2\} \cup \{1, 3, 4\}, \quad \{3\} \cup \{1, 2, 4\}, \quad \{4\} \cup \{1, 2, 3\},$$
$$\{1, 2\} \cup \{3, 4\}, \quad \{1, 3\} \cup \{2, 4\}, \quad \{1, 4\} \cup \{2, 3\}.$$

Thus $\left\{ {4 \atop 2} \right\} = 7$, which we also see in Figure 1.

Let's now look at our power sum formula featuring the Stirling numbers of the second kind.

Theorem 2.

$$\sum_{k=1}^{n} k^m = \sum_{k=0}^{m} \binom{n+1}{k+1} \left\{ {m \atop k} \right\} k!.$$

Proof. By Theorem 1, the left side is the number of functions $f : [m+1] \mapsto [n+1]$ such that, for all $i \in [m]$, $f(i) < f(m+1)$.

For the right side, let $k \in \{0, 1, \ldots, m\}$, and suppose $k+1$ is the number of elements in the image of f. Then there are $\binom{n+1}{k+1}$ ways to choose exactly which elements these will be. The largest element must be $f(m+1)$, and the remaining m elements in the domain must be mapped to the other k elements in the image. There are $\left\{ {m \atop k} \right\}$ ways to assign the remaining m elements to k nonempty groups, and then $k!$ ways to assign these groups to the k remaining elements in the image. (More generally, the number of onto functions from an m-set to a k-set is $\left\{ {m \atop k} \right\} k!$.) Finally, sum over all possible values of k. ■

As an example, take $m = 3$. Then Theorem 2 becomes

$$\sum_{k=1}^{n} k^m = \binom{n+1}{2} + 6\binom{n+1}{3} + 6\binom{n+1}{4}.$$

We see, then, that Theorem 2 gives us a formula for the power sum in terms of the binomial coefficients in row $n+1$ of Pascal's triangle.

The power sum via Eulerian numbers

Our second formula for the power sum involves the Eulerian numbers. Let's take a look at those numbers now.

As with the Stirling numbers of the second kind, the Eulerian numbers $\left\langle {n \atop k} \right\rangle$ satisfy a simple two-term recurrence relation. We have

$$\left\langle {n \atop k} \right\rangle = (k+1)\left\langle {n-1 \atop k} \right\rangle + (n-k)\left\langle {n-1 \atop k-1} \right\rangle,$$

valid for $n > k \geq 1$. For the boundary cases, we have $\left\langle {n \atop 0} \right\rangle = 1$ and, for $n > 0$, $\left\langle {n \atop n} \right\rangle = 0$. The first several rows of the triangle of Eulerian numbers are given in Figure 2.

n	$\left\langle {n \atop 0} \right\rangle$	$\left\langle {n \atop 1} \right\rangle$	$\left\langle {n \atop 2} \right\rangle$	$\left\langle {n \atop 3} \right\rangle$	$\left\langle {n \atop 4} \right\rangle$	$\left\langle {n \atop 5} \right\rangle$	$\left\langle {n \atop 6} \right\rangle$	$\left\langle {n \atop 7} \right\rangle$
0	1							
1	1	0						
2	1	1	0					
3	1	4	1	0				
4	1	11	11	1	0			
5	1	26	66	26	1	0		
6	1	57	302	302	57	1	0	
7	1	120	1191	2416	1191	120	1	0

Figure 2 Rows 0 through 7 of the triangle of Eulerian numbers.

Also like the Stirling numbers of the second kind, the Eulerian numbers have a combinatorial interpretation. To explain this combinatorial interpretation we need to provide some background.

Given a permutation $\pi : [m] \mapsto [m]$, we say that i, $1 \leq i \leq m-1$, is an *ascent* of π if $\pi(i) < \pi(i+1)$. For example, suppose we have the permutation

$$\pi = (5, 7, 2, 1, 6, 4, 9, 3, 8)$$

of $\{1, 2, \ldots, 9\}$ (so that $\pi(1) = 5$, $\pi(2) = 7$, and so forth). There are four locations in this permutation for which $\pi(i) < \pi(i+1)$: from 5 to 7, from 1 to 6, from 4 to 9, and from 3 to 8. Thus, π has four ascents; they occur at positions 1, 4, 6, and 8. For emphasis, these are underlined here:

$$(\underline{5}, 7, 2, \underline{1}, 6, \underline{4}, 9, \underline{3}, 8).$$

The Eulerian number $\left\langle {m \atop k} \right\rangle$ counts the number of permutations on $[m]$ containing exactly k ascents. For example, $\left\langle {m \atop m} \right\rangle = 0$ for $m \geq 1$; this is because a permutation on $[m]$ can have at most $m-1$ ascents. Moreover, $\left\langle {m \atop m-1} \right\rangle = 1$ because there is only one permutation on $[m]$ with exactly $m-1$ ascents: the identity permutation, which outputs values in increasing order. In addition, $\left\langle {m \atop 0} \right\rangle = 1$ because there is only one permutation on $[m]$ with zero ascents: the permutation that outputs values in decreasing order.

We need a bit more setup in order to prove our second formula for the power sum. Suppose we have a function $f : [m] \mapsto [n]$. Sort the function values so that

$$f(\pi(1)) \leq f(\pi(2)) \leq \cdots \leq f(\pi(m)),$$

where π is the resulting permutation of the domain set $[m]$ and ties are broken by requiring

$$f(\pi(i)) = f(\pi(j)) \implies \pi(i) < \pi(j).$$

For example, suppose we have the function f given by

$$f = (2, 7, 1, 8, 2, 8, 1, 8, 2)$$

(i.e., $f(1) = 2$, $f(2) = 7$, etc.). Sorting these by function value and using our rule for breaking ties, we have

$$f(3) \leq f(7) \leq f(1) \leq f(5) \leq f(9) \leq f(2) \leq f(4) \leq f(6) \leq f(8),$$

as well as the permutation

$$\pi = (3, 7, 1, 5, 9, 2, 4, 6, 8).$$

Given a nondecreasing function $g : [m] \mapsto [n]$, we say that g features a *duplication* at $i \in [m-1]$ if $g(i) = g(i+1)$. For example,

$$g = (1, 1, 2, 2, 2, 7, 8, 8, 8)$$

features duplications at positions 1, 3, 4, 7, and 8.

We also need the following lemma.

Lemma 1. *Given a function $f : [m] \to [n]$ and the implied permutation π of its domain set obtained by sorting the values of f, let $g = f \circ \pi$. If g features a duplication at i then π has an ascent at i.*

Proof. If g features a duplication at i, then $g(i) = g(i+1)$. This means that $f(\pi(i)) = f(\pi(i+1))$. By the rule for breaking ties in the definition of π, we have $\pi(i) < \pi(i+1)$, which means π has an ascent at i. ∎

We're now ready to give a combinatorial proof of the following power sum formula involving the Eulerian numbers.

Theorem 3.

$$\sum_{k=1}^{n} k^m = \sum_{k=0}^{m-1} \left\langle {m \atop k} \right\rangle \binom{n+k+1}{m+1}.$$

Proof. As we know, Theorem 1 says that the left side is the number of functions

$$f : [m+1] \mapsto [n+1]$$

such that, for all $i \in [m]$, $f(i) < f(m+1)$.

For the right side, let $k \in \{0, 1, \ldots, m-1\}$. Suppose $k+1$ is the number of ascents in π, where π is the implied permutation for a function f obtained by sorting the values of f. Since we're counting functions $f : [m+1] \mapsto [n+1]$ such that, for all $i \in [m]$, $f(i) < f(m+1)$, the rule for constructing π requires $\pi(m+1) = m+1$. In addition, $m+1$ is the largest possible value of $[m+1]$, so π must have at least one ascent; namely, at m. Because of these restrictions, choosing π can be accomplished by choosing a permutation σ on $[m]$ with k ascents and extending it via $\pi(i) = \sigma(i)$ for $i \in [m]$ and $\pi(m+1) = m+1$. By the definition of the Eulerian numbers, the selection of σ (and thus of π) can be done in $\left\langle {m \atop k} \right\rangle$ ways.

Denote the ascents in σ by $A_1, A_2, \ldots, A_k$, where $0 \le k \le m-1$. Then choose $m+1$ distinct elements from the set

$$\{1, 2, \ldots, n+1, A_1, A_2, \ldots, A_k\}.$$

There are $\binom{n+k+1}{m+1}$ ways to make this selection.

Now, construct a nondecreasing function $g : [m+1] \mapsto [n+1]$ by placing the chosen elements in a list of length $m+1$ according to the following scheme:

1. For each ascent A_i chosen, place a D (for duplication) in position A_i.
2. Place the elements chosen from $[n+1]$ in order in the remaining spaces.
3. Replace each D with the next numbered element that appears after it.

For example, suppose we have the permutation $\sigma = (2, 4, 1, 3, 5)$. It has ascents $A_1 = 1$, $A_2 = 3$, and $A_3 = 4$. (Remember that we have defined an ascent to be a position, so the ascents occur at positions 1, 3, and 4.) Suppose we choose from the set $\{1, \ldots, 9, A_1, \ldots, A_3\}$ the elements $\{1, 3, 4, 5, 9, A_1\}$. Since $A_1 = 1$, the scheme above gives us the following:

After Step 1: $(D, \_, \_, \_, \_, \_)$.

After Step 2: $(D, 1, 3, 4, 5, 9)$.

After Step 3: $(1, 1, 3, 4, 5, 9)$, which is g.

(Note that this scheme follows Lemma 1 in that duplications in g can only occur at ascents in σ. In particular, there will never be a duplication at position m, as the largest possible ascent in σ occurs at position $m-1$.)

Since π is a permutation it is invertible. Let $f = g \circ \pi^{-1}$, so that $f \circ \pi = g$. Since there are $\left\langle {m \atop k} \right\rangle$ ways to select π and $\binom{n+k+1}{m+1}$ ways to select g given π, there are

$$\left\langle {m \atop k} \right\rangle \binom{n+k+1}{m+1}$$

possible ways to construct f if its implied permutation π has $k+1$ ascents. Summing over all possible values of k gives the right side. ∎

In the example discussed in the proof of Theorem 3, requiring $f \circ \pi = g$ yields $f = (3, 1, 4, 1, 5, 9)$.

As we did with Theorem 2, let's take a look at the special case $m = 3$ of Theorem 3. We have

$$\sum_{k=1}^{n} k^3 = \binom{n+1}{4} + 4\binom{n+2}{4} + \binom{n+3}{4}.$$

In contrast to Theorem 2, Theorem 3 gives us a formula for the power sum in terms of the binomial coefficients in *column* $m + 1$ of Pascal's triangle.

Worpitzky's identity

As a side note, a slight simplification of the proof of Theorem 3 gives us what is known as *Worpitzky's identity*.

Corollary 1 (Worpitzky's identity)**.**

$$x^m = \sum_{k=0}^{m-1} \left\langle {m \atop k} \right\rangle \binom{x+k}{m}.$$

Proof. The left side is the number of functions f from $[m]$ to $[x]$.

For the right side, let π be a permutation of $[m]$. (Here is where the simplification occurs, as we are choosing π directly rather than choosing σ and then constructing π from σ.) Fix $k \in \{0, 1, \ldots, m-1\}$, and suppose k is the number of ascents in π. Then the selection of π can be done in $\left\langle {m \atop k} \right\rangle$ ways.

Then, as in the proof of Theorem 3, select m elements from the set

$$\{1, \ldots, x, A_1, \ldots, A_k\},$$

and construct a non-decreasing function $g : [m] \mapsto [x]$ from those elements. Given a π with k ascents, there are $\binom{x+k}{m}$ different non-decreasing functions g that can be constructed this way.

Finally, let $f = g \circ \pi^{-1}$, so that $f \circ \pi = g$. With $\left\langle {m \atop k} \right\rangle$ ways to construct π and $\binom{x+k}{m}$ ways to construct g, there are

$$\left\langle {m \atop k} \right\rangle \binom{x+k}{m}$$

ways to construct f. Summing over all possible values of k completes the proof. ■

The case $m = 3$ of Worpitzky's identity is the following:

$$x^3 = \binom{x}{3} + 4\binom{x+1}{3} + \binom{x+2}{3}.$$

This, of course, looks quite similar to the $m = 3$ case of Theorem 3.

Additional reading

As we have seen, the interpretation of the power sum given in Theorem 1 leads to combinatorial proofs of two different formulas for the power sum, as well as a combinatorial proof of Worpitzky's identity. Several others have done similar or related work as well.

For more on the Stirling numbers of the second kind, see Graham et al. [**6**, p. 258]. Treviño [**13**] gives an argument similar to our proof of Theorem 2. See also Mackiw [**8**].

Petersen [**10**] is a great resource for more information on the Eulerian numbers. Stanley [**12**] is as well. (Both authors define $\left\langle {m \atop k} \right\rangle$ as the number of permutations on $[m]$ with k *descents*, but the values of $\left\langle {m \atop k} \right\rangle$ are the same under this definition and ours.)

Engbers and Stocker [**3**] contain a combinatorial proof of a generalization of Theorem 3 extended to multisets.

Foata and Schützenberger [**4**], Knuth [**7**, pp. 36–37], and Rawlings [**11**] each contain proofs of Worpitzky's identity similar to ours. Dzhumadil'daev [**2**] uses *barred permutations* to prove a multipermutation generalization of Worpitzky's identity. An even further generalization of Worpitzky is due to MacMahon (see Equation (3.3), with $q = 1$, in Gessel [**5**] for a more modern formulation). In addition, Petersen [**9**] uses barred permutations to derive a variation of Worpitzky's identity for two-sided Eulerian numbers.

REFERENCES

[1] Benjamin, A. T., Quinn, J. J. (2003). *Proofs that Really Count*. Washington, DC: Mathematical Association of America.

[2] Dzhumadil'daev, A. S. (2011). Worpitzky identity for multipermutations. *Math. Notes*. 90(3): 448–450. doi.org/10.1134/S0001434611090136

[3] Engbers, J., Stocker, C. (2016). Two combinatorial proofs of identities involving sums of powers of binomial coefficients. *Integers*. 16: Article A58.

[4] Foata, D., Schützenberger, M. P. (1970). *Théorie géométrique des polynômes Eulériens*. Berlin: Springer-Verlag.

[5] Gessel, I. M. (2016). A historical survey of P-partitions. In: *The Mathematical Legacy of Richard P. Stanley*. Providence, RI: American Mathematical Society, pp. 169–188.

[6] Graham, R. L., Knuth, D. E., Patashnik, O. (1994). *Concrete Mathematics*, 2nd ed. Reading, MA: Addison-Wesley.

[7] Knuth, D. E. (1998). *The Art of Computer Programming, Vol. III: Sorting and Searching*, 2nd ed. Reading, MA: Addison-Wesley.

[8] Mackiw, G. (2000). A combinatorial approach to sums of integer powers. *Math. Mag*. 73(1): 44–46. doi.org/10.1080/0025570X.2000.11996799

[9] Petersen, T. K. (2013). Two-sided Eulerian numbers via balls in boxes. *Math. Mag.* 86(3): 159–176. doi.org/10.4169/math.mag.86.3.159

[10] Petersen, T. K. (2015). *Eulerian Numbers*. New York: Birkhäuser.

[11] Rawlings, D. (1981). Generalized Worpitzky identities with applications to permutation enumeration. *Eur. J. Combin*. 2: 67–78. doi.org/10.1016/S0195-6698(81)80023-6

[12] Stanley, R. P. (2012). *Enumerative Combinatorics, Vol. 1*, 2nd ed. Cambridge: Cambridge University Press.

[13] Treviño, E. (2018). A short proof of a sum of powers formula. *Amer. Math. Monthly.* 125(7): 659. doi.org/10.1080/00029890.2018.1460977

Summary. We give a combinatorial interpretation of the sum of powers of the first n positive integers. Then we use this interpreation to give combinatorial proofs of two formulas for the power sum: one featuring the Stirling numbers of the second kind and one featuring the Eulerian numbers. As a consequence of the latter, we present a combinatorial proof of Worpitzky's identity.

MICHAEL Z. SPIVEY (MR Author ID: 730955) is a professor of mathematics at the University of Puget Sound. His research interests include assignment problems and the binomial coefficients. He has written a book on proving binomial identities, as well as three mathematically inclined works of interactive fiction.

On the Rational Values of Trigonometric Functions of Angles that Are Rational in Degrees

BONAVENTURA PAOLILLO
Liceo Scientifico F. Severi
via G. D'Annunzio, Salerno, Italy
bpaolillo@unisa.com

GIOVANNI VINCENZI
Dipartimento di Matematica, Università di Salerno
via Giovanni Paolo II, 132, I-84084 Fisciano (SA), Italy
vincenzi@unisa.it

The concept of commensurable magnitudes can be traced back to the ancient Greeks [7]. Recall that two magnitudes are commensurable if their ratio is given by a pair of positive integers. An interesting theorem in number theory related to commensurable angles states:

Theorem 1. *If α is rational in degrees, say $\alpha = r360^\circ$ for some rational number r, then the only rational values of the trigonometric functions of α are as follows:*

$$\cos(\alpha),\ \sin(\alpha) = 0,\ \pm(1/2),\ \pm 1,$$
$$\sec(\alpha),\ \csc(\alpha) = \pm 1,\ \pm 2,$$
$$\tan(\alpha),\ \cot(\alpha) = 0,\ \pm 1.$$

This result is sometimes referred to as Niven's theorem, as it appears in two of his books (see [12, Corollary 3.12] or [13, Theorem 6.16]). On the other hand, Niven himself has written:

> A proof of [Theorem 1] ... was given by J. M. H. Olmsted [14]. The topic is a recurring one in the popular literature: as examples we cite H.A. Bradford and H. Eves [1]; R. W. Hamming [8]; E. Swift [16]; R. S. Underwood [17].

In the last fifty years, other authors have produced proofs of this result, and more recently many applications of it, both elementary and advanced, have arisen [2–6, 9–11, 13, 15].

We present a new proof that is very elementary. In our opinion, it is feasible for teachers and it is has proven easy to understand for high school students.

Proof of the theorem

Our proof avoids the advanced tools like induction, the de Moivre formulas, Chebyshev polynomials, or cyclotomic polynomials that are typically used. For instance, see Bergen [3], Calcut [6], Niven, Zuckerman, and Motgomery [13], or Underwood [17]. In Jahnel [11], the reader can find interesting insights for an elementary proof, even if some infinite processes are used in the argument.

The idea of our proof is essentially based on the periodicity of the function $\cos(x)$, which allows us to reduce the problem to the analysis of a few cases.

Math. Mag. **94** (2021) 132–134. doi:10.1080/0025570X.2021.1869479
MSC: 11A99; 97G40

Proof. It is sufficient to confine the proof to the cosine and tangent functions.

First, we assume that $\cos(\alpha)$ is a rational number different from 0. We will prove that

$$\cos(\alpha) \in \left\{\pm 1,\ \pm\frac{1}{2}\right\}.$$

Write

$$\cos(\alpha) = \frac{p}{q} \neq 0,$$

where $p, q \in \mathbb{Z}$ and are coprime.

Fix n such that $n\alpha$ is an integer multiple of 360°.

For every positive integer i, we put $\alpha_i = (\frac{i}{n})360°$. Let m be such that $\alpha_m = \alpha$, so that by hypothesis $\cos(\alpha_m)$ is a rational number. It follows that

$$T_n := \{\cos(\alpha_i) \in \mathbb{Q} \setminus \{0\} \mid i \in \mathbb{N}\},$$

is a finite, non-empty set of rational numbers. Each element of T_n is of the type $\cos(\alpha_i) := \frac{p_i}{q_i}$, where $p_i \in \mathbb{Z} \setminus \{0\}$ and $q_i \in \mathbb{N}$ are coprime. Among them we may choose an element, say $\cos(\alpha_k) = \frac{p_k}{q_k}$, whose denominator q_k is the greatest.

We now have that

$$\alpha_{2k} = 2\alpha_k = \left(2\,\frac{k}{n}\right) 360°.$$

It follows that

$$\cos(\alpha_{2k}) = \cos(2\alpha_k) = \frac{2p_k^2 - q_k^2}{q_k^2}$$

is a rational number.

Note that p_k and q_k are coprime. It follows that if q_k is odd, then $2p_k^2 - q_k^2$ and q_k^2 are both different from 0 and coprime. Hence, by the choice of q_k, we have that $q_k \geq q_k^2$. This yields $q_k = 1$.

If $q_k = 2s$ is even ($s \in \mathbb{N}$), then

$$\cos(2\alpha_k) = \frac{2p_k^2 - q_k^2}{q_k^2} = \frac{p_k^2 - 2s^2}{2s^2}.$$

On the other hand, p_k and q_k are coprime, and each divisor of s is also a divisor of q_k. Therefore, the last term above is a reduced fraction different from 0. By the choice of q_k, we have that

$$q_k \geq 2s^2 = \frac{q_k^2}{2}.$$

Thus, q_k is either 1 or 2, and hence $\cos(\alpha) \in \left\{\pm 1,\ \pm\frac{1}{2}\right\}$.

The $\tan(\alpha)$ part is routine, and we will only sketch the proof.

Suppose that $\tan(\alpha)$ is a rational number. Clearly, we may assume that $0 \leq \alpha < 180°$. It follows by a basic trigonometric relation that

$$\cos(2\alpha) = \frac{1 - \tan^2(\alpha)}{1 + \tan^2(\alpha)},$$

is a rational number. The first part of the proof shows that

$$2\alpha \in \{0°, 60°, 90°, 120°, 180°, 240°, 270°, 300°\}.$$

It follows that

$$\alpha \in \{0°, 30°, 45°, 60°, 90°, 120°, 135°, 150°\}.$$

By hypothesis $\tan(\alpha)$ is rational, so that the only possible values for α are $0°$, $45°$, $135°$.

This completes the proof. ■

REFERENCES

[1] Bradford, H. A., Eves H. (1949). A simple proof that, for odd $p > 1$ $\arccos(1/p)$ and π are incommensurable. *Amer. Math. Monthly.* 56: 20–21.
[2] Barbeau, E. J. (1983). Incommensurability proof: A pattern that Peters out. *Math. Mag.* 56(2): 82–90.
[3] Bergen, J. (2009). Values of trigonometric functions. *Math Horizons.* 16(3): 17–19.
[4] Berger, A. (2017). More grade school triangles. *Amer. Math. Monthly.* 124(4): 324–336.
[5] Berger, A. (2018). On linear independence of trigonometric numbers. *Carpathian J. Math.* 34(2): 156–166.
[6] Calcut, J. S. (2010). Grade school triangles. *Amer. Math. Monthly.* 117: 673–685.
[7] Filep, L. (2003). Proportion theory in Greek mathematics. *Acta Math. Acad. Paedagog. Nyregyháziensis*. 19: 167–174.
[8] Hamming, R. W. (1945). Convergent monotone series. *Amer. Math. Monthly.* 52: 336–337.
[9] Lupu, C. (2015). *Algebraic integer and application to elementary problems*. lupucezar.files.wordpress.com/2015/06
[10] Moreno, S. G., Garcìa-Caballero, E. M. (2013). To be integer or not be rational: That is $\sqrt{n}$. *Teach. Math.* XVI(2): 79–81.
[11] Jahnel, J. (2010). When co(sin) of a rational angle equal to a rational number? arXiv no. 1006.2938.
[12] Niven, I. (1956). *Irrational Numbers*. The Carus Mathematical Monograph. The Mathematical Association of America. Hoboken, NJ: Wiley.
[13] Niven, I., Zuckerman, H. S., Montgomery, H. L. (1991). *An Introduction to the Theory of Numbers*, 5th ed. New York: Wiley.
[14] Olmsted, J. M. H. (1945). Rational values of trigonometric functions. *Amer. Math. Monthly*. 52(9): 507–508.
[15] Schaumberger, N. (1974). A classroom theorem on trigonometric irrationalities. *The Two-Year College Math. J.* 5(1): 73–76.
[16] Swift, S. (1922). Note on trigonometric functions. *Amer. Math. Monthly*. 29: 404–405.
[17] Underwood, R. S. (1921). On the irrationality of certain trigonometric functions. *Amer. Math. Monthly*. 28: 374–376.

Summary. We give an elementary proof of the well-known theorem that gives the rational values of trigonometric functions of angles that are rational in degrees. Our proof avoids the traditional arguments based on induction, the de Moivre formulas, Chebyshev polynomials, or cyclotomic polynomials that are typically used.

BONAVENTURA PAOLILLO (MR Author ID: 928400, ORCID: 0000-0001-7773-5564) received his Ph.D. in mathematics from the University of Salerno (Italy). His main interest is in elementary mathematics from a higher point of view. He teaches at "Liceo Scientifico F. Severi" Secondary High School and collaborates with the Department of Mathematics at the University of Salerno.

GIOVANNI VINCENZI (MR Author ID: 329840, ORCID: 0000-0002-3869-885X) received his Ph.D. in mathematics from University of Napoli "Federico II" (Italy). He is a professor of algebra at the University of Salerno. He has interests in many branches of mathematics.

A New Proof of the Ionescu–Weitzenböck Inequality

NAM GU HEO
Sunchon National University
255 Jungangno, Suncheon
Jeonnam 57922, Korea
ngheo@scnu.ac.kr

Let $a \le b \le c$ be the sides of a triangle, and let T be its area. Prove:

$$a^2 + b^2 + c^2 \ge 4\sqrt{3}T.$$

In what case does equality hold?

This problem appeared in the third International Mathematical Olympiad (IMO) in 1961. We can prove the required inequality by using the trigonometric identities

$$T = \frac{bc \sin A}{2}$$

$$a^2 = b^2 + c^2 - 2bc \cos A$$

$$\frac{\sqrt{3}\sin A + \cos A}{2} = \cos(A - \pi/3),$$

and this method was the official solution that was presented [2]. This inequality has important applications and is useful in the theory of geometric inequalities [5]. The inequality was published in 1919 by Roland Weitzenböck [6]. I. Ionescu published a similar problem in 1897 (note that $\triangle$ denotes the area of the triangle):

Prove that there is no triangle for which the inequality

$$4\sqrt{3}\triangle > a^2 + b^2 + c^2$$

can be satisfied. [4]

Since this is equivalent to Weitzenböck's inequality, the inequality in the IMO problem is called the Ionescu–Weitzenböck inequality.

Engel subsequently presented eleven proofs of the inequality [3]. In 2008, Alsina and Nelsen presented a geometric proof [1]. And we now present a new algebraic proof of the Ionescu–Weitzenböck's inequality.

Theorem (Ionescu–Weitzenböck inequality)**.** *Let $a \le b \le c$ be the sides of a triangle, and T its area. Then*

$$a^2 + b^2 + c^2 \ge 4\sqrt{3}T.$$

Proof. With the notation as in Figure 1 we have that:

$$a^2 + b^2 + c^2 = \{(\frac{c}{2} + MH)^2 + h^2\} + \{(\frac{c}{2} - MH)^2 + h^2\} + c^2$$

Math. Mag. **94** (2021) 135–136. doi:10.1080/0025570X.2021.1869494
MSC: 51M25

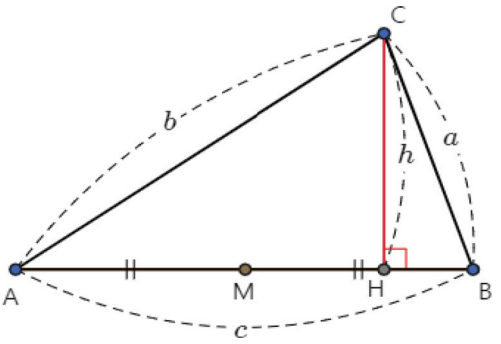

Figure 1 The diagram for our proof of the Ionescu–Weitzenböck inequality.

$$= \frac{c^2}{2} + 2MH^2 + 2h^2 + c^2$$
$$\geq \frac{3c^2}{2} + 2h^2.$$

Using the arithmetic-geometric mean inequality leads to:

$$\frac{3c^2}{2} + 2h^2 \geq 2\sqrt{\frac{3c^2}{2} \times (2h^2)} = 2\sqrt{3}ch = 4\sqrt{3}T.$$

Equality holds if and only if $MH = 0$ and $MC' = \sqrt{3}AM$. That is, equality holds if and only if $\triangle ABC$ is an equilateral triangle. This completes the proof. ■

REFERENCES

[1] Alsina, C., Nelsen, R. B. (2008). Geometric proofs of the Weitzenböck and Hadwiger-Finsler inequalities. *Math. Mag.* 81(3): 216–219.
[2] Djukić, D., Janković, V., Matić, I., Petrovic, N. (2006). *The IMO Compendium*. New York: Springer.
[3] Engel, A. (1998). *Problem Solving Strategies*. Berlin: Springer Verlag.
[4] Ionescu, I. (1897). Problem 273. *Rom. Math. Gaz.* 3(2): 52.
[5] Stoica, E., Minculete, N., Barbu, C. (2016). New aspects of Ionescu-Weitzenböck's inequality. *Balkan J. Geom. Appl.* 21(2): 95–101.
[6] Weitzenböck, R. (1919). Uber eine Ungleichung in der Dreiecksgeometrie. *Math. Z.* 5(1–2): 137–146.

Summary. We prove the Ionescu–Weitzenböck inequality using algebraic and geometric methods.

NAM GU HEO (MR Author ID: 1106949, ORCID: 0000-0002-6584-4971) studied mathematics education and received an Ed.D. from the Korea National University of Education. Currently he is a professor at Sunchon National University, Korea.

Plato's Approximation of Pi

ROGER B. NELSEN
Lewis & Clark College
Portland, OR 97219
nelsen@lclark.edu

Did Plato approximate π? There is no evidence that he did so. The myth that he did seems to have originated in the book *The Open Society and its Enemies* by the British philosopher Karl Popper (1902–1994) [1]. In note 9 to Chapter 6, Popper writes: "It is a curious fact that $\sqrt{2}+\sqrt{3}$ very nearly approximates π. . . . A kind of explanation of this curious fact is that it follows from the fact that the arithmetical mean of the areas of the circumscribed hexagon and the inscribed octagon is a good approximation of the area of the circle."

After noting that Plato was interested in adding irrational numbers and must have added $\sqrt{2}+\sqrt{3}$, Popper writes: "It seems a plausible hypothesis that Plato knew of $[\sqrt{2}+\sqrt{3} \approx \pi]$, but was unable to prove whether or not is was a strict inequality or only an approximation. . . . I must again emphasize that no direct evidence is known to me to show that this was in Plato's mind: but if we consider the indirect evidence here marshaled, then the hypothesis does perhaps not seem too far-fetched."

The approximation is actually quite good, as it yields $\pi \approx 3.146264$ for a relative error of about 0.1487%. The purpose of this note is to establish the inequality in the approximation, that is, to show analytically that $\pi < \sqrt{2}+\sqrt{3}$. We do this with simple rational approximations to the three constants. For the square roots we have $\sqrt{2} > 41/29$ since $2 > 1681/841$, and $\sqrt{3} > 71/41$ since $3 > 5041/1681$. Thus,

$$\sqrt{2}+\sqrt{3} > \frac{41}{29}+\frac{71}{41} = 3\frac{173}{1189} > 3\frac{1}{7} > \pi.$$

The rational approximations to $\sqrt{2}$ and $\sqrt{3}$ were obtained by observing that $(x, y) = (41, 29)$ is a solution to the Pell equation $x^2 - 2y^2 = -1$ and $(x, y) = (71, 41)$ is a solution to the Pell equation $x^2 - 3y^2 = -2$. A proof of the rightmost inequality follows from solving problem A-1 on the 1968 Putnam examination:

$$\text{Prove } \frac{22}{7} - \pi = \int_0^1 \frac{x^4(1-x)^4}{1+x^2}\,dx$$

and noting that the integral is positive. To solve the problem, write the integrand as

$$\frac{x^4(1-x)^4}{1+x^2} = x^6 - 4x^5 + 5x^4 - 4x^2 + 4 - \frac{4}{1+x^2}.$$

Acknowledgments The author wishes to thank an anonymous reviewer for very helpful comments and suggestions on an earlier draft of this note.

REFERENCE

[1] Popper, K. R. (1963). *The Open Society and its Enemies*, Vol. 1. Princeton, NJ: Princeton University Press.

Summary. We discuss the approximation $\pi \approx \sqrt{2}+\sqrt{3}$.

ROGER B. NELSEN (MR Author ID 237909, ORCID: 0000-0002-3632-6577) is a professor emeritus at Lewis & Clark College, where he taught mathematics and statistics for 40 years.

Math. Mag. **94** (2021) 137. doi:10.1080/0025570X.2021.1869482
MSC: 51M16, 26D20

Report on the 49th Annual USA Mathematical Olympiad

BÉLA BAJNOK
Gettysburg College
Gettysburg, PA 17325
bbajnok@gettysburg.edu

The American Mathematics Competitions (AMC) program of the Mathematical Association of America consists of a series of examinations for middle school, high school, and college students, designed to build problem solving skills, foster a love of mathematics, and identify and nurture talented students across the United States. The final round at the high-school level is the USA Mathematical Olympiad (USAMO). This competition follows the style of the International Mathematics Olympiad: It consist of three problems each on two consecutive days, with an allowed time of four and a half hours both days.

The 49th annual USAMO was given on June 19–20, 2020. About 230 students were invited to take the exam; for the first time in history, the competition was administered online. The names of winners and honorable mentions, as well as more information on the AMC program, can be found on the site maa.org/math-competitions.

The problems of the USAMO are chosen—from a large collection of proposals submitted for this purpose—by the USAMO Editorial Board, whose co-editors-in-chief are Evan Chen and Jennifer Iglesias, with associate editors John Berman, Zuming Feng, Sherry Gong, Alison Miller, Maria Monks Gillespie, and Alex Zhai. This year's problems were created by Ankan Bhattacharya, Antonia Bluher, Zuming Feng, Carl Schildkraut, David Speyer, Richard Stong, and Alex Zhai.

The solutions presented here were composed by the present author, and are based on the competition papers of Ankit Bisain (11th grade, Canyon Crest Academy, CA), Jeffrey Kwan (12th grade, Harker Upper School, CA), Rupert Li (12th grade, Jesuit High School, OR), Holden Mui (11th grade, Naperville North High School, IL), Yuru Niu (12th grade, Suncoast High School, FL), Ishika Shah (12th grade, Cupertino High School, CA), and Brandon Wang (12th grade, Saratoga High School, CA). Each problem was worth 7 points; the nine-tuple $(n; a_7, a_6, a_5, a_4, a_3, a_2, a_1, a_0)$ states the number of students who submitted a paper for the relevant problem, followed by the numbers who scored $7, 6, \ldots, 0$ points, respectively.

Problem 1 (186; 143, 4, 0, 0, 0, 8, 16, 15).

Let ABC be a fixed acute triangle inscribed in a circle ω with center O. A variable point X is chosen on minor arc AB of ω, and segments CX and AB meet at D. Denote by O_1 and O_2 the circumcenters of triangles ADX and BDX, respectively. Determine all points X for which the area of triangle OO_1O_2 is minimized.

SOLUTION. Let points M, N, R, and S denote, in order, the midpoints of $\overline{CX}$, $\overline{DX}$, $\overline{AD}$, and $\overline{DB}$. Since C and X are equidistant from O, $\overline{OM}$ is the perpendicular bisector of $\overline{CX}$. Similarly, $\overline{RO_1}$ is the perpendicular bisector of $\overline{AD}$, $\overline{SO_2}$ is the perpendicular bisector of $\overline{DB}$, and $\overline{O_1N}$ and $\overline{O_2N}$ are both perpendicular bisectors of $\overline{DX}$; in particular, O_1, N, and O_2 are collinear. This is shown in Figure 1. We then see that $RS = \frac{1}{2}AB$

Math. Mag. **94** (2021) 138–147. doi:10.1080/0025570X.2021.1867408
MSC: 00-01

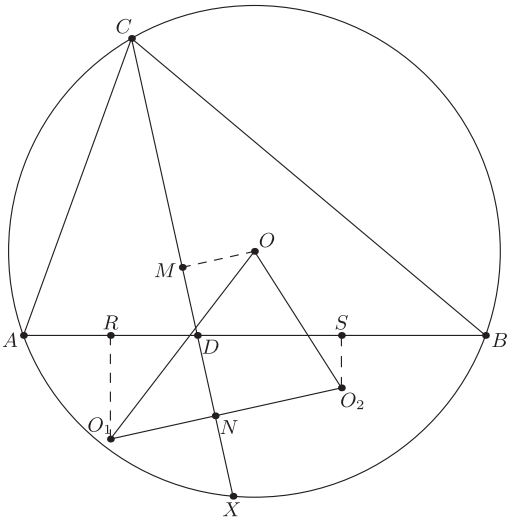

Figure 1 The diagram for Problem 1.

and

$$MN = MX - NX = \frac{1}{2}CX - \frac{1}{2}DX = \frac{1}{2}CD.$$

Since in quadrilateral $RDNO_1$ the angles at D and O_1 are supplementary, the angles $\angle ADC$ and $\angle RO_1O_2$ are equal. Therefore,

$$RS = O_1O_2 \sin \angle ADC,$$

and thus

$$O_1O_2 = \frac{AB}{2 \sin \angle ADC}.$$

Furthermore, since lines OM and O_1O_2 are parallel, the distance from O to $\overline{O_1O_2}$ equals MN.

We can now see that the area of triangle OO_1O_2 equals

$$\frac{1}{2}\,(O_1O_2)\,(MN) = \frac{(AB)\,(CD)}{8 \sin \angle ADC}.$$

Note that CD is minimized when $\overline{CD} \perp \overline{AB}$, and $\sin \angle ADC$ is maximized when $\angle ADC = \pi/2$. This is a happy coincidence, as the same point X works for both of these conditions: the area of triangle OO_1O_2 is minimized when X is the (unique) point with $\overline{CX} \perp \overline{AB}$.

Problem 2 (156; 57, 35, 8, 2, 3, 9, 7, 35).

An empty $2020 \times 2020 \times 2020$ cube is given, and a 2020×2020 grid of square unit cells is drawn on each of its six faces. A *beam* is a $1 \times 1 \times 2020$ rectangular prism. Several beams are placed inside the cube subject to the following conditions:

- The two 1×1 faces of each beam coincide with unit cells lying on opposite faces of the cube. (Hence, there are $3 \cdot 2020^2$ possible positions for a beam.)

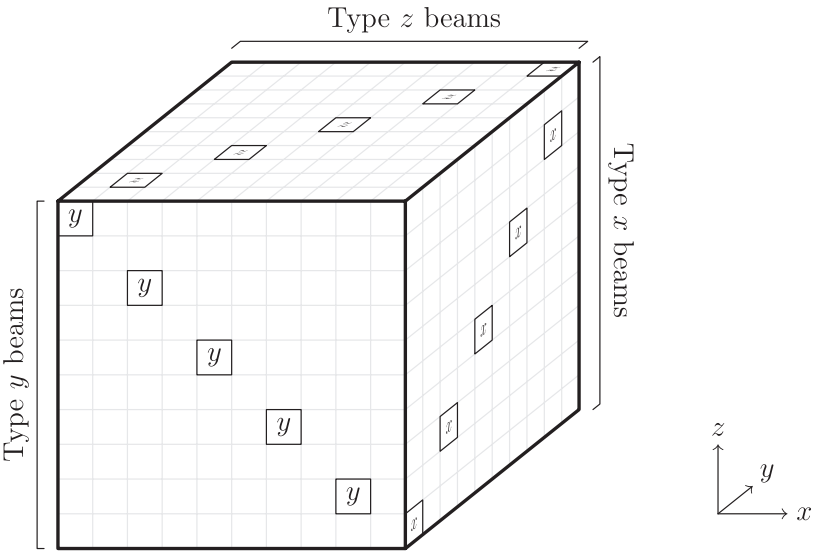

Figure 2 The diagram for Problem 2.

- No two beams have intersecting interiors.
- The interiors of each of the four 1×2020 faces of each beam touch either a face of the cube or the interior of the face of another beam.

What is the smallest positive number of beams that can be placed to satisfy these conditions?

SOLUTION. Let n be a positive even integer, and consider an $n \times n \times n$ cube. We claim that the smallest positive number of beams satisfying the three analogous conditions (where 2020 is replaced by n) is $3n/2$ (and thus equals 3030 for the case of $n = 2020$).

To facilitate our deliberation, we place the cube into the Cartesian coordinate system so that its edges are parallel to the coordinate axes, with one of its corners at the origin and another at the point (n, n, n). We can then label the n^3 cells of the cube by their corners furthest from the origin. For positive integers $a, b \leq n$, we then let $B_x(a, b)$ denote the *type x beam* consisting of cells (t, a, b) with $t = 1, 2, \ldots, n$; similarly, we let $B_y(a, b)$ denote the *type y beam* consisting of cells (a, t, b), and $B_z(a, b)$ denote the *type z beam* consisting of cells (a, b, t).

To see that there is a valid configuration with $3n/2$ beams, consider the collection consisting of beams

$$B_x(1, 1), B_x(3, 3), \ldots, B_x(n - 1, n - 1),$$

$$B_y(1, n), B_y(3, n - 2), \ldots, B_y(n - 1, 2),$$

and

$$B_z(2, 2), B_z(4, 4), B_z(6, 6), \ldots, B_z(n, n),$$

illustrated for $n = 10$ in Figure 2.

Clearly, our collection consists of $3n/2$ beams satisfying the first condition.

We can verify that our collection also satisfies the second condition, as follows. Note that

- each type x beam in the collection consists of cells whose second and third coordinates are odd,
- each type y beam consists of cells whose first coordinate is odd and third coordinate is even, and
- each type z beam consists of cells whose first and second coordinates are even.

Therefore, no two beams in the collection have intersecting interiors, and thus the second condition holds.

Finally, to see that our third condition is satisfied, consider first a type x beam B. We see that the interior of each horizontal face (that is, each face perpendicular to the z axis) of B touches the interior of a type y beam or a face of the cube, and the interior of each vertical face (that is, each face perpendicular to the y axis) of B touches the interior of a type z beam or a face of the cube. Since analogous observations apply to type y beams and type z beams, we conclude that our collection of beams satisfies all three required conditions.

It remains to be shown that any valid construction must use at least $3n/2$ beams. Let N_x, N_y, and N_z denote the number of beams of type x, y, and z, respectively. If any two of these three quantities are zero, then the third must equal n^2, since the collection must then contain all possible beams of that type. Since $n^2 > 3n/2$, we may assume that at least two of N_x, N_y, or N_z are nonzero.

Next, we prove that $N_x + N_y \geq n$. By a *horizontal beam*, we mean a beam of type x or type y; by the previous paragraph, we must have at least one horizontal beam. According to the third condition, the interior of each horizontal face of each horizontal beam must touch the face of the cube or the interior of a face of another beam; clearly, this other beam would also need to be a horizontal beam. Repeating this observation, we find that we must have at least n horizontal beams, proving our claim.

By a similar argument, we have $N_y + N_z \geq n$ and $N_z + N_x \geq n$, and so

$$N_x + N_y + N_z = \frac{1}{2}(N_x + N_y) + \frac{1}{2}(N_y + N_z) + \frac{1}{2}(N_z + N_x) \geq \frac{3}{2}n,$$

proving our claim.

Problem 3 (148; 30, 1, 1, 0, 5, 3, 11, 97).

Let p be an odd prime. An integer x is called a *quadratic non-residue* if p does not divide $x - t^2$ for any integer t. Denote by A the set of all integers a such that $1 \leq a < p$, and both a and $4 - a$ are quadratic non-residues. Calculate the remainder when the product of the elements of A is divided by p.

Solution. We prove that the requested remainder is 2. As one can easily see that for $p = 3$ we have $A = \{2\}$, from here we will assume that $p \geq 5$, and work in the finite field $\mathbb{F}_p$, which here we identify with the set $\{0, 1, 2, \ldots, p-1\}$ with operations carried out mod p.

An element n of $\mathbb{F}_p$ is a *quadratic residue* when $n = t^2$ holds for some $t \in \mathbb{F}_p$ (it can be easily seen that there are at most two such t) and is a *quadratic non-residue* otherwise (this corresponds to the definition as stated in the problem). We will need the following facts: the product of two quadratic residues is a quadratic residue; the product of two quadratic non-residues is a quadratic residue; and the product of a quadratic residue and a quadratic non-residue is a quadratic non-residue.*

*For a proof of these claims and other properties of quadratic residues see, for example, Chapter VI of Hardy and Wright [2].

We let A be the set of all elements $a \in \mathbb{F}_p$ such that both a and $4 - a$ are quadratic non-residues, and we let B denote the set of all $b \in \mathbb{F}_p$ for which both b and $4 - b$ are quadratic residues. Note that $0 \in B$, $4 \in B$, and $2 \in A \cup B$.

Now consider an element $n \in A \cup B$. Since $n(4 - n)$ is then either the product of two quadratic residues or two quadratic non-residues, it must be a quadratic residue. Furthermore, the element $4 - n(4 - n)$ is a quadratic residue as well, because it is equal to $(n - 2)^2$. This then implies that $n(4 - n) \in B$.

Conversely, we prove that for every $b \in B$, there is an element $n \in A \cup B$ such that $n(4 - n) = b$. Indeed, since $b \in B$, we have $4 - b \in B$ as well, so there must be an element $n \in \mathbb{F}_p$ for which $(n - 2)^2 = 4 - b$, that is, $n(4 - n) = b$. But b is a quadratic residue, so either both n and $4 - n$ are quadratic residues or they are both quadratic non-residues, so $n \in A \cup B$. Moreover, we can see that, unless $b = 4$, in which case $n = 2$ is the only solution, the equation $n(4 - n) = b$ has exactly two solutions, n and $4 - n$.

We thus see that there is a bijection between the unordered pairs $\{n, 4 - n\}$ (allowing for the pair $\{2, 2\}$) of $A \cup B$ and the elements of B, given by the map

$$\{n, 4 - n\} \mapsto n(4 - n).$$

Note that $\{0, 4\}$ maps to 0, and $\{2, 2\}$ maps to 4. Consequently, when $2 \in A$, the product of the elements of $(A \cup B) \setminus \{0, 2, 4\}$ equals the product of the elements in $B \setminus \{0, 4\}$. This means that the product of the elements in $A \setminus \{2\}$ must be 1, and thus the product of the elements in A equals 2.

The situation is similar when $2 \in B$, but this time the product of the elements of $(A \cup B) \setminus \{0, 2, 4\}$ equals twice the product of the elements in $B \setminus \{0, 4\}$. This implies that the product of the elements in A again equals 2.

Problem 4 (179; 73, 1, 0, 0, 0, 0, 88, 17).

Suppose that

$$(a_1, b_1), (a_2, b_2), \ldots, (a_{100}, b_{100})$$

are distinct ordered pairs of nonnegative integers. Let N denote the number of pairs of integers (i, j) satisfying $1 \le i < j \le 100$ and $|a_i b_j - a_j b_i| = 1$. Determine the largest possible value of N over all possible choices of the 100 ordered pairs.

First Solution. We claim that the answer is $N = 2n - 3$ for $n \ge 2$ ordered pairs (197 for $n = 100$). Let

$$P_1 = (a_1, b_1), \ldots, P_n = (a_n, b_n).$$

We say that points P_i and P_j are *enchanted* if $|a_i b_j - a_j b_i| = 1$; note that, by the Shoelace Formula, this is equivalent to triangle OP_iP_j (where O is the origin) having area $1/2$. It is easy to see that the n points

$$P_1 = (0, 1), P_2 = (1, 2), P_3 = (1, 3), \ldots, P_n = (1, n)$$

contain $2n - 3$ enchanted pairs: P_1 is enchanted with the other $n - 1$ points, and P_i is enchanted with P_{i+1} for each $i = 2, 3, \ldots, n - 1$.

We will now use induction to prove that $N \le 2n - 3$ for every $n \ge 2$. This being trivial for $n = 2$, assume that our claim holds for each collection of $n - 1$ points for some $n \ge 3$, and consider a collection

$$P_1 = (a_1, b_1), \ldots, P_n = (a_n, b_n).$$

Without loss of generality, we assume that $a_n + b_n \geq a_i + b_i$ for all $1 \leq i \leq n$. By our inductive assumption, it suffices to show that P_n is enchanted with at most two other points.

If this were not the case, then we would have two points P_i and P_j that have the same distance from line OP_n and are on the same side of that line. But then P_iP_j is parallel to OP_n, so

$$\overrightarrow{P_iP_j} = t \cdot \overrightarrow{OP_n} = \langle ta_n, tb_n \rangle$$

for some scalar t, and we may assume that $t > 0$. Since P_i and P_j have integer coordinates, ta_n and tb_n are integers, so $|b_i ta_n - a_i tb_n| = t$ is an integer as well. Therefore, $t \geq 1$, and since $P_i \neq O$, we arrive at

$$a_j + b_j = (a_i + ta_n) + (b_i + tb_n) > a_n + b_n,$$

contradicting our choice of P_n.

Second Solution. First, we recall that the *Farey sequence* of order m is the increasing sequence of fractions a/b of relatively prime integers a and b with $0 \leq a \leq b \leq m$. The property of Farey sequences that we need here is that a/b and a'/b' are consecutive terms in some Farey sequence if, and only if, $|a'b - ab'| = 1$.[†]

Suppose now that

$$(a_1, b_1), (a_2, b_2), \ldots, (a_n, b_n)$$

are distinct ordered pairs of nonnegative integers, so that there are N pairs of integers (i, j) satisfying $1 \leq i < j \leq n$ and $|a_i b_j - a_j b_i| = 1$. We shall use induction to prove that $N \leq 2n - 3$ for every $n \geq 2$. This obviously holds for $n = 2$ and $n = 3$, so let $n \geq 4$. Without loss of generality, we arrange our points so that $\max(a_n, b_n) \geq \max(a_i, b_i)$ for each $1 \leq i \leq n$. Furthermore, we may assume that $a_n \leq b_n$, since if this were not the case, we could instead consider the mirror image of our n points with respect to the line $y = x$. Note that our assumptions imply that $b_n \geq 2$, since we can only have $b_n = 1$ for $n \leq 3$. Our goal is to show that there are at most two indices $1 \leq i \leq n - 1$ for which $|a_i b_n - a_n b_i| = 1$. Our claim will then follow by induction.

Observe that if $|a_i b_n - a_n b_i| = 1$, then $a_i \leq b_i$. Indeed, if this were not the case, then we would have $a_i \geq b_i + 1$, so

$$\begin{aligned} 1 = |a_i b_n - a_n b_i| &= a_i b_n - a_n b_i \\ &\geq (b_i + 1) b_n - a_n b_i \\ &= b_i (b_n - a_n) + b_n \geq b_n \geq 2, \end{aligned}$$

a contradiction. Note also that $|a_i b_n - a_n b_i| = 1$ implies that $b_i \neq 0$ and

$$\gcd(a_i, b_i) = \gcd(a_n, b_n) = 1.$$

Therefore, a_i/b_i and a_n/b_n are consecutive terms in some Farey sequence. We need to show that this can happen for at most two indices i. But this is clearly the case: a_n/b_n appears only in Farey sequences of order b_n or more; it can have at most two neighbors in the Farey sequence of order b_n; and if a_i/b_i and a_n/b_n are not consecutive in the Farey sequence of order b_n, then they are also not consecutive in one with order more than b_n.

[†]For this and other interesting features of Farey sequences see, for example, Chapter III of Hardy and Wright [2].

To show that $N = 2n - 3$ is achievable, we may start with any two fractions a/b and a'/b' that are consecutive in some Farey sequence. Inserting $(a + a')/(b + b')$ between them results in three consecutive fractions, since

$$|b(a + a') - a(b + b')| = 1$$

and

$$|b'(a + a') - a'(b + b')| = 1.$$

Repeating this process then yields n points with $N = 2n - 3$ pairs with the desired property. (For example, starting with $0/1$ and $1/2$, and inserting the just-described fraction next to $0/1$ each time, yields the sequence $0/1, 1/n, 1/(n-1), \ldots, 1/2$, corresponding to the example of the first solution.)

Problem 5 (140; 21, 9, 1, 9, 17, 17, 49, 17).

A finite set S of points in the coordinate plane is called *overdetermined* if $|S| \geq 2$ and there exists a nonzero polynomial $P(t)$, with real coefficients and of degree at most $|S| - 2$, satisfying $P(x) = y$ for every point $(x, y) \in S$. For each integer $n \geq 2$, find the largest integer k (in terms of n) such that there exists a set of n distinct points that is *not* overdetermined, but has k overdetermined subsets.

Solution. Recall that for every nonempty finite set S in the coordinate plane consisting of points with distinct x coordinates, there exists a unique polynomial f_S, called the *interpolating polynomial of* S, which has real coefficients and degree at most $|S| - 1$, and which satisfies $f(x) = y$ for every point $(x, y) \in S$. Thus we can say that S is overdetermined if and only if it has at least two elements and its interpolating polynomial has degree at most $|S| - 2$. (Note that sets containing points that share their x coordinates do not have interpolating polynomials.)

Let $n \geq 2$, and consider the set

$$A = \{(1, 2)\} \cup \{(2, 1), (3, 1), \ldots, (n, 1)\}.$$

Then

$$f_A(x) = 1 + \frac{1}{(n-1)!}(2 - x)(3 - x) \cdot \cdots \cdot (n - x),$$

so A is not overdetermined. However, each of its subsets not containing $(1, 2)$ and having size at least 2 has interpolating polynomial of degree 0 and is thus overdetermined. So we have found a non-overdetermined set of size n with at least

$$\binom{n-1}{2} + \binom{n-1}{3} + \cdots + \binom{n-1}{n-1} = 2^{n-1} - n \tag{1}$$

overdetermined subsets. We will now prove that we cannot do better.

Let A be a set of $n \geq 2$ distinct points in the coordinate plane. We will prove that if it has more than $2^{n-1} - n$ overdetermined subsets, then it is overdetermined. Let N_m denote the number of overdetermined m-subsets of A. By (1), it suffices to show that if $N_m > \binom{n-1}{m}$ for some $2 \leq m \leq n - 1$, then A is overdetermined. We will, in fact, prove the stronger statement that if $N_m > \binom{n-1}{m}$ for some $2 \leq m \leq n - 1$, then not just A but all its subsets of size at least m are overdetermined.

Keeping m as fixed, we use induction on n. Suppose first that $n = m + 1 \geq 3$ and that $N_m > 1$. Let $P_1 = (x_1, y_1)$ and $P_2 = (x_2, y_2)$ be distinct points in A for which

$A \setminus P_1$ and $A \setminus P_2$ are overdetermined. Then $f_{A\setminus P_1}$ and $f_{A\setminus P_2}$ are polynomials of degree at most $|A| - 3$; since they agree on $|A| - 2$ values of x, they must be equal for all values of x, and thus

$$f_{A\setminus P_1}(x_1) = f_{A\setminus P_2}(x_1) = y_1$$

and

$$f_{A\setminus P_2}(x_2) = f_{A\setminus P_1}(x_2) = y_2.$$

This means that A has an interpolating polynomial and it is of degree at most $|A| - 3$, which then implies that A and all its subsets of size $|A| - 1$ are overdetermined, as claimed.

Suppose now that our claim holds for all sets of size $n - 1$, and consider a set A of size n with $N_m > \binom{n-1}{m}$ for some $2 \le m \le n - 1$. Since each m-subset of A is in $n - m$ subsets of size $n - 1$, and since

$$\frac{\binom{n-1}{m}}{\binom{n-2}{m}} = \frac{n-1}{n-m-1} > \frac{n}{n-m},$$

at least one of the n subsets of A of size $n - 1$ has more than $\binom{n-2}{m}$ overdetermined subsets of size m. Let one such subset be $A \setminus \{P\}$. By our inductive assumption, all subsets of $A \setminus \{P\}$ of size at least m are overdetermined. Since $N_m > \binom{n-1}{m}$, there is an overdetermined set of A of size m that is not a subset of $A \setminus \{P\}$. Let S be one of these sets. Let $Q \notin S$, and consider $A \setminus \{Q\}$.

Note that the $\binom{n-2}{m}$ m-subsets of $A \setminus \{Q, P\}$ are all overdetermined, and so is S. Therefore, by our inductive hypothesis again, all subsets of $A \setminus \{Q\}$ of size at least m are overdetermined. But now we have at least two overdetermined subsets of A of size $n - 1$, so A is overdetermined as well.

It remains to be shown that all subsets of A containing both P and Q and having size between m and $n - 1$, inclusive, are overdetermined. For this purpose, we let R be an arbitrary element of $A \setminus \{P, Q\}$, and we show that all subsets of $A \setminus \{R\}$ of size at least m are overdetermined. Note that all m-subsets of $A \setminus \{P, R\}$ and all m-subsets of $A \setminus \{Q, R\}$ are overdetermined, giving a total of more than $\binom{n-2}{m}$ overdetermined m-subsets of $A \setminus \{R\}$, so our claim follows from our inductive hypothesis. Our proof is now complete.

Problem 6 (88; 4, 2, 1, 0, 0, 0, 1, 80).

Let $n \ge 2$ be an integer. Let $x_1 \ge x_2 \ge \cdots \ge x_n$ and $y_1 \ge y_2 \ge \cdots \ge y_n$ be $2n$ real numbers such that

$$0 = x_1 + x_2 + \cdots + x_n = y_1 + y_2 + \cdots + y_n$$

and

$$1 = x_1^2 + x_2^2 + \cdots + x_n^2 = y_1^2 + y_2^2 + \cdots + y_n^2.$$

Prove that

$$\sum_{i=1}^{n} (x_i y_i - x_i y_{n+1-i}) \ge \frac{2}{\sqrt{n-1}}.$$

SOLUTION. We will use the rearrangement inequality, which can be stated as follows. Suppose that $x_1 \geq x_2 \geq \cdots \geq x_n$ and $y_1 \geq y_2 \geq \cdots \geq y_n$ are real numbers. Let S_n be the set of permutations of $\{1, 2, \ldots, n\}$, and for each $\sigma \in S_n$, set

$$f(\sigma) = \sum_{i=1}^{n} x_i y_{\sigma(i)}.$$

With these notations, $f(\sigma)$ is maximized when σ is the identity permutation (that is, $\sigma(i) = i$ for each $1 \leq i \leq n$) and minimized when σ is the reverse identity permutation (that is, $\sigma(i) = n + 1 - i$ for each $1 \leq i \leq n$).[‡]

We will also need the following.

Lemma 1. *Suppose that $a_1, \ldots, a_k$ are real numbers, with $a_1 \geq a_i \geq a_k$ for all $1 \leq i \leq k$. Suppose that $0 = \sum_{i=1}^{k} a_i$ and $A = \sum_{i=1}^{k} a_i^2$. Then*

$$a_1 - a_k \geq 2\sqrt{A/k}.$$

Proof. Let $a = (a_1 + a_k)/2$. Then

$$\sum_{i=1}^{k} (a_i - a)^2 = \sum_{i=1}^{k} a_i^2 - 2a \sum_{i=1}^{k} a_i + \sum_{i=1}^{k} a^2 \geq A.$$

Note that

$$(a_1 - a)^2 = (a_k - a)^2 \geq (a_i - a)^2$$

for all $1 \leq i \leq k$, so

$$a_1 - a \geq \sqrt{A/k} \qquad \text{and} \qquad a - a_k \geq \sqrt{A/k}.$$

Adding these two inequalities proves our claim. ∎

We will now compute

$$\sum_{\sigma \in S_n} f(\sigma) \qquad \text{and} \qquad \sum_{\sigma \in S_n} f^2(\sigma)$$

under the conditions of this problem. The first of these is easy: since $\sum_{i=1}^{n} x_i = 0$, we have

$$\sum_{\sigma \in S_n} f(\sigma) = \sum_{\sigma \in S_n} \sum_{i=1}^{n} x_i y_{\sigma(i)} = \sum_{i=1}^{n} x_i \sum_{\sigma \in S_n} y_{\sigma(i)} = 0.$$

In order to compute $\sum_{\sigma \in S_n} f^2(\sigma)$, we first rewrite it as

$$\sum_{\sigma \in S_n} \left(\sum_{i=1}^{n} x_i y_{\sigma(i)} \right)^2 = \sum_{\sigma \in S_n} \left(\sum_{i=1}^{n} x_i^2 y_{\sigma(i)}^2 + \sum_{i \neq j} x_i x_j y_{\sigma(i)} y_{\sigma(j)} \right)$$

$$= \sum_{i=1}^{n} x_i^2 \sum_{\sigma \in S_n} y_{\sigma(i)}^2 + \sum_{i \neq j} x_i x_j \sum_{\sigma \in S_n} y_{\sigma(i)} y_{\sigma(j)}.$$

[‡]See Chapter 10 of Hardy, Littlewood, and Pólya [1].

Here $\sum_{i=1}^{n} x_i^2 = 1$, and

$$\sum_{i \neq j} x_i x_j = \left(\sum_{i=1}^{n} x_i \right)^2 - \sum_{i=1}^{n} x_i^2 = 0^2 - 1 = -1.$$

Next, note that for each $1 \leq i, i' \leq n$ there are exactly $(n-1)!$ permutations $\sigma \in S_n$ for which $\sigma(i) = i'$, so

$$\sum_{\sigma \in S_n} y_{\sigma(i)}^2 = (n-1)! \sum_{i'=1}^{n} y_{i'}^2 = (n-1)! \cdot 1.$$

Similarly, observe that for each $1 \leq i, i', j, j' \leq n$ with $i \neq j$ and $i' \neq j'$ there are exactly $(n-2)!$ permutations $\sigma \in S_n$ for which $\sigma(i) = i'$ and $\sigma(j) = j'$, so

$$\sum_{\sigma \in S_n} y_{\sigma(i)} y_{\sigma(j)} = (n-2)! \sum_{i' \neq j'} y_{i'} y_{j'} = (n-2)! \cdot (-1).$$

In summary, we find that

$$\sum_{\sigma \in S_n} f^2(\sigma) = 1 \cdot (n-1)! \cdot 1 + (-1) \cdot (n-2)! \cdot (-1) = n(n-2)!.$$

Now let $\sigma_1, \sigma_2, \ldots, \sigma_{n!}$ be the elements of S_n in some order so that σ_1 is the identity permutation and $\sigma_{n!}$ is the reverse identity permutation. Set $k = n!$ and $a_i = f(\sigma_i)$. Then, by the rearrangement inequality, we have

$$f(\sigma_{n!}) \leq f(\sigma_i) \leq f(\sigma_1),$$

so our lemma yields

$$f(\sigma_1) - f(\sigma_{n!}) \geq 2\sqrt{n(n-2)!/n!}$$

or

$$\sum_{i=1}^{n} (x_i y_i - x_i y_{n+1-i}) \geq \frac{2}{\sqrt{n-1}},$$

as claimed.

Acknowledgments The author wishes to express his immense gratitude to everyone who contributed to the success of the competition: the students and their teachers, coaches, and proctors; the problem authors; the USAMO Editorial Board; the graders; the Art of Problem Solving; and the AMC Headquarters of the MAA. I am also grateful to Evan Chen for proofreading this article and for providing the two figures.

REFERENCES

[1] Hardy, G. H., Littlewood, J. E., Pólya, G. (1952). *Inequalities*, 2nd ed. London: Cambridge University Press.
[2] Hardy, G. H., Wright, E. M. (2008). *An Introduction to the Theory of Numbers.* Oxford: Oxford University Press.

Summary. We present the results of the 49th Annual USA Mathematical Olympiad. We also present the problems used in the competition and their solutions.

BÉLA BAJNOK (MR Author ID: 314851, ORCID: 0000-0002-9498-1596) is a professor of mathematics at Gettysburg College and the Director of the American Mathematics Competitions program of the MAA.

HM-LM-AM Inequalities

ÁNGEL PLAZA
Universidad de Las Palmas de Gran Canaria, Spain
angel.plaza@ulpgc.es

Let $a, b \in \mathbb{R}$, with $a \neq b$. The harmonic, logarithmic, and arithmetic means of a and b are respectively defined by $H(a,b) = \frac{2}{\frac{1}{a}+\frac{1}{b}} = \frac{2ab}{a+b}$, $L(a,b) = \frac{b-a}{\ln b - \ln a}$, and $A(a,b) = \frac{a+b}{2}$.

Theorem. For $0 < a < b$, $\dfrac{2}{a+b} < \dfrac{\ln b - \ln a}{b-a} < \dfrac{a+b}{2ab}$, which may be written as $(AM)^{-1} < (LM)^{-1} < (HM)^{-1}$.

Proof. Let us consider functions $2/(a+b)$, $1/x$, and the linear interpolation between points $(a, 1/a)$ and $(b, 1/b)$.

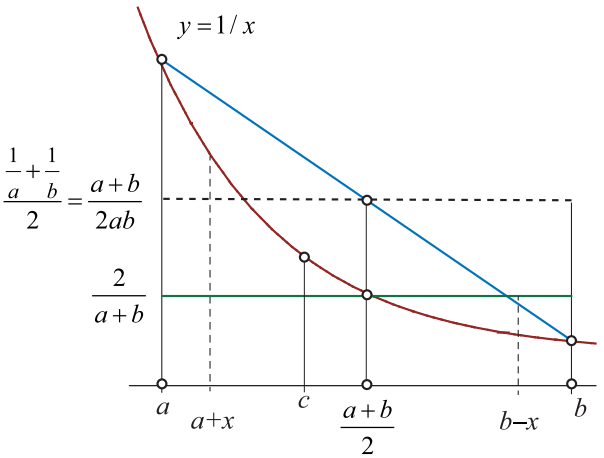

$$\frac{2}{a+b} < \frac{\ln b - \ln a}{b-a} < \frac{a+b}{2ab}$$

For $x \in (0, (b-a)/2)$, $\dfrac{1}{a+x} + \dfrac{1}{b-x} \geq \dfrac{4}{a+b}$ by the AM-HM inequality.

Then, by the mean value theorem for definite integrals there exists $c \in (a, (a+b)/2)$ such that $\dfrac{1}{c} = \dfrac{\ln b - \ln a}{b-a}$. □

Summary. We demonstrate visually the inequalities among the harmonic mean, the logarithmic mean and the arithmetic mean of two positive numbers.

ÁNGEL PLAZA (MR Author ID: 350023, ORCID: 0000-0002-5077-6531) received his master's degree from Universidad Complutense de Madrid in 1984 and his Ph.D. from Universidad de Las Palmas de Gran Canaria in 1993, where he is a Full Professor in Applied Mathematics.

Math. Mag. **94** (2021) 148. doi:10.1080/0025570X.2021.1867451
MSC: Primary 97H30, Secondary 11B39

A Double Angle Relationship

REX H. WU
New York Presbyterian
Lower Manhattan Hospital
New York, NY 10038
rexhwu@yahoo.com

Theorem. *Let $x > 1$ be a real number. Then $\theta = \arctan x^{-1}$ if and only if*

$$2\theta = \arcsin\frac{2}{x+x^{-1}}, \quad 2\theta = \arccos\frac{x-x^{-1}}{x+x^{-1}}, \quad \textit{or} \quad 2\theta = \arctan\frac{2}{x-x^{-1}}.$$

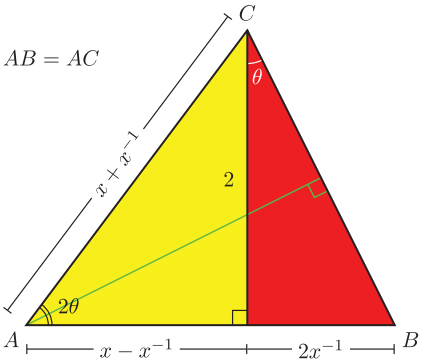

When the ratio of the legs in the red (dark) triangle is $\tan\theta$ (not necessary that just $x^{-1} = \tan\theta$), this theorem and diagram serve as the basis for many double angle formulas. When $x^{-1} = \tan\theta$ ($x = \cot\theta$), we have

$$\sin 2\theta = \frac{2}{\cot\theta + \tan\theta} \qquad \text{and} \qquad \cos 2\theta = \frac{\cot\theta - \tan\theta}{\cot\theta + \tan\theta}.$$

When $\tan\theta = (2\sin^2\theta)/(2\sin\theta\cos\theta)$, we have $\sin 2\theta = 2\sin\theta\cos\theta$ and $\cos 2\theta = 1 - 2\sin^2\theta$. If $\tan\theta = (\tan\theta\tan 2\theta)/\tan 2\theta$, we have $\tan\theta\tan 2\theta + 1 = \sec 2\theta$. And the list goes on.

Other interesting identities can be derived:

(1) Let φ be the golden ratio, and let F_i and L_i be the Fibonacci and Lucas numbers, respectively. If we set $x = \varphi^{2n}$, then $x^{-1} = \varphi^{-2n}$, and we have

$$2\arctan(\varphi^{-2n}) = \arcsin(2/L_{2n}) = \arccos[(\sqrt{5}F_{2n})/L_{2n}] = \arctan[2/(\sqrt{5}F_{2n})]$$

(2) If $x = e^{\vartheta}$, then we have

$$2\arctan(e^{-\vartheta}) = \arcsin(\operatorname{sech}\vartheta) = \arccos(\tanh\vartheta) = \arctan(\operatorname{csch}\vartheta).$$

Summary. We provide a visual proof to a double angle trigonometric relationship that serves as the basis for many double angle identities.

REX H. WU (MR Author ID: 1293646, ORCID 0000-0003-0970-3741) wishes to thank the editor for his suggestions.

Math. Mag. **94** (2021) 149. doi:10.1080/0025570X.2021.1869478
MSC: 97G60

PROBLEMS

LES REID, *Editor*
Missouri State University

EUGEN J. IONAŞCU, *Proposals Editor*
Columbus State University

RICHARD BELSHOFF, Missouri State University; *MAHYA GHANDEHARI*, University of Delaware; *EYVINDUR ARI PALSSON*, Virginia Tech; *GAIL RATCLIFF*, Eastern Carolina University; *ROGELIO VALDEZ*, Centro de Investigación en Ciencias, UAEM, Mexico; *Assistant Editors*

Proposals

To be considered for publication, solutions should be received by September 1, 2021.

2116. *Proposed by Fook Sung Wong, Temasek Polytechnic, Singapore.*

Evaluate

$$\int_0^\infty \frac{e^{\cos x}\cos(\alpha x + \sin x)}{x^2+\beta^2}\,dx,$$

where α and β are positive real numbers.

2117. *Proposed by Ahmad Sabihi, Isfahan, Iran.*

Find all positive integer solutions to the equation

$$(m+1)^n = m! + 1.$$

2118. *Proposed by Moubinool Omarjee, Lycée Henri IV, Paris, France.*

It is well known that the series

$$\sum_{k=1}^{\infty} \frac{\sin k}{k}$$

converges. Does the series

$$\sum_{k=1}^{\infty} e^{-\lfloor \ln k \rfloor} \sin k$$

converge or diverge?

Math. Mag. **94** (2021) 150–158. doi:10.1080/0025570X.2021.1873039

We invite readers to submit original problems appealing to students and teachers of advanced undergraduate mathematics. Proposals must always be accompanied by a solution and any relevant bibliographical information that will assist the editors and referees. A problem submitted as a Quickie should have an unexpected, succinct solution. Submitted problems should not be under consideration for publication elsewhere.

Proposals and solutions should be written in a style appropriate for this MAGAZINE.

Authors of proposals and solutions should send their contributions using the Magazine's submissions system hosted at http://mathematicsmagazine.submittable.com. *More detailed instructions are available there. We encourage submissions in PDF format, ideally accompanied by LaTeX source. General inquiries to the editors should be sent to* mathmagproblems@maa.org.

2119. *Proposed by Viktors Berstis, Portland, OR.*

A point in the plane is a distance of a, b, and c units from the vertices of an equilateral triangle in the plane. Denote the side length of the equilateral triangle by s.

(a) Find a polynomial relation between a, b, c, and s.
(b) Give a simple compass and straightedge construction of a segment of length s given segments of lengths a, b, and c.
(c) Generalize part (a) to the case of a point at a distance of a_i units, $i = 1, \ldots, n+1$, from the vertices of a regular n-dimensional simplex having sides of length s.

2120. *Proposed by Gregory Dresden, Jackson Gazin (student), and Kathleen McNeill (student), Washington & Lee University, Lexington, VA.*

Recall that the normalizer of a subgroup H of G is defined as

$$N_G(H) = \left\{ g \in G | ghg^{-1} \in H \text{ for all } h \in H \right\}.$$

Determine $N_G(H)$, when $G = GL_2(\mathbb{R})$, the group of all invertible 2×2 matrices with real entries, and

$$H = SO_2(\mathbb{R}) = \left\{ \begin{pmatrix} \cos\theta & -\sin\theta \\ \sin\theta & \cos\theta \end{pmatrix} \middle| \, \theta \in \mathbb{R} \right\}.$$

Quickies

1109. *Proposed by George Stoica, Saint John, NB, Canada.*

Let z_1, z_2, z_3 denote complex numbers of modulus 1. Prove that if

$$z_1 + z_2 + z_3 = -1,$$

then one of the numbers z_1, z_2, z_3 must be -1.

1110. *Proposed by Ovidiu Furdui and Alina Sîntămărian, Technical University of Cluj-Napoca, Cluj-Napoca, Romania.*

Let $n \geq 0$ be an integer. Calculate

$$\lim_{x \to 0} \left((n+1)! \frac{e^x - 1 - x - \frac{x^2}{2!} - \cdots - \frac{x^n}{n!}}{x^{n+1}} \right)^{\frac{1}{x}}.$$

Solutions

A geometric inequality — April 2020

2091. *Proposed by Marian Tetiva, National College "Gheorghe Roşca Codreanu," Bârlad, Romania.*

Let ABC be a triangle with sides of lengths a, b, c, altitudes h_a, h_b, h_c, inradius r, and circumradius R. Prove that the following inequality holds:

$$h_a + h_b + h_c \geq 9r + \frac{a^2 + b^2 + c^2 - ab - ac - bc}{4R},$$

with equality if and only if $\triangle ABC$ is equilateral.

Solution by Robert Calcaterra, University of Wisconsin-Platteville, Platteville, WI.
Let K denote the area of $\triangle ABC$. We have

$$r = \frac{2K}{a+b+c},$$
$$R = \frac{abc}{4K},$$
$$h_a = \frac{2K}{a},$$
$$h_b = \frac{2K}{b}, \text{ and}$$
$$h_c = \frac{2K}{c}.$$

Note that

$$\frac{abc}{K}(h_a + h_b + h_c) = 2(ab + ac + bc),$$

and

$$\frac{abc}{K}\left(9r + \frac{a^2 + b^2 + c^2 - ab - ac - bc}{4R}\right)$$
$$= \frac{18abc}{a+b+c} + a^2 + b^2 + c^2 - ab - ac - bc.$$

Therefore, it will suffice to show that

$$2(ab + ac + bc) \geq \frac{18abc}{a+b+c} + a^2 + b^2 + c^2 - ab - ac - bc,$$

or equivalently,

$$f(a, b, c) = 2a^2b + 2ab^2 + 2a^2c + 2ac^2 + 2b^2c + 2bc^2 - a^3 - b^3 - c^3 - 9abc \geq 0.$$

Without loss of generality, we may assume that $c \geq b \geq a$. Note that

$$f(a, b, c) = (a + b - c)(c - a)(c - b) + (3c - a - b)(b - a)^2.$$

Since a, b, and c are the side lengths of a triangle, $a + b - c > 0$. Also,

$$3c - a - b = c + c - a + c - b > 0$$

as well. Hence $f(a, b, c) > 0$ if $c > b$ or $b > a$, and consequently $f(a, b, c) = 0$ can only occur when $a = b = c$. This concludes the proof.

Also solved by Arkady Alt, Farrukh Rakhimjanovich Ataev (Uzbekistan), Herb Bailey, Michel Bataille (France), Elton Bojaxhiu (Germany) & Enkel Hysnelaj (Australia), Scott H. Brown, Habib Y. Far, Subhankar Gayen & Vivekananda Mission Mahavidyalaya & Haldia Purba Medinipur (India), Finbarr Holland (Ireland), Walther Janous (Austria), Parviz Khalili, Koopa Tak Lun Koo (Hong Kong), Omran Kouba (Syria), Sushanth Sathish Kumar. Elias Lampakis (Greece), Kee-Wai Lau (China), Antoine Mhanna (Lebanon), Quan Minh Nguyen (Canada), Sang-Hoon Park (Korea), Volkhard Schindler (Germany), Albert Stadler (Switzerland), Daniel Văcaru (Romania), Michael Vowe (Switzerland), John Zacharias, and the proposer.

An integral involving the tail of a Maclaurin series **April 2020**

2092. *Proposed by Seán M. Stewart, Bomaderry, Australia.*

Let n be a non-negative integer. Evaluate

$$\int_0^\infty \frac{1}{x^{2n+3}} \left(\sin x - \sum_{k=0}^{n} \frac{(-1)^k x^{2k+1}}{(2k+1)!} \right) dx.$$

Solution by Omran Kouba, Higher Institute for Applied Sciences and Technology, Damascus, Syria.
The answer is

$$(-1)^{n+1} \frac{\pi}{2(2n+2)!}.$$

We define

$$F_{2n}(x) = (-1)^n \left(\cos x - \sum_{k=0}^{n} \frac{(-1)^k x^{2k}}{(2k)!} \right), \text{ and}$$

$$F_{2n+1}(x) = (-1)^n \left(\sin x - \sum_{k=0}^{n} \frac{(-1)^k x^{2k+1}}{(2k+1)!} \right)$$

One easily sees that $F_m' = F_{m-1}$. Further,

$$F_m(x) = O(x^m) \text{ as } x \to \infty, \text{ and}$$

$$F_m(x) = O(x^{m+2}) \text{ as } x \to 0,$$

so the integral

$$I_m = \int_0^\infty \frac{F_m(x)}{x^{m+2}}\, dx$$

is convergent. A straightforward integration by parts shows that

$$\begin{aligned} I_m &= \frac{-F_m(x)}{(m+1)x^{m+1}}\bigg|_{x=0}^{\infty} + \frac{1}{m+1} \int_0^\infty \frac{F_{m-1}(x)}{x^{m+1}} dx \\ &= \frac{1}{m+1} I_{m-1}. \end{aligned}$$

This implies that

$$I_m = \frac{I_0}{(m+1)!}.$$

Another integration by parts gives

$$\begin{aligned} I_0 &= \int_0^\infty \frac{\cos x - 1}{x^2}\, dx \\ &= \left.\frac{1-\cos x}{x}\right|_{x=0}^{\infty} - \int_0^\infty \frac{\sin x}{x} dx \\ &= -\int_0^\infty \frac{\sin x}{x} dx \\ &= -\frac{\pi}{2}. \end{aligned}$$

Thus,

$$I_m = -\frac{\pi}{2(m+1)!}.$$

In particular,

$$\begin{aligned} \int_0^\infty \frac{1}{x^{2n+3}} \left(\sin x - \sum_{k=0}^{n} \frac{(-1)^k x^{2k+1}}{(2k+1)!} \right) dx &= (-1)^n I_{2n+1} \\ &= (-1)^{n+1} \frac{\pi}{2(2n+2)!}, \end{aligned}$$

which is the desired conclusion.

Also solved by Michel Bataille (France), Paul Bracken, Brian Bradie, David M. Bradley, Robert Calcaterra, William Chang, Robin Chapman (UK), Hongwei Chen, G.A. Edgar, Russell Gordon, Lixing Han, Eugene A. Herman, Finbarr Holland (Ireland), Sushanth Sathish Kumar, Elias Lampakis (Greece), Kee-Wai Lau (China), Quan Minh Nguyen (Canada), and the proposer. There were three incomplete or incorrect solutions.

A permutation probability — April 2020

2093. *Proposed by Jacob Siehler, Gustavus Adolphus College, Saint Peter, MN.*

Suppose π is a permutation of $\{1, 2, \ldots, 2m\}$, where m is a positive integer. Consider the (possibly empty) subsequence of $\pi(m+1), \pi(m+2), \ldots, \pi(2m)$ consisting of only those values which exceed $\max\{\pi(1), \ldots, \pi(m)\}$. Let $P(m)$ denote the probability that this subsequence never decreases (note that the empty sequence has this property), when π is a randomly chosen permutation of $\{1, \ldots, 2m\}$. Evaluate $\lim_{m\to\infty} P(m)$.

Solution by José Heber Nieto, Universidad del Zulia, Maracaibo, Venezuela.
The limit is $\sqrt{e}/2$. Let

$$k = \max\{\pi(1), \ldots, \pi(m)\}.$$

Clearly $m \le k \le 2m$. A permutation π with a given k satisfies the condition if and only if $k+1, k+2, \ldots, 2m$ is a (possibly empty, if $k = 2m$) subsequence of $\pi(m+1)$, $\pi(m+2), \ldots, \pi(2m)$. In the sequence $\pi(1), \ldots, \pi(2m)$ the number k may occupy any of the first m positions. The numbers $k+1, k+2, \ldots, 2m$ may occupy any $2m-k$ places among the last m places (i.e., $\binom{m}{m-k}$ possibilities), and the $2m-1-(m-k) = m+k-1$ remaining elements may be distributed in $(m+k-1)!$ ways. Therefore

$$P(m) = \frac{1}{(2m)!} \sum_{k=m}^{2m} m \binom{m}{2m-k} (m+k-1)!.$$

Putting $j = k - m$ we have

$$P(m) = \frac{1}{(2m)!} \sum_{j=0}^{m} m \binom{m}{j} (2m - j - 1)!.$$

Now

$$\begin{aligned} a_{j,m} &= \frac{1}{(2m)!} m \binom{m}{j} (2m - j - 1)! \\ &= \frac{m(m-1)(m-2)\cdots(m-j+1)}{2j!(2m-1)\cdots(2m-j)}. \end{aligned}$$

For fixed j, we have

$$\begin{aligned} \lim_{m\to\infty} a_{j,m} &= \lim_{m\to\infty} \frac{(1-\frac{1}{m})(1-\frac{2}{m})\cdots(1-\frac{j-1}{m})}{2j!(2-\frac{1}{m})\cdots(2-\frac{j}{m})} \\ &= \frac{1}{j!\,2^{j+1}}. \end{aligned}$$

Also

$$a_{j,m} < \frac{m^j}{2j!(2m-m)^j} = \frac{1}{2j!}$$

and

$$\sum_{j=0}^{\infty} \frac{1}{2j!} = e/2.$$

Hence by the dominated convergence theorem we have

$$\begin{aligned} \lim_{m\to\infty} P(m) &= \lim_{m\to\infty} \sum_{j=0}^{m} a_{j,m} \\ &= \sum_{j=0}^{\infty} \lim_{m\to\infty} a_{j,m} \\ &= \sum_{j=0}^{\infty} \frac{1}{j!\,2^{j+1}} \\ &= \frac{\sqrt{e}}{2}, \end{aligned}$$

as claimed.

Also solved by Elton Bojaxhiu (Germany) & Enkel Hysnelaj (Australia), Robert Calcaterra, Robin Chapman (UK), Kenneth Schilling, Edward Schmeichel, Albert Stadler (Switzerland), and the proposer. There was one incomplete or incorrect solution.

An upper bound for a vector sum **April 2020**

2094. *Proposed by George Stoica, Saint John, NB, Canada.*

Find the smallest number $f(n)$ such that for any set of unit vectors $x_1, \ldots, x_n$ in $\mathbb{R}^n$, there is a choice of $a_i \in \{-1, 1\}$ such that $|a_1x_1 + \cdots + a_nx_n| \le f(n)$.

Solution by Sushanth Sathish Kumar, student, Portola High School, Irvine, CA.
We claim that $f(n) = \sqrt{n}$. To see that this is minimal, consider the unit vectors $x_i = (0, \ldots, 1, \ldots, 0)$, where the ith term is 1 and the rest are 0. Then,

$$a_1x_1 + \cdots + a_nx_n = (\pm 1, \ldots, \pm 1)$$

has magnitude $\sqrt{n}$ regardless of choice of the a_i's.

We now show that $f(n) = \sqrt{n}$ does indeed work. Randomly and independently choose each a_i to be 1 or -1, both with probability $1/2$. We will prove that

$$\mathbb{E}\left[|a_1x_1 + \cdots + a_nx_n|^2\right] = n.$$

To see this, note that

$$\begin{aligned}\mathbb{E}[|a_1x_1 + \cdots + a_nx_n|^2] &= \mathbb{E}\left[\sum_{i=1}^{n}\sum_{j=1}^{n} a_ix_i \cdot a_jx_j\right] \\ &= \sum_{i=1}^{n}\mathbb{E}\left[a_i^2|x_i|^2\right] + 2\sum_{i=1}^{n}\sum_{j=i+1}^{n}\mathbb{E}[a_ix_i \cdot a_jx_j],\end{aligned}$$

by the dot product and linearity of expectation. Since $a_i^2 = 1$, and x_i is a unit vector, the first sum is just n. To compute the second sum, we note that

$$\begin{aligned}\mathbb{E}[a_ix_i \cdot a_jx_j] &= \mathbb{E}[a_ia_j|x_i||x_j|\cos\theta_{ij}] \\ &= \mathbb{E}[a_ia_j\cos\theta_{ij}] \\ &= 0,\end{aligned}$$

where θ_{ij} is the angle between vectors x_i and x_j. It follows that

$$\mathbb{E}\left[|a_1x_1 + \cdots + a_nx_n|^2\right] = n,$$

as claimed. Hence, there is a choice of $a_1, \ldots, a_n$ for which

$$|a_1x_1 + \cdots + a_nx_n|^2 \le n,$$

and we are done.

Also solved by Elton Bojaxhiu (Germany) & Enkel Hysnelaj (Australia), Robert Calcaterra, William Chang, Lixing Han, Eugene Herman, Omran Kouba (Syria), Miguel A. Lerma, José Nieto (Venezuela), Celia Schacht, Albert Stadler (Switzerland), Edward Schmeichel, and the proposer. There was one incomplete or incorrect solution.

A floor function sum **April 2020**

2095. *Proposed by Mircea Merca, University of Craiova, Romania.*

Show that

$$\sum_{k=1}^{n} k\left\lfloor\frac{n+1-k}{d}\right\rfloor = \begin{cases}\lceil (n+1)(n-1)(2n+3)/24\rceil & \text{if } d=2\\ \lceil (n+1)^2(n-2)/18\rceil & \text{if } d=3\\ \lceil (n+1)(2n+1)(n-3)/48\rceil & \text{if } d=4\\ \lceil (n+1)n(n-4)/30\rceil & \text{if } d=5\end{cases}.$$

Solution by Russell Gordon, Whitman College, Walla Walla, WA.
We first observe that these four formulas can be combined into one formula by noting that

$$\sum_{k=1}^{n} k \left\lfloor \frac{n+1-k}{d} \right\rfloor = \left\lceil \frac{(n+1)(n+1-d)(2n+5-d)}{12d} \right\rceil$$

is equivalent to the equation above for $d = 2, 3, 4, 5$. We will also show that the analogous formula holds when $d = 1$. It is easy to verify that the formulas are valid for $n = 1, 2, \ldots, d$ for each of these values of d; we omit the simple arithmetic computations that generate 0's and 1's for these values of n and d. Hence, by induction, it is sufficient to show that the equation for a given d is valid for $n + d$ when it is valid for n. To verify this, we will use the fact that

$$\lfloor m + x \rfloor = m + \lfloor x \rfloor \text{ and } \lceil m + x \rceil = m + \lceil x \rceil$$

for any positive integer m and positive number x. We then have

$$\begin{aligned}
&\sum_{k=1}^{n+d} k \left\lfloor \frac{n+d+1-k}{d} \right\rfloor \\
&\quad = \sum_{k=1}^{n} k \left(1 + \left\lfloor \frac{n+1-k}{d} \right\rfloor \right) + (n+1) \\
&\quad = \sum_{k=1}^{n+1} k + \sum_{k=1}^{n} k \left\lfloor \frac{n+1-k}{d} \right\rfloor \\
&\quad = \frac{(n+1)(n+2)}{2} + \left\lceil \frac{(n+1)(n+1-d)(2n+5-d)}{12d} \right\rceil \\
&\quad = \left\lceil \frac{(n+1)(n+2)}{2} + \frac{(n+1)(n+1-d)(2n+5-d)}{12d} \right\rceil \\
&\quad = \left\lceil \frac{(n+1)\left(6dn + 12d + 2n^2 + (7-3d)n + (1-d)(5-d)\right)}{12d} \right\rceil \\
&\quad = \left\lceil \frac{(n+1)\left(2n^2 + (7+3d)n + (1+d)(5+d)\right)}{12d} \right\rceil \\
&\quad = \left\lceil \frac{(n+1)(n+1+d)(2n+5+d)}{12d} \right\rceil,
\end{aligned}$$

as desired.

Remark. The analogous formulas do not hold for $d \geq 6$. For example, when $d = 6$ the two sides agree for all n, except when $n \equiv 0 \pmod 6$. In that case, we must subtract 1 from the right-hand side to maintain equality.

Also solved by Robert Calcaterra, William Chang, Dmitry Fleischman, Walther Janous (Austria), Elias Lampakis (Greece), Jacob Petry, Albert Stadler (Switzerland), and the proposer.

Answers

Solutions to the Quickies from page 151.

A1109. If $z_1 = -1$, we are done. If $z_1 = 1$ we have $z_2 + z_3 = -2$, which gives $z_2 = z_3 = -1$. So we may assume $z_1 \neq \pm 1$. Then the points $A = 0$, $B = 1$, $C = 1 + z_1$ form a triangle, in which AB has length 1 and BC has length $|z_1| = 1$. Let D be the point $1 + z_1 + z_2$. Note that CD has length $|z_2| = 1$ and DA has length $|z_3| = 1$. It follows that the triangles ABC and ADC are congruent. Then ABC and ADC either coincide (in which case $B = D$, so $z_1 + z_2 = 0$ and hence $z_3 = -1$), or they form a rhombus (in which case AB is parallel to DC and hence $z_2 = -1$). Either way, the claim follows.

A1110. The limit is $e^{1/(n+2)}$.

By Taylor's formula, there is a $\theta_{n,x} \in (0, 1)$ such that

$$e^x - 1 - x - \frac{x^2}{2!} - \cdots - \frac{x^n}{n!} = \frac{e^{x\theta_{n,x}}}{(n+1)!}x^{n+1}, \quad x \in \mathbb{R}.$$

It follows that

$$\begin{aligned} L_n &= \lim_{x\to 0} \frac{e^x - 1 - x - \frac{x^2}{2!} - \cdots - \frac{x^n}{n!}}{x^{n+1}} \\ &= \lim_{x\to 0} \frac{e^{x\theta_{n,x}}}{(n+1)!} \\ &= \frac{1}{(n+1)!}. \end{aligned}$$

We note that the limit we seek is indeterminate of the form 1^∞. Standard calculations show that if

$$\lim_{x\to a} f(x) = 0 \text{ and } \lim_{x\to a} g(x) = \infty,$$

then

$$\lim_{x\to a} (1 + f(x))^{g(x)} = \exp\left(\lim_{x\to a} f(x)g(x)\right).$$

In our case, we have

$$\begin{aligned} &\lim_{x\to 0} \left((n+1)! \frac{e^x - 1 - x - \frac{x^2}{2!} - \cdots - \frac{x^n}{n!}}{x^{n+1}} \right)^{\frac{1}{x}} \\ &= \lim_{x\to 0} \left(1 + \frac{(n+1)!\left(e^x - 1 - x - \frac{x^2}{2!} - \cdots - \frac{x^n}{n!}\right) - x^{n+1}}{x^{n+1}} \right)^{\frac{1}{x}} \\ &= \exp\left(\lim_{x\to 0} \frac{(n+1)!\left(e^x - 1 - x - \frac{x^2}{2!} - \cdots - \frac{x^n}{n!} - \frac{x^{n+1}}{(n+1)!}\right)}{x^{n+2}} \right) \\ &= \exp\left((n+1)!\, L_{n+1}\right) \\ &= \exp\left(\frac{1}{n+2}\right) \end{aligned}$$

and the problem is solved.

REVIEWS

PAUL J. CAMPBELL, *Editor*
Beloit College

Assistant Editor: Eric S. Rosenthal, West Orange, NJ. Articles, books, and other materials are selected for this section to call attention to interesting mathematical exposition that occurs outside the mainstream of mathematics literature. Readers are invited to suggest items for review to the editors.

Austin, David, Pooling strategies for COVID-19 testing, ams.org/publicoutreach/feature-column/fc-2020-10.

Public frustration at how long it took to get results of a Covid-19 test finally led the FDA in August to authorize pooling samples from individuals; doing so can reduce the number of tests necessary and hence the wait time compared to testing one sample at a time. The mathematics involved has been known for some time, and the basic idea goes back to tests for syphilis during World War II. Further developments include both adaptive methods (using results from a round of testing to decide how to test further) and more-complex non-adaptive methods (which produce results in a single round of tests).

Toscano, Fabio, *The Secret Formula: How a Mathematical Duel Inflamed Renaissance Italy and Uncovered the Cubic Equation*, Princeton University Press, 2020; viii + 161 pp, $24.95. ISBN 978-0-691-18367-1.

Author Toscano tells in detail the tale of Scipione del Ferro, Niccolo Tartaglia, Gerolamo Cardano, and Ludovico Ferrari—"the four glittering musketeers who lit up the sky of algebra"—and their interpersonal involvements in the discovery of solutions for cubic and quartic equations. The story centers on Tartaglia and quotes copiously from *his* detailed accounts of conversations and events. As Toscano ably relates and concludes, the discoveries were the result not only of clever mathematical investigation, but also of "passion, dedication, perseverance, rivalry, jealousy, ambition, esteem, resentment, impetuosity, and suffering … all the human emotions and feeling that can be hidden in a mathematical formula."

Ramond, Paul, Abel–Ruffini's theorem: Complex but not complicated, arxiv.org/abs/2011.05162.

Katz, Boaz, Short proof of Abel's theorem that 5th degree polynomial equations cannot be solved, youtube.com/watch?v=RhpVSV6iCko.

This paper offers valuable insight and intuition into why a general solution to a polynomial equation of degree five or more, in terms of radicals of the coefficients, does not exist. Using a simple logic of "loops" traversed in the complex plane by solutions, plus the concept of commutators of permutation cycles of the solutions, the author shows that a formula to solve the general quadratic equation cannot be found that involves only the coefficients and the four arithmetic operations ($+, -, \times, \div$). Similar impossibility results apply to cubic equations with only one level of cube roots, and to quartic equations with two levels of square roots; "commutators reject formulae with too few nested roots in their expressions." But those cases can indeed be solved just by allowing one more level of roots. Why can't we solve the quintic that way? Well, being able to write a three-cycle of roots as a number n of commutators allows rejecting formulas with n levels of roots. Having a fifth root to permute results in being able to write a three-cycle as a commutator of arbitrarily many commutators, thus rejecting formulas with any number of roots. This imaginative and enlightening exposition is based on a 1963 proof by V.I. Arnold; the video by Katz gives animations of the loops involved.

Math. Mag. **94** (2021) 159–160. doi:10.1080/0025570X.2021.1873042

Ward, Matthew, The Hodge conjecture: Get $1 million if you solve this math problem, medium.com/cantors-paradise/the-hodge-conjecture-5fabdf1dfb54.

_____, Faltings's theorem and the Mordell conjecture: On the number of rational solutions to polynomials, medium.com/cantors-paradise/faltingss-theorem-and-the-mordell-conjecture-59e1917f5cdb.

Veisdal, Jørgen, The Riemann hypothesis, explained, medium.com/cantors-paradise/the-riemann-hypothesis-explained-fa01c1f75d3f.

_____, The Poincaré conjecture: What is the shape of the universe?, medium.com/cantors-paradise/the-poincare-conjecture-cb4ca7014cc5.

Want to write short pieces about math for a popular audience? *You can get paid.* The subscription site medium.com ($5/month, after three free articles per month) offers at medium.com/cantors-paradise daily articles about mathematics, with 350 currently available. The site pays a median of $57 and an average of $147 per mathematics story, with payment based on number of views and the time that readers spend reading it. The four excellent essays cited are a recent sample, each focusing on a notable problem in mathematics. Each builds up the concepts and intuition necessary to understand the mathematical problem of its title and progress on it, at a level that undergraduate mathematics majors and others can both learn from and appreciate.

Gelman, Andrew, and Aki Vehtari, What are the most important statistical ideas of the past 50 years?, statmodeling.stat.columbia.edu/2020/12/09/what-are-the-most-important-statistical-ideas-of-the-past-50-years/.

The ideas presented, not in order of importance, are exploratory data analysis and data visualization, bootstrapping and simulation-based inference, hierarchical models (e.g., in Bayesian analysis), efficient statistical algorithms, robust inference, adaptive decision analysis, counterfactual causal inference, and overparameterized models and regularization. The full paper goes on to note what the ideas have in common and how they differ, mention the most important statistical ideas of 1920–1970 and 1870–1920, and speculate on future developments.

Strang, Gilbert, *Linear Algebra for Everyone*, SIAM, 2020; xii + 356 pp, $85. ISBN 978-1-713314663-0.

Gilbert Strang is the author of several leading textbooks on linear algebra. This one is a "new start," marked by more numerical examples but the same spirit of analyzing a matrix in terms of the four subspaces (row space, column space, nullspace, left nullspace). Featured are the "great factorizations" of linear algebra, including diagonalization and the singular value decomposition. Notable is a novel chapter on data science, focusing on continuous piecewise linear functions of data vectors, neural nets, and gradient descent. The book would embrace more of "everyone" if the price were considerably lower.

Arney, Chris, *Ars Mathematica: Mathematics as an Art Form, Art as a Mathematical Endeavor*, Patriot Publications (9328 Blind Sodus Bay Road, Red Creek, NY 13143), 2020; xvi + 248 pp, $10.50(P), ISBN 979-856780448-3.

What makes mathematics artful? How is art mathematical? This volume attempts the difficult task of bringing out the artistic aspects of mathematics of all kinds and mathematical aspects in the arts. For images, the book concentrates on frontispieces of mathematics books, geometric models, and mathematical curves and shapes. The emphasis is on "remarkable people and their incredible pursuits"; the bulk of the book consists of highlights about particular mathematicians and artists, with detailed profiles of Cardano, Erdős, Leonardo, Escher, Dürer, Dalí, Ramanujan, and Joseph Arkin. Arkin (1923–2002), whom author Arney knew personally and calls a "master artistic mathematician," was a prolific untrained amateur number theorist who took up mathematics at age 40 and collaborated with Arney and Erdős. [Disclosure: The author and I collaborate in work for COMAP and *The UMAP Journal*.]